ZOOTAXA

1571

Skeletomusculature of Scelionidae (Hymenoptera: Platygastroidea): head and mesosoma

ISTVÁN MIKÓ, LARS VILHELMSEN, NORMAN F. JOHNSON, LUBOMIR MASNER & ZSOLT PÉNZES

Magnolia Press
Auckland, New Zealand

ISTVÁN MIKÓ, LARS VILHELMSEN, NORMAN F. JOHNSON, LUBOMIR MASNER & ZSOLT PÉNZES
Skeletomusculature of Scelionidae (Hymenoptera: Platygastroidea): head and mesosoma
(*Zootaxa* 1571)

78 pp.; 30 cm.

31 August 2007

ISBN 978-1-86977-135-5 (paperback)

ISBN 978-1-86977-136-2 (Online edition)

FIRST PUBLISHED IN 2007 BY

Magnolia Press

P.O. Box 41-383

Auckland 1346

New Zealand

e-mail: zootaxa@mapress.com

http://www.mapress.com/zootaxa/

ISSN 1175-5326 (Print edition)

ISSN 1175-5334 (Online edition)

Zootaxa 1571: 1–78 (2007)
www.mapress.com/zootaxa/

ISSN 1175-5326 (print edition)
ZOOTAXA
ISSN 1175-5334 (online edition)

Skeletomusculature of Scelionidae (Hymenoptera: Platygastroidea): head and mesosoma

ISTVÁN MIKÓ[1], LARS VILHELMSEN[2] NORMAN F. JOHNSON[3], LUBOMIR MASNER[4] & ZSOLT PÉNZES[5, 6]

[1]*Vas County Plant Protection and Soil Conservation Service, Tanakajd, Ambrózy st. 2. 9730, Hungary.*
E-mail: istvan.miko@gmail.com
[2]*Zoological Museum, Entomology Department, DK-2100 Copenhagen Ø Denmark.*
E-mail: lbvilhelmsen@snm.ku.dk
[3]*Department of Entomology, The Ohio State University, 1315 Kinnear Road, Columbus, OH 43212, USA.*
E-mail: johnson.2@osu.edu
[4]*Agriculture and Agri-Food Canada, Research Branch, K. W. Neatby Building, Ottawa, Ontario K1A 0C6, Canada.*
E-mail: lmasner@gmail.com
[5]*Institute of Genetics, Biological Research Center of Hungarian Academy of Sciences, Temesvári krt, 62 Szeged, 6726, Hungary.*
E-mail: penzes@bio.u-szeged.hu
[6]*Department of Ecology, University of Szeged, Egyetem str.2. Szeged, 6721, Hungary*

Table of contents

Abstract 3
Introduction 4
Materials and Methods 5
Results 11
Discussion 24
Acknowledgments 33
References 33
Appendix 36

Abstract

The skeletomusculature of the head and mesosoma of the parasitoid wasp family Scelionidae is reviewed. Representatives of 27 scelionid genera are examined together with 13 non-scelionid taxa for comparison. Terms employed for other groups of Hymenoptera are reviewed, and a consensus terminology is proposed. External characters are redescribed and correlated with corresponding apodemes, muscles and putative exocrine gland openings; their phylogenetic importance is discussed. 229 skeletal structures were termed and defined, from which 84 are newly established or redefined. 67 muscles of the head and mesosoma are examined and homologized with those present in other Hymenoptera taxa.

The presence of the cranio-antennal muscle, an extrinsic antennal muscle originating from the head capsule, is unique for Scelionidae. The dorsally bent epistomal sulcus and the corresponding internal epistomal ridge extend to the anterior margin of the oral foramen, the clypeo-pleurostomal line is absent and the tentorium is fused with the pleurostomal condyle. The frontal ledge is present in those scelionid genera having the anterior mandibular articulation located on the lateral margin of the oral foramen. The ledge corresponds to the site of origin of the mandibular abductor muscle, which is displaced from the genal area to the top of the frons. The protractor of the pharyngeal plate originates dorsally of the antennal foramen in Scelionidae. All scelionid genera have a postgenal bridge developed between the oral and occipital foramina. The propleural arm is reduced, muscles originating from the propleural arm in other Hymenoptera are situated on other propectal structures in Scelionidae. The profurcal bridge is absent. The first flexor of the fore wing originates from the posteroventral part of the pronotum in Scelionidae and Vanhorniidae, whereas the muscle originates

Accepted by M. Buffington: 7 Jun.; published: 31 Aug. 2007

from the mesopleuron in all other Hymenoptera. The netrion apodeme anteriorly limits the site of origin of the first flexor of the fore wing. Three types of netrion are described on the basis of the relative position of the netrion apodeme and the posterior pronotal inflection. The occlusor muscle apodeme is absent in basal Scelionidae, the fan-shaped muscle originates from the pronotum. In *Nixonia* the muscle originates posterior to the netrion apodeme. The skaphion apodeme crosses the site of origin of the longitudinal flight muscle. The lateral and dorsal axillar surfaces and the axillar carina are defined and described for the first time in Platygastroidea. The retractor of the mesoscutum is reported in Scelionidae and the variability of the muscle and corresponding skeletal structures within the family is described. The term sternaulus is redefined on the basis of the site of origin of the mesopleuro-mesobasalare muscle. The term speculum is adopted from Ichneumonidae and Cynipoidea taxonomy on the basis of the site of origin of the mesopleuro-mesofurcal muscle. The remnants of the mesopleural ridge, sulcus and mesopleural arm and pit and the putative border between the mesepisternum and mesepimeron is discussed. The mesopleural depressor of the mesotrochanter sensu Gibson 1985 originates from the anterior extension of the mesofurca and therefore the muscle is redefined and referred to in the present study as the lateral mesofurco-mesotrochanteral muscle. In *Nixonia*, *Sparasion*, *Idris* and *Gryon* both the lateral and median mesofurco-mesotrochanteral muscles are present. The lateral mesofurco-mesotrochanteral muscle is present in Platygastridae. The second flexor of the hind wing at least partly originates from the posteriorly delimited area of the mesopectus in Scelionidae similarly to some other Proctotrupomorpha and Chalcidoidea. The serial homology of this area and the netrion is discussed. The possible serial homology of the medially elevated area of the metanotum and mesoscutellum and the usage of the term metascutellum in Apocrita is discussed with the descriptions of correlated internal structures. The anterior metanotal wing process is located on the independent humeral sclerite in Scelionidae, similar to other Apocrita except Cynipoidea. The metanotal depressor of the metatrochanter originates from the humeral sclerite in Scelionidae as well as in some other Proctotrupoidea. The metapleuron is extended secondarily dorsally of the metapleural ridge and corresponding metapleural sulcus in Scelionidae. In Telenominae, Gryonini and Baeini the metafurca is located posteriorly on the metadiscrimenal lamella.

Key words: Scelionidae, morphology, terminology, comparative anatomy, skeletomusculature, parasitoid wasps

Introduction

Anatomical characters are an important source of data in systematic and taxonomic research, and an elaborate and arcane language has developed over the years to describe these features (for entomological terms see, e.g., Torre-Bueno 1989). Unfortunately, the specialists in different taxonomic groups have often developed independent terminologies, resulting in numerous synonymies and a general barrier to effective communication. Even though the latest edition of the Torre-Bueno Glossary of Entomology numbers over 800 pages, for only English words, new and important morphological features are continually discovered, all of which need names. The intimate relationship between form and function and the correspondence of internal and external anatomy is well known and was amply demonstrated in even the early textbooks on insect morphology (e.g., Snodgrass 1935). External structures, such as sulci and pits, are often functionally correlated with internal skeleto-muscular features. Proper recognition of homologies between structures, and of synonymies between terms, is facilitated by a consideration of both external and internal features.

This paper is a contribution toward a comprehensive examination of the internal and external morphology of the family Scelionidae (Hymenoptera: Platygastroidea). One of the goals is to reconcile the different terms used in the taxonomic literature of this family of parasitoid wasps and to coordinate with the nomenclature used for other groups of Hymenoptera. Our work builds upon the recent important contributions of numerous authors, particularly those of Gibson (1985, 1986, 1993, 1997, 1999), Ronquist (1995), Ronquist & Nordlander (1989), and Vilhelmsen (1996, 1999, 2000a, 2000b, 2003). Secondly, we seek to provide a precise nomenclature for scelionid anatomy for use in systematics, and thus to contribute to further advances in our understanding of the taxonomy and interrelationships of its constituent groups. Given the enigmatic position of the family in the Apocrita (summarized in Austin *et al*. 2005), the recognition of homologous characters with other hymenopterans will facilitate work toward a robust phylogenetic hypothesis for the entire order.

The scope of this contribution encompasses the anatomy of the head and mesosoma. Most extrinsic muscles associated with appendages are treated, but those associated with the mouthparts and antennae only partially.

Materials and Methods

Members of 27 scelionid genera were examined. Most of the examined specimens were obtained from the collection of the Systematic Parasitoid Laboratory (Kőszeg, Hungary), but specimens of *Nixonia* were provided by N. F. Johnson, those of *Archaeoteleia* and *Calliscelio* from Chile by J. Heraty (University of California, Riverside, USA), and those of *Tiphodytes* by F. Bin (Università di Perugia, Italy). The non-scelionid Hymenoptera specimens were donated primarily by L. Vilhelmsen, but specimens of *Proctotrupes*, *Helorus*, *Andricus*, *Belyta*, *Trichopria*, *Isocybus*, *Trichacis* and *Inostemma* from Hungary came from the collection of the Systematic Parasiotid Laboratory. A list of examined species with locations is given in Table 1.

TABLE 1. Species examined during this study and the origin of the material. Number of specimens examined in brackets.

Species	Origin
SCELIONIDAE	
Apegus sp. (2)	Hungary
Archaeoteleia sp. (7)	Chile
Baeus seminulum (1)	Hungary
Baryconus sp. (2)	South Africa
Baryconus sp. (3)	Hungary
Calliscelio sp. (1)	South Africa
Calloteleia sp. (4)	South Africa
Calloteleia sp. (5)	Chile
Doddiella sp. (1)	Republic of Congo
Dyscritobaeus sp. (1)	Thailand
Dyscritobaeus sp. (1)	South Africa
Eremioscelio cydnoides (1)	Hungary
Eremioscelio sp. (1)	China
Gryon misellum (4)	Hungary
Gryon sp. (1)	China
Gryon sp. (3)	South Africa
Idris flavicornis (1)	Hungary
Idris sp. (1)	South Africa
Macroteleia sp. (1)	Hungary
Neoscelio (*2*)	Australia
Nixonia sp. (4)	South Africa
Paratelenomus saccharalis (3)	South Africa
Psilanteris bicolor (3)	Hungary

..... *continued on the next page*

TABLE 1 (continued)

Species	Origin
Psix sp. (2)	South Africa
Scelio sp. (12)	Hungary
Scelio sp. (4)	South Africa
Sparasion sp. (4)	China
Sparasion sp. (6)	Hungary
Teleas lamellatus (4)	Hungary
Telenomus chloropus (6)	Hungary
Telenomus sp. (2)	South Africa
Thoron metalicus (1)	Hungary
Tiphodytes gerriphagus (2)	Italy
Trichoteleia sp. (2)	Thailand
Trimorus flavipes (3)	Hungary
Trimorus hungaricus (5)	Hungary
Trimorus opacus (3)	Hungary
Trimorus sp. (2)	South Africa
Trimorus varicornis (2)	Hungary
Trissolcus semistriatus (4)	Hungary
Trissolcus sp. (4)	South Africa
Xenomerus sp. (2)	South Africa
OTHER HYMENOPTERA	
Inostemma sp. (Platygastridae) (4)	Hungary
Isocybus sp. (Platygastridae) (3)	Hungary
Trichacis sp. (Platygastridae) (3)	Hungary
Andricus lignicolus (Cynipidae) (4)	Hungary
Belyta sp. (Diapriidae) (3)	Hungary
Evaniella semaeoda (Evaniidae) (4)	USA
Helorus sp. (Heloridae) (2)	Hungary
Pelecinus polyturator (Pelecinidae) (3)	USA
Pristaulacus strangaliae (Aulacidae) (2)	USA
Proctotrupes gravidator (Proctotrupidae) (6)	Hungary
Pseudofoenus sp. (Gasteruptiidae) (4)	Australia
Trichopria sp. (Diapriidae) (2)	Hungary
Vanhornia eucnemidarum (Vanhorniidae) (3)	USA

Specimens dissected for examination of musculature were preserved in 70% ethanol. All specimens were transferred to 96% ethanol and critical-point dried. The specimens were transferred to Blu Tack (Bostik Findley 2001) and dissected with insect pins (size: 000) or minuten needles. For examination of pleural musculature, specimens were bisected along the median sagittal plane with a razor blade. Most muscles were removed successively from the body parts during dissections. The remnants of the specimens are deposited in the collection of the Systematic Parasitoid Laboratory, Kőszeg.

Dissections for skeletal structures were based on dried or ethanol-preserved specimens. The dissected specimens were macerated in KOH and transferred to 96% ethanol. Part of the series was critical-point dried and examined with SEM and part was transferred to clove oil and examined under stereo (Leica MZ6) and polarizing (Olympus BH2) microscopes.

Critical-point dried and dissected specimens were mounted with double adhesive tape on stubs and coated with gold prior to SEM examination.

Critical-point dried and dissected specimens were transferred to Blu Tack for digital imaging. Specimens were imaged at different stages of dissection. Digital images were taken with a Nikon Coolpix 4500 camera attached to an Olympus BH2 polarizing microscope. To avoid glare and light reflections a sheet of tracing paper was used to disperse light. A series of photographs were prepared by focusing on different levels of the structure and these combined by CombineZ5 (Hadley 2006) using "do combine" and "do average and filter" commands. Images were processed in Adobe Photoshop 6.0. Line drawings were made in Adobe Photoshop 6.0. based on dissected specimens stored in clove oil and examined under the stereomicroscope.

The terms propectus, mesopectus, and metapectus are used to refer to the fused pleural and sternal components of the thoracic segments. Terms for skeletal structures generally follow Masner (1980), Ronquist & Nordlander (1989), and Vilhelmsen (2000a, 2000b). Additional terms are derived from Bin and Dessart (1983), Duncan (1939), Gibson (1985, 1986, 1997), Gordh & Headrick (2001), Heraty *et al*. (1994), Huber & Sharkey (1993), Johnson (1984, 1996), Johnson & Masner (1985), Masner (1972, 1979a, 1979b, 1983, 1991), Ronquist (1995), Snodgrass (1942), Vilhelmsen (1999), and Yoder (2004).

Terms referring to skeletal structures appear in bold face the first time they occur in the text. Abbreviations and figure references are given in parenthesis following the term. Abbreviations referring to muscles are italicized. Abbreviations, the reference to works where the terms were defined or redefined and proposed, and synonyms are given in Appendix. New or modified terms are denoted with an asterisk (*).

We generally do not use names for muscles that refer to their function, because the function may be ambiguous, difficult to discern, may differ among taxa, or different muscles may have the same function in different taxa. Instead, we follow Vilhelmsen (1996, 2000a, 2000b) and refer to muscles as follows: the first component of the name refers the site of origin, the second component to the site of insertion of the muscle. Suffixes may be used to indicate the relative position of muscles with the same origin and insertion. Muscles usually have a fan-shaped origin and insert on a tendon. If the muscle is rodlike, i.e., attaching with tendons at both ends, then its site of origin is decided by its function. For example, the third mesopleuro-mesonotal muscle is a retractor of the mesoscutum; therefore its site of origin is the mesopleuron and its site of insertion is the mesoscutum. Terms referring to muscles appear in bold and italics the first time they occur in the text. Figure references are given in parentheses following the term. The terms for muscles used in the present paper, figure references, function and possible homologies are given in Table 2.

TABLE 2. Muscle homologies between Scelionidae and other Hymenoptera (–: absent; ?: questionable or unknown; other papers: **a**, compiled from Alam 1951; **b**, compiled from Daly 1963; **c**, compiled from Gibson 1985; **d**, compiled from Gibson 1986; **e**, compiled from Gibson 1993; **f**, compiled from Heraty et al. 1994; **g**, compiled from Johnson 1988; **h**, compiled from Ronquist & Nordlander 1989; **i**, compiled from Vilhelmsen 2000a; **j**, compiled from Vilhelmsen 2000b; **k**, compiled from Vilhelmsen 1996; **l**, compiled from Gibson 1999; **m**, compiled from Krogmann & Vilhelmsen 2006).

abbreviation	term	figs	function	Duncan 1939	Snodgrass 1942	Others
crpl-md, crpm-md	*posterior cranio-mandibular*	2, 21, 29, 33	mandibular adductor	admd	9	?
cra-md	*anterior cranio-mandibular*	1a, 21, 34, 156, 157	mandibular abductor	abmd	8	?

..... *continued on the next page*

TABLE 2 (continued)

abbreviation	term	figs	function	Duncan 1939	Snodgrass 1942	Others
cr-A1	*cranio-antennal*	1a, 21, 34	–	–	–	?
not figured	*tentorio-antennal*		depressors and elevators of the antenna	ial, iad, ead, eal	2–5	?
not figured	*tentorio-labial*		tentorial depressor of the labium	plad	18	?
not figured	*tentorio-stipital*		tentorial depressor of the stipes	flst	11, 12, 13	?
cr-phr	*cranio-pharyngeal plate*	1a, 34	protractor of the pharyngeal plate	dlph	34, 35	ppp: **h;** 11: **k**
t1-sp2	*pronoto-mesothoracic spiracle*	3, 4, 55, 58	occlusor of the mesothoracic spiracle	2osp	73	om: **c**; 6: **d**; 110, ism-sp2: **e**
t1-cx1	*pronoto-procoxal*	3, 4, 57, 63, 65, 98, 116,	pronotal remotor of the procoxal	Ilm6	55	11: **j**
t1-poc	*pronoto-postoccipital*	3, 4, 42, 55, 98, 116	pronotal levator of the head	–	40, 41?	4?: **j**, 43, 44: **a**
t1-cv	*pronoto-laterocervical*	3, 4, 42, 57, 116	pronotal elevato of the propleuron and head	l pm1, 2	47	5: **j**
t1-pl1	*pronoto-propleural*	3, 4, 6, 42, 55, 57, 116	pronotal protractor of the propleuron	lpm3 , 4	48	9: **j**
t1-fu1	*pronoto-profurca*	3, 4, 8, 39, 57, 116	pronotal protractor of the propleuron	lpm5,6	49, 50	10: **j**
pl1(m, l)-poc	*propleuro-postoccipital*	5, 6, 42, 43, 46	propleural elevator of the head	Ois1	42	1: **j**
pl1-cx1	*propleuro-procoxal*	5, 43	propleural promotor of the procoxal	l lm2	53	12: **j**
pl1-tr1	*propleuro-protrochanteral*	5, 42, 43	propleural depressor of the protrochanter	llm3	61	17: **j**
fu1-cv	*profurco-laterocervical*	6, 7, 39, 44	retractor of the prosternum	lfp	51	6: **j**
cv-cx1	*laterocervico-procoxal*	7	diagonal rotator of the procoxa	llm7	mcr	7: **j**
fu1d-poc	*dorsal profurco-postoccipital*	6, 7, 39, 44, 46	furcal elevator of the head	Ois2	43	2: **j;** profurco-postoccipital muscle: **m**
fu1v-poc	*ventral profurco-postoccipital*	6, 7, 44, 46	furcal depressor of the head	Oi s3,4	44	3: **j;** profurco-postoccipital muscle: **m**
fu1-cx1m	*median profurco-procoxal*	7, 46	median furcal remotor of the procoxa	l lm4	56	15: **j**
fu1-cx1l	*lateral profurco-procoxal*	7, 37, 46, 57	lateral furcal remotor of the procoxa	llm5	57	14: **j** profurco-procoxal muscle: **m**
s1-cx1	*prosterno-procoxal*	8	sternal promotor of the procoxa	Ilm1	54	13: **j**

..... continued on the next page

TABLE 2 (continued)

abbreviation	term	figs	function	Duncan 1939	Snodgrass 1942	Others
ph1-ph2	*first phragmo-second phragmal*	46, 70, 81, 98, 122	longitudinal indirect flight muscle; indirect depressor of the fore wing	IIdl1	71	2: **d**; 112(1ph-2ph): **f**; 1ph-2ph: **b**
ph1(t1)-pl1	*first phragmo-propleural*	9, 66	phragmal protractor of the propleuron	lpm 3, 4	48?	9: **j**
ph1(t1)-poc	*first phragmo-postoccipital*	9, 66	phragmal levator of the head	–	40, 41	4: **j**?; 43, 44: **a**
t1-ph1	*pronoto-prophragmal*	7, 8, 55, 57, 58, 63, 98, 116	pronotal retractor of the mesoscutum	l is1,2	45	19: **j**
pl2-t2a	*first mesopleuro-mesonotal*	70, 98	dorsoventral indirect flight muscle; indirect elevator of the fore wing	IIdv1	72	3: **d**; t2-pl2: **b**; 128/129, t2-prep2: **e**
pl2-t2c	*third mesopleuro-mesonotal*	9, 12, 66, 70–72	retractor of the mesoscutum	–	–	5: **d**; 142, t2-plr2: **e**
t1-3ax2	*pronoto-third axillary sclerite of fore wing*	7, 8, 10, 57, 58, 62–65	pronotal flexor of the fore wing	m3Ax?	76a?	7?: **d**; 163, plr2-3ax2: **e**
pl2-3ax2a	*anterior mesopleuro-third axillary sclerite of fore wing*	10, 12, 62, 63, 65, 72, 103, 104	second pleural flexor of the fore wing	IIpm2	76b	8: **d**; 163, plr2-3ax2: **e**
pl2-3ax2p	*posterior mesopleuro-third axillary sclerite of fore wing*	10, 12, 62–65, 67, 72, 103, 104, 112, 118	third pleural flexor of the fore wing	IIpm3	76c	9: **d**; 164, epm2-3ax2: **e**
pl2-ba2	*mesopleuro-mesobasalar*	10, 12, 67, 103, 104, 118	mesopleural muscle of the mesobasalare	IIpm1	77	10: **d**; pl2-ba2b: **b**; 154, prep2-ba2: **e**
ism1,2-ba2	*intersegmental membrane-mesobasalar*	10, 12, 64, 67, 103, 118	intersegmental muscle of the mesobasalare	–	–	144: **e**
t1-ba2	*pronoto-mesobasalar*	7	pronotal muscle of the mesobasalare	–	–	144, ismba2?: **e**
pl2-3ax3	*mesopleuro-third axillary sclerite of the hind wing*	11, 104, 109, 110, 113–116	mesopleural flexor of the hind wing	I IIpm2a?	100	19: **d**
pl2-t2b	*second mesopleuro-mesonotal*	9, 10, 12, 62–65, 67, 102, 112, 118, 119	retractor of the scutellar axillar complex	IIpm4	75	4: **d**; 153, t2-epm2: **e**
pl2-cx2	*mesopleuro-mesocoxal*	10, 12, 62–65, 67, 102–104, 112, 118	lateral promotor of the mesocoxa	IIlm1	80	13: **d**; 157, prep2-cx2: **e**
cx2-sa2	*mesocoxo-mesosubalar*	11, 64, 67, 109–111, 113	lateral remotor of the mesocoxa	–	82	160, cx2-sa2: **e**; cx2-sa2: **b**
s2-cx1	*mesosterno-procoxal*	10	mesosternal retractor of the propectus	l is3	58	16: **j**
pl2-fu2	*mesopleuro-mesofurcal*	10, 12, 108, 111, 112, 114	mesothoracic furcopleural muscle	IIfpl1	79	12: **d**; 151(pl2-fu2a): **f**

..... continued on the next page

TABLE 2 (continued)

abbreviation	term	figs	function	Duncan 1939	Snodgrass 1942	Others
fu2l-tr2	*lateral mesofurco-mesotrochanteral*	10–12, 67, 109, 111, 114, 115, 118, 119	lateral furcal depressor of the mesotrochanter	IIlm3b	–	pl2-tr2: **c**; **l**
fu2m-tr2	*median mesofurco-mesotrochanteral*	10, 11, 111	median furcal depressor of the mesotrochanter	IIlm3a	–	fu2-tr2: **c; l**; 174(fu2-tr2): **f**
fu2-cx2	*mesofurco-mesocoxal*	10, 11, 46, 109, 110, 113	furcal remotor of the mesocoxa	IIlm4	83	15: **d**; 173(fu2-cx2p): **f**
s2-cx2	*mesosterno-mesocoxal*	10, 46, 104	sternal promotor of the mesocoxa	IIlm2	81	14: **d**; 169(fu2-cx2a): **f**
fu2-fu1d	*dorsal mesofurco-profurcal*	10–12, 46, 116	lateral mesofurcal retractor of the propectus	lis5	–	21: **j**; 124(fu2-fu1): **f**
fu2-fu1v	*ventral mesofurco-profurcal*	10–12, 46, 116, 117	median mesofurcal retractor of the propectus	lis4	52	2 2: **j** ; 1: **d**; 124(fu2-fu1): **f**
fu2-ph2	*mesofurco-mesolatero-phragmal*	10–12, 109–111, 115, 121	furcal retractor of the second phragma	IIdv2	78	11: **d**; 150a,b(fu2-pn2a,p): **f**
t2-t3	*mesoscutello-metanotal*	9, 81, 87, 89, 92, 120, 125	retractor of the mesoscutellum	IIis1	70	2: **i** ; 114(t2-t3): **f**
pl3-t3 (a, b)	*metapleuro-metanotal*	14c, 15a, 132, 144, 151, 152	pleural depressor of the metanotum	IIIpm4	97–99	10: **i**; pl3-t3: **h**
t3-tr3	*metanoto-metatrochanteral*	13, 15a, 67, 143, 145, 146, 151	metanotal depressor of the metatrochanter	–	–	t3-tr3: **b**; 20: **i**
pl3-ba3	*metapleuro-metabasalar*	14c, 15a, 67	metapleural muscle of the metabasalare	IIIpm1	101	13: **i**; pl3-ba3: **h**; pl3-ba3: **b**
pl3-3ax3	*metapleuro-third axillary sclerite of hind wing*	14c, 104, 143, 144, 151, 152	second flexor of the hind wing	IIIpm2b	100	12b: **i**; pl3-3ax3: **h**
pl3-sa3	*metapleuro-metasubalar*	14c, 147, 149, 150	metapleural muscle of the metasubalare	IIIpm3a& b	102	15: **i**; pl3-sa3: **h**; pl3-sa3a,b: **b**
cx3-sa3	*metacoxo-metasubalar*	13, 150, 152	subalar remotor of the metacoxa	IIIp m5	105	22: **i**; cx3-sa3: **b**
pl3-cx3m	*median metapleuro-metacoxal*	14c, 15a, b, 145–147, 149	sternal promotor of the metacoxa	IIIl m1	104	25: **i**
pl3-cx3l	*lateral metapleuro-metacoxal*	13, 14c, 15a, 67, 149, 152	pleural promotor of the metacoxa	IIIlm4	103	26: **i**; pl3-cx3: **h**
pl3-tr3	*metapleuro-metatrochanteral*	13, 15a	pleural depressor of the metatrochanter	IIIl m3	109	31?: **i**
fu3-tr3	*metafurco-metatrochanteral*	13, 15a, 67, 148, 149	furcal depressor of the metatrochanter	IIIl m3	109?	31: **i**
fu3-cx3(m,l)	*metafurco-metacoxal*	13, 15a, b, 67, 148, 151	remotor of the metacoxa	IIIlm2	106	30: **i**

..... continued on the next page

TABLE 2 (continued)

abbreviation	term	figs	function	Duncan 1939	Snodgrass 1942	Others
fu3-fu2	*metafurco-mesofurcal*	10, 15a	interfurcal muscle	IIis2	–	27: **i**; 181(fu3-fu2): **f**; fu3-fu2: **h**
fu3-S2 (m, l)	*metafurco-second abdominal sternal*	13, 14c, 104, 145–147, 151, 153–155	depressor of the metasoma	IIIis1, 2	118	35: **i**
ph3-ph2	*second phragmo-third phragmal*	13	indirect flight muscle of the metathorax	IIIdl	96	5: **i**; 112m(2ph-3ph): **f**; 2ph-3ph: **b**; 18: **d**
ph3-T2	*third phragmo-second abdominal tergal*	13, 14c, 67, 143, 145–147, 149, 151–155	propodeal elevator of the metasoma	Iadl1	120	32: **i**
T1-T2	*propodeo-second abdominal tergal*	13, 152–155	tergal torsion muscle of the metasoma	Iadl2	119	32a:**i**
T1-S2	*propodeo-second abdominal sternal*	13, 14c, 104, 145, 152–155	sternal torsion muscle of the metasoma	IIIis3	121	35: **i**
T1-T1sp	*propodeo-first metasomal spiracle*	13, 14c	muscle of the first metasomal spiracle	dspI	123	?

Results

Head

Skeletal structures. The **vertex** (**vrx**: Fig. 2) is the dorsal part of the head between the level of the dorsal margin of the **occipital carina** (**occ**: Figs 2, 30, 32, 33) and the level of the ventral margin of the **anterior ocellus** (**aoc**: Fig. 1b). The anterior ocellus and the **lateral ocelli** (**loc**: Fig. 1b, 156, 157) delimit the triangular **interocellar space** (**ics**: Fig. 1b) on the vertex. The **hyperoccipital carina** (**hyc**: Fig. 2) crosses the vertex and extends just posterior to the lateral ocellus in some Scelionidae. The **vertex patch*** (**vpt**: Fig. 1a) is on the vertex between the lateral ocellus and the inner margin of the eye.

The **frons** (**fro**: Fig. 1a) is the anterior surface of the head between the level of the ventral margin of the anterior ocellus and the dorsal margin of the **antennal foramen** (**anfo**: Figs 1a, b). The unpaired **preocellar pit** (**prp**: Figs 1a, 20) is just ventral of the anterior ocellus in some Telenominae and corresponds internally with a cup or bell-shaped apodeme. The **frontal ledge** (**fld**: Fig. 21) crosses the dorsal part of the frons in *Sparasion, Acanthoscelio, Breviscelio, Tyrannoscelio*, and *Encyrtoscelio*, separating a vertical and a horizontal area. The **orbital band** (**obb**: Fig. 22) is a vertically elongated reticulate area along the inner orbit of the eye in Telenominae. In Teleasinae, a coriaceous **frontal patch*** (**frp**: Figs 1a, 23) occurs near the inner orbit. The longitudinal **central keel** (**ctk**: Figs 1a, 23, 25) extends between the anterior ocellus and the **interantennal process** (**iap**: Figs 1a, 20, 21, 26) in some Scelionidae. The central keel bifurcates ventrally to surround the antennal foramen, thereby delimiting the usually setaceous **torular triangle*** (**trt**: Figs 1a, 23, 25) or extends to the interantennal process without bifurcating. The **antennal scrobe** (**asc**: Figs 1a, 23, 25) is a smooth area lateral of the central keel. In some Scelionidae the frons has a more or less well-developed **frontal depression** (**fdp**: Figs 22, 24). In *Baryconus* and some members of the *Psix*-group of genera of Telenominae the frontal depression is limited laterally by the **submedian carina** (**sbc**: Figs 1a, 24). The interantennal process is situated ventrally on the frons and laterally bears the antennal foramen in most Scelionidae, but is absent from *Nixonia*.

The **malar region** (**mlr**: Fig. 1a) is the ventrolateral part of the anterior surface of the head limited later-

ally by the lower orbit of the eye and the **malar sulcus** (**mas**: Figs 1a, 23, 25). The malar sulcus extends between the lower orbit and the base of the mandible. The **facial striae*** (**fas**: Figs 1a, 23, 25) radiate from the base of the **mandible** (**mdb**: Figs 1a, 21, 156, 157) onto the malar region. Some of the facial striae extend to the frons and vertex along the inner orbit. The **orbital carina** (**obc**: Figs 1a, 25), present in *Psix*, extends from the base of the mandible along the inner orbit.

The externally convex **clypeus** (**cly**: Figs 1a, 23, 25) is ventral to the interantennal process. The anterior margin of the **oral foramen** (**orf**: Figs 156, 157) lateral to the clypeus is impressed to the **pleurostomal condyle** (**pscy**: Figs 1b, 26, 28) and serves as the anterior mandibular articulation. It is usually polished and fused to the ventral surface of the anterior part of the **tentorium** (**tntr**: Figs 1b, 27, 29). The tentorium is vertically flattened anteriorly and corresponds externally to the **anterior tentorial pit** (**atp**: Fig. 28), which is lateral to the clypeus just dorsal to the impressed margin of the oral foramen in *Sparasion* and some Telenominae (Bin & Dessart 1983), but is absent from other Scelionidae.

Internally, the **epistomal ridge** (**epsr**: Figs 1b, 34) and the **ventral ridge of the clypeus*** (**vrcl**: Figs 1b, 34) extend from the pleurostomal condyle medially. The epistomal ridge bifurcates before reaching the antennal foramen, with a dorsal branch extending just medial to the antennal foramen and a ventral branch delimiting the clypeus internally. The two dorsal branches and the ventral branch delimit an internally concave area that corresponds externally with the interantennal process. The ventral ridge of the clypeus serves as the site of attachment of the **labrum** (**lbr**: Figs 1b, 26, 28). The weakly sclerotized labrum is usually concealed by the clypeus. The number of **labral setae** (**lbrs**: Figs 1a, 26) along the ventral margin of the labium varies in Scelionidae (e.g. 15-20 in *Scelio*, 4-6 in Teleasinae and *Gryonini*). The **pleurostomal ridge** (**plsr**: Figs 1b, 34) extends from the pleurostomal condyle along the lateral margin of the oral foramen to the **pleurostomal fossa** (**plsf**: Figs 2, 26, 28), which serves as the posterior mandibular articulation. The pleurostomal fossa is on the posterior margin of the oral foramen in most Scelionidae (Fig. 26). In *Sparasion*, the pleurostomal fossa is on the lateral margin of the oral foramen (Fig. 28). The **hypostoma** (**hy**: Figs 2, 31) is posterior to the pleurostomal fossa and is limited dorsally by the **hypostomal sulcus** (**hys**: Figs 2, 30, 31). The margin of the oral foramen is produced into a **hypostomal tooth*** (**hyst**: Figs 2, 26, 30, 32) at the junction of the hypostoma and the pleurostomal fossa. The inflected hypostoma serves as the site of articulation of the **maxilla** (**maxl**: Figs 2, 31). The stipes is the only part of the maxilla visible externally; the reduced cardo is hidden by the **postgenal bridge** (**pgb**: Figs 2, 30–32). The postgenal bridge is the median part of the **postgena** (**pg**: Fig. 2) between the **occipital foramen** (**ocf**: Fig. 2) and the hypostomal sulcus. The usually setaceous **median sulcus of the postgenal bridge*** (**mspb**: Figs 2, 31) is situated in the middle of the postgenal bridge in most Scelionidae. The **postgenal sulcus*** (**pos**: Figs 2, 30, 32) laterally delimits the postgenal bridge in some Scelionidae. The tentorium fuses posteriorly with the postgenal bridge lateral to the occipital foramen. A posteriorly widened **ventral lamella*** (**vla**: Figs 1b, 27, 29) arises ventrally from the median part of the tentorium. The **postgenal pit*** (**pgp**: Figs 2, 30, 32) corresponds with the ventralmost point of the posterior site of fusion of the ventral lamella. The **tentorial bridge** (**tbr**: Figs 2, 29) originates just medially of the posterior end of the tentorium and corresponds with the **posterior tentorial pit** (**ptp**: Figs 1b, 2, 30, 32).

The distance between the posterior tentorial and postgenal pits varies in Scelionidae. In most cases the postgenal pit is in or just ventral to the **fossa** (**fos**: Figs 2, 30), much closer to the occipital foramen than to the oral foramen (Fig. 30). In some species of *Gryon, Eremioscelio, Encyrtoscelio, Breviscelio, Dyscritobaeus*, and in some Teleasinae (Fig. 32), the postgenal pit is closer to the oral foramen than to the occipital foramen.

The **postocciput** (**pooc**: Fig. 2) surrounds the occipital foramen; the fossa is the circular depression surrounding the postocciput. The **occipital condyle** (**ocy**: Figs 2, 30) is located ventrolaterally on the postocciput and articulates with the **cervical prominence** (**cvpr**: Figs 6, 7, 16, 35) of the prothorax. The occipital carina is an inverted U-shaped carina that extends from the oral foramen dorsal to the occipital foramen and that delimits a ventral area on the posterior surface of the head (Fig. 2). The **occiput** (**ocp**: Fig. 2) is limited dorsally by the occipital carina and ventrally by the occipital foramen. The **gena** (**gen**: Figs 1a, 2) is the posterolateral area

of the head limited laterally by the outer orbit and the malar sulcus and medially by the occipital carina. Dorsally, the gena extends to the level of the dorsal margin of the occipital foramen. The **genal patch*** (**gnp**: Figs 2, 30) is a small area of fine sculpture on the dorsal part of the gena.

Muscles. The posterior cranio-mandibular muscle is the largest muscle in the head, having several muscle bands that insert on the **mandibular adductor muscle apodeme** (**maa**: Figs 2, 21). The ***posterior cranio-mandibular muscle*** is subdivided, the margin of the site of origin of the median band (***crpm-md***: Figs 2, 21, 29, 33) corresponds externally with the median part of the occipital carina, whereas the lateral part of occipital carina crosses the origins of the lateral bands (***crpl-md***: Figs 2, 21). The anterior extension of the lateral bands of the posterior cranio-mandibular muscle varies in Scelionidae. In some cases the site of origin of the muscle extends to the frons (*Scelio*, *Gryon*, *Trissolcus*) and to the interocellar space. The anterior margin of the site of origin of the median band of the posterior cranio-mandibular muscle corresponds externally with the hyperoccipital carina. In *Archaeoteleia*, the ***anterior cranio-mandibular muscle*** (***cra-md***: Figs 1a, 21, 34) originates exclusively from the internal surface of the gena, and the malar region serves as the site of origin of the ***cranio-antennal muscle*** (***cr-A1***: Figs 1a, 21, 34). The border between the sites of origin of the anterior cranio-mandibular muscle and the cranio-antennal muscle corresponds externally to the malar sulcus. In other Scelionidae the site of origin of the anterior cranio-mandibular muscle extends distinctly anteriorly of the malar sulcus. The dorsal extension of the site of origin of the anterior cranio-mandibular muscle and cranio-antennal muscle and the corresponding external structures vary in Scelionidae. In some Teleasinae and the *Psix* group of genera of Telenominae, the attachment sites of the muscles extend towards the midlevel of the eye and correspond with the dorsally extended facial striae along the inner orbit (Fig. 25). In the *Psix* group of genera the orbital carina corresponds to the border between the anterior cranio-mandibular muscle and cranio-antennal muscle. The site of origin of the anterior cranio-mandibular muscle corresponds with the orbital band in Telenominae and the frontal patch in Teleasinae. The anterior cranio-mandibular muscle extends to the top of the head and originates partly from the horizontal area of the frons delimited by the frontal ledge in *Sparasion* (Fig. 21). The ***cranio-pharyngeal plate muscle*** (***cr-phr***: Figs 1a, 34) originates from the frons above the antennal foramina. The size of the muscle varies and usually is enlarged in taxa having a well developed frontal depression. The ***tentorio-antennal muscle*** originates from the dorsal surface of the anterior broadened part of the tentorium, and the ***tentorio-labial*** and ***tentorio-stipital muscles*** from the ventral surface.

Pronotum

Skeletal structures. The pronotum is rigidly attached to the mesothorax. The posteroventral corners of the pronotum extend ventrally and fuse medially behind the procoxae to form a sclerotized ring encircling the propectus. The **anterior rim of the pronotum** (**arp**: Figs 16, 19, 48, 56) is the elevated area along the anterior margin of the pronotum, delimited posteriorly by the **pronotal cervical sulcus*** (**prcs**: Figs 3, 16, 19, 48, 56, 61, 105). In Teleasinae, the **anterior process of the pronotum*** (**apr**: Figs 35, 47) is a beaklike projection on the median broadened part of the anterior rim of the pronotum. The longitudinal **epomial carina** (**epc**: Figs 3, 16, 19, 48, 49, 51, 56, 61) extends from the anterior rim of the pronotum to the **pronotal suprahumeral sulcus*** (**pss**: Figs 3, 16, 19, 36, 48, 49, 56, 105) and is usually straight or slightly curved, but bends medially in *Nixonia* (Fig. 51). The epomial carina separates the concave and usually setaceous **cervical pronotal area*** (**cpa**: Figs 16, 19, 49, 56, 59, 61) and the usually bare **lateral pronotal area*** (**lpa**: Figs 16, 19, 49, 56, 59, 61). The pronotal suprahumeral sulcus extends along the dorsal margin of the pronotum and delimits the **dorsal pronotal area*** (**dpa**: Figs 3, 16, 19, 39, 48, 49, 56, 105), which is usually narrow and not visible dorsally. In some scelionids the dorsal pronotal area is enlarged, triangular, and visible dorsally (Figs 39, 56). In *Archaeoteleia*, a **dorsal incision of the pronotum*** (**dipr**: Figs 48–50) is on the posterior part of the dorsal margin of pronotum. The incision fits with the **anterior extension of the preaxilla*** (**epax**: Figs 48, 75). The **posterior pronotal inflection** (**ppi**: Figs 4, 48, 50, 52–55, 60, 62) extends along the posterior margin of the

pronotum delimiting a narrow posterior area of the pronotum. In *Sparasion,* the posterior area of the pronotum is enlarged, and the posterior pronotal inflection corresponds with the **posterior pronotal sulcus*** (**ppsu**: Figs 35, 56, 96). The posterior pronotal sulcus is usually absent from other Scelionidae, but is present dorsally in Teleasinae (Figs 35, 96).

The **mesothoracic spiracle** (**sp2**: Figs 4, 19, 48, 52, 60, 61) is near the posterior margin of the pronotum. The trachea of the mesothoracic spiracle extends through an opening between the dorsal part of the posterior pronotal inflection and the lateral wall of the pronotum (Figs 4, 50, 52). The posterior pronotal inflection merges dorsally with the **dorsal pronotal inflection** (**dpi**: Figs 4, 50, 52–54, 60) and forms the **posterodorsal edge of pronotum*** (**pdep**: Figs 4, 48, 52–54, 97, 105).

The **netrion** (**net**: Figs 3, 16, 19, 35, 36, 48, 49, 51, 96, 97, 105) is a posteroventral region of the pronotum that is differentiated in sculpture from the lateral pronotal area and is delimited anteriorly by the **netrion sulcus** (**nes**: Figs 3, 16, 49, 51). The netrion sulcus usually is distinct and usually extends to the posterolateral margin of the pronotum ventral to the mesothoracic spiracle; it corresponds internally to the **netrion apodeme** (**nea**: Figs 4, 50, 52, 53, 57, 58, 64, 65). The netrion apodeme originates anteriorly from the anterior margin of the **ventral bridge of the pronotum** (**vbp**: Figs 3, 16, 35, 49, 50, 56, 57, 59–61) and usually fuses with the posterior pronotal inflection below the mesothoracic spiracle. The ventral bridge of the pronotum extends between the ventral ends of the netrion on opposite sides of the pronotum.

Both the netrion apodeme and corresponding external structures vary in Scelionidae. In *Scelio* (Figs 57, 58), *Baryconus, Apegus,* and *Calliscelio* the netrion apodeme is well developed, whereas in *Nixonia* (Fig. 53), *Archaeoteleia* (Figs 50, 52), *Gryon*, *Idris,* Telenominae (Fig. 60), and Teleasinae (Figs 59, 65) the netrion apodeme is marked only by a shallow ridge or is reduced. The netrion apodeme and the netrion sulcus is absent from *Sparasion* (Figs 54, 55, 62). In *Nixonia* (Fig. 53), the netrion apodeme extends parallel to the posterior pronotal inflection and the trachea extends between the netrion apodeme and the posterior pronotal inflection. The **occlusor muscle apodeme** (**oma**: Figs 50, 52, 58, 59) is located anterior to the netrion apodeme. The occlusor muscle apodeme is present in *Archaeoteleia* (Figs 50, 52), Teleasinae (Fig. 59), *Calliscelio, Scelio* (Fig. 58), *Gryon, Probaryconus* and *Idris*, but absent from *Nixonia*, *Sparasion* (Figs 53–55), *Trissolcus, Telenomus* (Fig. 60), *Baryconus* and *Apegus.*

Muscles. In many Scelionidae, the ***pronoto-first thoracic spiracle muscle*** (***t1-sp2***: Figs 3, 4, 55, 58) originates from the occlusor muscle apodeme. If the apodeme is absent, then the muscle originates partly from the anterior surface of the netrion apodeme and partly from the lateral wall of the pronotum anterior to the netrion apodeme or the posterior pronotal inflection (Fig. 55) in most Scelionidae. In *Nixonia,* the muscle originates posterior to the netrion apodeme.

The dorsal pronotal area serves as the site of origin of the ***pronoto-procoxal*** (***t1-cx1***: Figs 3, 4, 57, 63, 65, 98, 116), ***pronoto-postoccipital*** (***t1-poc***: Figs 3, 4, 42, 55, 98, 116), ***pronoto-laterocervical*** (***t1-cv***: Figs 3, 4, 42, 57, 116), and the ***pronoto-propleural*** (***t1-pl1***: Figs 3, 4, 6, 42, 55, 57, 116) muscles. The pronoto-procoxal muscle originates from the lateral most part of the dorsal pronotal area and extends to the procoxa. The pronoto-postoccipital muscle originates anterior to the site of origin of the pronoto-procoxal muscle and dorsal of the site of origin of the pronoto-laterocervical muscle. The pronoto-propleural muscle originates anterior of the site of origin of the pronoto-laterocervical muscle and extends lateral to the pronoto-postoccipital muscle and medial of the pronoto-laterocervical muscle.

Propleuron, prosternum and profurca

Skeletal structures. The propleuron and prosternum are connected to the pronotum and mesopectus (mesopleuron + mesosternum) by extensive membranous areas, which provide for a high degree of mobility. The site of fusion of the cervical prominence corresponds with the **propleural cervical sulcus*** (**pcs**: Figs 5, 16, 19, 35, 36), which extends along the anterodorsal margin of the ventral propleural area. The cervical

prominence articulates with the occipital condyle. The **cervical apodeme** (**crva**: Figs 6, 7, 42, 44, 46) is the posterior extension of the cervical prominence and is fused with the dorsal part of the propleuron.

The **longitudinal carina of the propleuron*** (**lcp**: Figs 5, 36) separates the **ventral*** and the **lateral propleural areas*** (**vpa**, **lpal**: Figs 5, 7, 8, 36). The weakly sclerotized **dorsal propleural area*** (**dpl**: Figs 5, 7, 40) is posterodorsal of the well-sclerotized lateral propleural area and usually differs from it in sculpture. The **dorsal incision of the propleuron*** (**dip**: Fig. 6) is on the dorsal margin, whereas the reduced **propleural arm** (**ppa**: Figs 5, 40, 41) is on the posteroventral corner of the dorsal propleural area. The dorsal propleural area is usually smooth externally, which may allow for free movement between it and the pronotum. The **propleural epicoxal sulcus*** (**pes**: Figs 5, 16, 19, 35) sets off the **epicoxal lobe*** (**epl**: Figs 5, 16, 19, 35) from the ventral part of the ventral propleural area. The **lateral articular process** (**lapr**: Figs 7, 8, 37) for the procoxa lies anterolaterally on the ventral margin of the propleuron. The **ventral edge of the propleuron*** (**vgp**: Figs 7, 8, 35, 37) sets off the **ventral vertical lobe of the propleuron*** (**vvl**: Figs 7, 8, 37, 38, 41, 45), which is inflected 90° relative the ventral propleural area.

The prosternum is divided into two parts: the well sclerotized, externally visible **basisternum** (**bstr**: Figs 6–8, 37, 38, 41, 45) and the weakly sclerotized **furcasternum** (**fust**: Figs 6–8, 37, 41, 45), which is concealed by the ventral bridge of the pronotum. The basisternum and furcasternum are almost entirely separated by the deep, transverse **prosternal incisions*** (**psin**: Figs 7, 8, 37, 38, 41, 45), only being continuous for a short distance medially. The **lateral basisternal projection*** (**lbp**: Figs 6–8, 37, 38, 41, 45) extends anterolaterally and forms the **median articular process** for the procoxa. The **anterior process of the prosternum** (**app**: Figs 7, 8, 35, 37, 45) fits into the incision between the ventral vertical lobes. The **profurcal arms** (**fu1a**: Figs 5, 7, 8, 40, 41, 45) originate medially from the furcasternum and correspond to the externally separated **profurcal pits** (**fu1p**: Figs 8, 37, 38, 41, 45). The profurcal arm articulates laterally with the propleural arm.

The **dorsal profurcal lamella** (**dprl**: Figs 5, 7, 8, 37, 41, 45) extends along the dorsal surface of the profurcal arm. The **longitudinal line of the dorsal profurcal lamella*** (**ldl**: Figs 5, 7, 8, 45) divides the dorsal profurcal lamella into a median and a lateral area. The triangular **anterior profurcal lamella*** (**aprl**: Figs 5, 7, 8, 39, 40, 44) extends anteriorly along the longitudinal line of the dorsal profurcal lamella, whereas the longitudinal **posterior profurcal lamella** (**pprl**: Figs 5, 8, 40, 44, 45) extends along the posterior margin of the dorsal profurcal lamella. The **ventral profurcal lamella*** (**vpl**: Figs 5, 7, 8, 40, 41, 45) extends along the anteroventral surface of the profurcal arm.

Muscles. The pronoto-propleural muscle inserts on the dorsal incision of the propleuron. The ***pronoto-profurcal muscle*** (***t1-fu1***: Figs 3, 4, 8, 39, 57, 116) originates from the lateral pronotal area and inserts on the lateral part of the dorsal margin of the dorsal profurcal lamella. The ***propleuro-postoccipital muscle*** originates from the propleuron and has two bands. The ***median band*** (***pl1m-poc***: Figs 5, 6, 42, 43, 46) originates from the propleural epicoxal sulcus. The ***lateral band*** (***pl1l-poc***: Figs 5, 42) originates from the anterior part of the lateral propleural area. The tendon of the propleuro-postoccipital muscle extends lateral to the cervical prominence. The ***propleuro-procoxal muscle*** (***pl1-cx1***: Figs 5, 43) originates anteriorly on the lateral propleural area, posterodorsal of the origin of the lateral band of the propleuro-postoccipital muscle. The ***propleuro-protrochanteral muscle*** (***pl1-tr1***: Figs 5, 42, 43) originates from the dorsal propleural area. The ***profurco-laterocervical muscle*** (***fu1-cv***: Figs 6, 7, 39, 44) originates from a tendon arising from the anterior edge of the anterior profurcal lamella and inserts on the cervical apodeme. The rodlike ***laterocervico-procoxal muscle*** (***cv-cx1***: Fig. 7) originates from the cervical apodeme and inserts on the coxa on the opposite side from which it arises. The ***dorsal profurco-postoccipital muscle*** (***fu1d-poc***: Figs 6, 7, 39, 44, 46) originates from the dorsal part of the lateral area of the dorsal profurcal lamella. The ***ventral profurco-postoccipital muscle*** (***fu1v-poc***: Figs 6, 7, 44, 46) originates partly from the anterior surface of the dorsal profurcal lamella ventral to the site of origin of the dorsal profurco-postoccipital muscle and partly from the median area of the dorsal profurcal lamella. The anterior profurcal lamella separates the dorsal and ventral profurco-postoccipital muscles. The

lateral profurco-procoxal muscle (***fu1-cx1l***: Figs 7, 37, 46, 57) originates partly from the posterior surface of the dorsal profurcal lamella and partly from the ventral surface of the posterior profurcal lamella. The ***medial profurco-procoxal muscle*** (***fu1-cx1m***: Figs 7, 46) originates partly from the posteroventral surface of the ventral profurcal lamella and partly from the ventral surface of the profurcal arm laterally. The ***prosterno-procoxal muscle*** (***s1-cx1***: Fig. 8) originates partly from the prodiscrimenal lamella.

Mesoscutum

Skeletal structures. The vertical, weakly sclerotized **first phragma** (**ph1**: Figs 9, 66, 68–72, 78, 122) extends along the anteroventral margin of the mesoscutum between the **preaxillae** (**pax**: Figs 9, 17, 18, 19, 72, 74–79). It is entirely hidden by the pronotum and is continuous anterodorsally with the well sclerotized **vertical lobe of the mesoscutum*** (**vrtm**: Figs 9, 69, 70, 72). The first phragma is well developed and partly divided ventrally by an incision in *Nixonia* and *Sparasion* (Fig. 68), but is reduced and undivided (Figs 66, 69) in other Scelionidae. The **ventral apodeme of the first phragma*** (**aph1**: Figs 9, 66, 71, 73) is lateral on the ventral margin of the first phragma. In *Calliscelio*, *Calotelea* and *Anteromorpha* the apodeme is well developed, and its ventral end curves posteriorly (Figs 72, 73). In Teleasinae, Gryonini, *Idris*, *Probaryconus* and Telenominae the apodeme is cup-shaped and on the posterior part of the first phragma (Fig. 71). In *Apegus*, *Baryconus*, and *Scelio* the cup-shaped apodeme is just anterior to the posterior end of the first phragma (Fig. 66). The apodeme is absent from *Nixonia* and *Sparasion*.

The **lateral margin of mesoscutum*** (**lmms**: Figs 9, 17) fits into the dorsal pronotal inflection. The **mesoscutal suprahumeral sulcus** (**shms**: Figs 9, 16, 17, 19, 72, 75, 83, 84) corresponds externally to the first phragma and the vertical lobe of the mesoscutum. The **mesoscutal humeral sulcus** (**mshs**: Figs 9, 17–19, 72, 75, 83, 84) extends between the posterior end of the mesoscutal suprahumeral sulcus and the posterolateral edge of the mesoscutum.

The **antero-admedian line** (**aal**: Figs 16, 17, 69, 75, 80) originates from the anterior margin of the mesoscutum. The transverse **skaphion carina*** (**skpc**: Figs 9, 16, 17, 80, 81) delimits the **skaphion** (**sk**: Figs 9, 16, 17, 19, 80, 81) anteriorly on the mesoscutum in some Scelionidae.

The vertical preaxilla is separated from the horizontal part of the mesoscutum by the **parascutal carina** (**psc**: Figs 9, 17, 18, 72, 74–79). The **anterior notal wing process** (**anwp**: Figs 9, 17, 18, 75, 77, 79) is on the ventrolateral part of the preaxilla. The anterior part of the first axillary sclerite articulates with the anterior notal wing process. The preaxilla extends anteriorly to form the anterior extension of the preaxilla in *Archaeoteleia* (Figs 48, 75). The anterior extension of the preaxilla fits into the dorsal incision of the pronotum. The preaxilla extends posteriorly to form the **posterior extension of the preaxilla*** (**pep**: Figs 9, 17, 85, 123). The oblique **preaxillar carina*** (**pxc**: Figs 9, 17, 18, 76, 78, 79) extends across the preaxilla and separates the articulation for the **tegula** (**tga**: Figs 16, 19, 74, 76, 97;) from the anterior notal wing process. The anterior margin of the tegula fits to the posterodorsal edge of the pronotum.

The longitudinal **median mesoscutal line** (**mml**: Figs 17, 18, 82, 83) extends medially for most of the mesoscutum in some Scelionidae, terminating posteriorly in the transscutal articulation. Although the line is well developed in some genera, it never corresponds with an internal carina. The **notaulus** (**not**: Figs 9, 17–19, 75, 80, 82, 83, 84; Gibson 1985) is a submedial longitudinal furrow extending anteriorly from the posterior edge of the mesoscutum. The notaulus may be abbreviated anteriorly. Lateral to the notaulus is the usually indistinct **parapsidal line** (**prsl**: Figs 9, 17, 18, 75, 77, 82, 84). The presence of notauli varies in Scelionidae and in some Teleasinae only males have notauli. Each notaulus usually is marked by a foveolate or simple sulcus (Figs 75, 82), but in some *Sparasion* species it is marked by a row of foveae (Fig. 84) and in a few taxa it is expressed as a distinct ridge (Fig. 83).

Muscles. The first phragma serves as the anterior attachment site for the ***first phragmo-second phragmal muscle*** (***ph1-ph2***: Figs 46, 70, 81, 98, 122). The anterior site of attachment of the muscle extends from the phragma onto the mesonotum and corresponds with the antero-admedian line. The skaphion carina posteriorly

crosses the anterior attachment site of the first phragmo-second phragmal muscle. The ***first phragmo-propleural muscle*** (***ph1(t1)-pl1***: Figs 9, 66) and ***first phragmo-postoccipital muscle*** (***ph1(t1)-poc***: Figs 9, 66) originate from the anterior surface of the first phragma. The ***pronoto-first phragmal muscle*** (***t1-ph1***: Figs 7, 8, 55, 58, 63, 98, 116) originates from the lateral pronotal area and inserts on the anterior surface of the first phragma.

The median mesoscutal line extends along the border between the two bands of the first phragmo-second phragmal muscles. The notauli mark the border between the attachment sites of the first phragmo-second phragmal and ***first mesopleuro-mesonotal muscle*** (***pl2-t2a***: Figs 70, 98). The posterior part of the site of origin of the first mesopleuro-mesonotal muscle corresponds to the parapsidal line.

Scutellar-axillar complex

Skeletal structures. The mesoscutum is separated from the scutellar-axillar complex by the **transscutal articulation** (**tsa**: Figs 9, 17–19, 72, 74, 75, 78, 83, 84, 86, 90). The usually foveolate **scutoscutellar sulcus** (**sss**: Figs 9, 17–19, 72, 74, 75, 78, 83, 84, 86, 90, 95) separates the lateral axilla (Gibson 1985) from the **mesoscutellum** (**scu**: Figs 9, 17–19, 75, 83–88, 90) and usually merges dorsomedially with the transscutal articulation. The scutoscutellar sulcus corresponds internally to the **scutoscutellar ridge** (**ssr**: Figs 85, 87, 89, 91, 92). The oblique **scutellar bridge*** (**scbr**: Figs 87, 89) originates from the scutoscutellar ridge in Telenominae and Teleasinae and fuses with the posterior part of the mesoscutellum. The scutellar bridge is absent from other Scelionidae. The lateral part of the scutoscutellar sulcus bends anteriorly and extends to the ventral end of the **axillar carina** (**axc**: Figs 9, 17, 18, 76, 77, 79, 88, 90, 91, 93, 95, 96). The axillar carina separates the **dorsal axillar area** (**daa**: Figs 9, 17–19, 76, 77, 79, 88, 90, 93, 95, 96) from the **lateral axillar area** (**laa**: Figs 9, 17, 19, 76, 77, 79, 88, 90, 93, 95, 96). The posterior extension of the preaxilla abuts the anterior part of the **anterior extension of the lateral axillar area*** (**lapa**: Figs 9, 67, 79, 85, 87, 89, 90, 91–93, 123). The **posterior notal wing process** (**pnwp**: Figs 9, 17, 77, 90, 91, 93) is on the posterior part of the anterior extension of lateral axillar area just behind the posterior extension of the preaxilla. The **transaxillar carina*** (**tac**: Figs 9, 17–19, 75, 77–79, 88, 95, 96) divides the dorsal axillar area into horizontal and vertical areas. The **axillula** (**axu**: Figs 9, 17–19, 74, 79) is a lateral, vertical area of the mesoscutellum delimited by the **axillular carina** (**auc**: Figs 9, 17–19, 78, 86, 93, 95, 96). In some Scelionidae the axillular carina fuses with the transaxillar carina and forms a longitudinal carina, which delimits the anterolateral, vertical area of scutellar axillar complex (Figs 95, 96). *Archaeoteleia* lacks an axillular carina (Fig.74) and in *Nixonia* (Fig. 93) it is a weak, reduced carina that arises from the posterolateral margin of the mesoscutellum. In *Archaeoteleia*, *Gryonoides*, and *Neoscelio* the **lateral mesoscutellar spine*** (**lmsp**: Figs 74, 75, 94, 95) arises laterally from the posterodorsal margin of the axillula. The **postalar process** (**pap**: Figs 9, 17–19, 75, 77, 78, 84, 86–92, 123, 124) arises from the ventral margin of the axilla anteriorly and from the ventral margin of the mesoscutellum posteriorly. In *Xenomerus* and some *Trimorus* the median mesoscutellar spine is located on the posterodorsal part of the mesoscutellum. The **posterior mesoscutellar sulcus*** (**psu**: Figs 9, 17–19, 84, 86, 88, 90) corresponds internally to the **vertical apodemal lobe of the mesoscutellum*** (**valm**: Figs 9, 85, 87, 92, 93, 120).

Muscles. For the descriptions of muscles attaching to the scutellar axillar complex (*pl2-t2b* and *t2-t3*) see the descriptions of musculature of the mesopectus and metanotum.

Mesopectus

Skeletal structures. The **mesobasalare** (**ba2**: Figs 10, 12, 76, 101) fits into the **anterodorsal incision of the mesopleuron*** (**adi**: Figs 76, 100).

The oblique **acropleural sulcus** (**asu**: Figs 19, 76, 94, 96, 97, 100, 105, 107) is on the anterodorsal part of mesopleuron and corresponds internally to the **acropleural apodeme* (acra: Figs 12, 71, 101, 106)** in most Scelionidae. The acropleural apodeme is absent from *Sparasion* and *Nixonia*. The oblique, externally concave

femoral depression (**fed**: Figs 19, 74, 94, 96, 97, 99, 100, 105, 107) extends between the speculum (see below) and the posteroventral edge of the mesopleuron. The **pleural pit** (**pp**: Figs 19, 94, 96, 97, 100, 107) on the anterodorsal part of the femoral depression corresponds internally with the **pleural apodeme*** (**pa**: Figs 10, 12, 64, 65, 67, 101–104, 106, 118). The pleural apodeme is absent from *Nixonia*, and is reduced in *Archaeoteleia* and *Sparasion*. The femoral depression is usually limited anteroventrally by the **mesopleural carina** (**mc**: Figs 19, 36, 94, 96, 97, 99). In some Scelionidae a ventral and a dorsal foveolate sulcus extend alongside the mesopleural carina.

The **acetabulum** (**act**: Figs 10, 11, 16, 35) on the anteroventral part of the mesopleuron accommodates the procoxa. The **acetabular carina** (**ac**: Figs 10–12, 16, 35, 74, 94, 96, 99, 100, 134) delimits the acetabulum posteriorly. The **postacetabular sulcus*** (**ats**: Figs 16, 19, 35, 94, 96, 99, 100, 134) extends posteriorly along the acetabular carina. The coriaceous **postacetabular patch*** (**papc**: Figs 19, 35, 96, 100, 134) is on the lateroventral, convex part of the mesopleuron posterior to the postacetabular sulcus in most Scelionidae. The **sternaulus** (**str**: Figs 16, 19, 96, 134) is an anteriorly curved sulcus extending between the dorsal part of the mesopleural carina and the dorsal end of the postacetabular sulcus. In some cases the sternaulus is well developed and distinctly separated from the foveolate sulcus extending ventrally to the mesopleural carina (Fig. 96), but usually is less distinct and obscured by other mesopleural structures or by the overall sculpture of the mesopleuron (Figs 36, 94, 97).

The **mesocoxal depression*** (**mcp**: Figs 10, 99, 134) is the ventral depressed area of the mesothorax that abuts the base of the mesocoxa, in the bottom of which is the mesocoxal cavity. The transverse **ventral mesopleural carina*** (**vplc**: Figs 10, 12, 16, 19, 96, 99, 100, 134) surrounds the mesocoxal depression. The **mesopleural epicoxal sulcus*** (**mes**: Figs 16, 19, 96, 99, 100, 134) extends dorsally along the ventral mesopleural carina.

The **posterior mesepimeral inflection** (**mepi**: Figs 11, 12, 106, 108–110, 112–115) extends along the posterior margin of the mesopleuron, curving anteriorly and widened on the dorsal margin of the mesopleuron where it fuses with the impressed dorsal margin of the mesopleuron to form the **posterodorsal edge of the mesopleuron*** (**pdem**: Figs 10–12, 101, 103, 106, 108–110, 113, 115). The postalar process of the scutellar-axillar complex fits into the impression on the dorsal margin of the mesopleuron. The posterodorsal edge of the mesopleuron extends to the **subalar pit** (**sapi**: Figs 10, 11, 19, 36, 74, 76, 94, 96, 100, 105) and is connected with the mesosubalare. The **mesepimeral ridge** (**meer**: Figs 10–12, 106, 108–115) arises from the mesopleurocoxal condyle and extends along the posterior margin of the mesopleuron anterior to the posterior mesepimeral inflection. Most Scelionidae have a mesepimeral ridge, but it is reduced in *Apegus* and *Baryconus* and absent from *Scelio*. The mesepimeral ridge and the externally corresponding **mesepimeral sulcus*** (**mees**: Figs 19, 36, 74, 94, 96, 97, 100, 105, 107, 136) delimit the narrow **posterior mesepimeral area*** (**pmma**: Figs 19, 36, 74, 96, 97, 100). Dorsally, the mesepimeral ridge bends anteriorly and fuses with the posterodorsal edge of mesopleuron. The **dorsal mesopleural inflection** (**dmi**: Figs 10, 94, 103, 108) is anterior to the subalar pit and accommodates the second axillary sclerite (Snodgrass 1942). The **speculum** (**spec**: Figs 19, 36, 74, 94, 96, 97, 100, 105) is the area of the mesopleuron just ventral of the posterodorsal edge of mesopleuron; internally, it corresponds to a concavity. The speculum is limited posteriorly by the mesepimeral ridge and ventrally by the femoral depression. The internal **anterior margin of the speculum*** (**amsp**: Figs 10, 12, 101, 103, 104, 106, 112) limits the speculum anteriorly. It is a distinct, vertical apodeme that dorsally is fused with the posterodorsal edge of the mesopleuron and externally corresponds to the **prespecular sulcus*** (**pssu**: Figs 19, 74, 94, 96, 97, 105). The anterior margin of speculum usually diminishes dorsal to the pleural apodeme. In *Telenomus* and *Trissolcus* the pleural apodeme fuses with the anterior margin of the speculum, forming an oblique, concave apodeme. In *Psix* and *Paratelenomus* the anterior margin of the speculum is not fused with the pleural apodeme, but extends ventrally to the mesocoxal articulation (Figs 103, 104) and corresponds externally to the **transpleural sulcus** (**tps**: Figs 19, 105).

A median longitudinal line along the venter of the mesopectus, the **mesodiscrimen** (**dscr2**: Fig. 134), internally corresponds to the **mesodiscrimenal lamella** (**dscl2**: Figs 12, 104), which extends between the acetabulum and the **mesofurca** (**fu2**: Figs 11, 12, 46, 108–110, 113). The site of origin of the mesofurca corresponds with the **mesofurcal pit** (**fu2p**: Figs 12, 99, 134), which is situated between the mesocoxal depressions. The mesofurca is Y-shaped, with the **lateral mesofurcal arms** (**lmfa**: Figs 10–12, 108–110, 113, 115) connected by the **mesofurcal bridge** (**frb**: Figs 10, 11, 108–110, 113, 116, 117). The **anterior process of the mesofurcal bridge** (**apfb**: Figs 10, 117) is present in *Calliscelio* and *Archaeoteleia*, but not in other Scelionidae. The lateral mesofurcal arm is flattened laterally and extends to the speculum to form the **anterior extension of the mesofurca*** (**anem**: Figs 10, 12, 108, 112–115). The lateralmost part of the lateral mesofurcal arm is twisted posterodorsally.

Muscles. The ventral, convex area of the mesopectus is the ventral site of attachment of the first mesopleuro-mesonotal muscle. The ***third mesopleuro-mesonotal muscle*** (***pl2-t2c***: Figs 9, 12, 66, 70–72) originates from the ventral apodeme of the first phragma and inserts on the acropleural apodeme of the mesopleuron. The size of the muscle varies depending on how anteriorly the ventral apodeme is located on the first phragma.

The ***pronoto-third axillary sclerite of the fore wing muscle*** (***t1-3ax2***: Figs 7, 8, 10, 57, 58, 62–65) originates from the netrion in most Scelionidae. The site of origin of the muscle is usually limited anteriorly by the netrion apodeme. In *Sparasion*, the muscle originates from the posterior area of the pronotum that is delimited by the posterior pronotal inflection. The muscle inserts on the 3rd axillary sclerite of the fore wing, sharing a common tendon with the ***anterior mesopleuro-third axillary sclerite of the fore wing muscle*** (***pl2-3ax2a***: Figs 10, 12, 62, 63, 65, 72, 103, 104, 112). The ***posterior mesopleuro-third axillary sclerite of the fore wing muscle*** (***pl2-3ax2p***: Figs 10, 12, 62–65, 67, 72, 103, 104, 112, 118) originates dorsal to the site of origin of the ***mesopleuro-mesobasalare muscle*** (***pl2-ba2***: Figs 10, 12, 67, 103, 104, 118). The anterior mesopleuro-third axillary sclerite of the fore wing muscle originates dorsal to the origin of the posterior mesopleuro-third axillary sclerite of the fore wing muscle.

The number and the sites of origin of muscles inserting on the mesobasalare vary in Scelionidae. All Scelionidae have an ***intersegmental membrane-mesobasalare muscle*** (***ism1,2-ba2***: Figs 10, 12, 64, 67, 103, 118). In *Scelio, Telenomus, Trissolcus, Gryon,* Teleasinae, *Calliscelio* and *Probaryconus* the mesopleuro-mesobasalare muscle originates just anteroventral of the origin of the mesopleuro-third axillary sclerite of the fore wing muscles and corresponds externally to the sternaulus. *Archaeoteleia* and *Idris* lack the mesopleuro-mesobasalare. In these two genera the ***pronoto-mesobasalare muscle*** (***t1-ba2***: Fig. 7) originates from the ventral bridge of the pronotum medial to the site of origin of the pronoto-third axillary sclerite of the fore wing muscle.

The ***mesopleuro-third axillary sclerite of the hind wing muscle*** (***pl2-3ax3***: Figs 11, 104, 109, 110, 113–116) originates at least partly from the mesopectus. In most Scelionidae, it originates from the posterior surface of the mesepimeral ridge, but in *Scelio, Apegus,* and *Baryconus* where the mesepimeral ridge is absent or reduced, the muscle originates from the mesopectus posteroventral to the site of origin of the mesopleuro-mesofurcal muscle (Figs 67, 109, 115). In *Sparasion, Nixonia,* and *Scelio* the site of origin of the muscle is shared between the meso- and metapleuron..

In most Scelionidae the ***second mesopleuro-mesonotal muscle*** (***pl2-t2b***: Figs 9, 10, 12, 62–65, 67, 102, 118, 119) is rod-like, originating from the dorsal surface of the pleural apodeme and inserting on the ventral surface of the lateral axillar area. In *Archaeoteleia, Nixonia,* and *Sparasion*, where the pleural apodeme is absent, the muscle is fan-shaped and originates from the dorsal part of femoral depression. The ***mesopleuro-mesocoxal muscle*** (***pl2-cx2***: Figs 10, 12, 62–65, 67, 102–104, 112, 118) originates from the dorsal part of the femoral depression just ventral to the site of origin of the second mesopleuro-mesonotal muscle, at least partly from the ventral surface of the pleural apodeme if present. In *Telenomus* and *Trissolcus* the second mesopleuro-mesonotal muscle originates from the dorsal surface of the fused pleural pit apodeme and the

anterior margin of the speculum, and the mesopleuro-mesocoxal muscle originates from the ventral part of this structure (Fig. 102).

The ***mesocoxo-mesosubalare muscle*** (***cx2-sa2***: Figs 11, 64, 67, 109–111, 113), originates from the mesocoxa and extends posterior to the mesopleuro-mesofurcal muscle to the subalare. The ***mesosterno-procoxal muscle*** (***s2-cx1***: Fig. 10) originates from the anterior part of the mesodiscrimenal lamella.

The ***mesopleuro-mesofurcal muscle*** (***pl2-fu2***: Figs 10, 12, 108, 111, 112, 114) originates from the anterior surface of the mesepimeral ridge and inserts on the external surface of the flattened, membranous anterior extension of the mesofurca. The site of origin extends anterior of the mesepimeral ridge dorsally and covers the internal surface of the speculum. The ***lateral mesofurco-mesotrochanteral muscle*** (***fu2l-tr2***: Figs 10–12, 67, 109, 111, 112, 114, 115, 118, 119) originates from the internal part of the mesofurca. In *Nixonia*, *Sparasion*, *Gryon*, *Idris*, and *Archaeoteleia* ***the median mesofurco-mesotrochanteral muscle*** (***fu2m-tr2***: Figs 10, 11, 111) originates from the ventral surface of the lateral mesofurcal arm medial to the site of origin of the lateral mesofurco-mesotrochanteral muscle. The ***mesofurco-mesocoxal muscle*** (***fu2-cx2***: Figs 10, 11, 46, 109, 110, 113) originates partly from the lateral mesofurcal arms and partly from the base of the mesofurca. The ***mesosterno-mesocoxal muscle*** (***s2-cx2***: Figs 10, 46, 104) originates partly from the base of the mesofurca and partly from the posterior part of the mesodiscrimenal lamella. The slender, rodlike ***dorsal mesofurco-profurcal muscle*** (***fu2-fu1d***: Figs 10–12, 46, 116) originates from the lateral part of the lateral mesofurcal arm and inserts on the posterior surface of the posterior profurcal lamella. The fan-shaped ***ventral mesofurco-profurcal muscle*** (***fu2-fu1v***: Figs 10–12, 46, 116, 117) originates from the mesofurcal bridge and inserts on the base of the profurca. In *Calliscelio* and *Archaeoteleia* the muscle originates partly from the anterior process of the mesofurcal bridge.

Mesopostnotum and the second phragma

Skeletal structures. The mesopostnotum is concealed by the mesonotum and the metanotum. The sclerotized, transverse, **ventral mesopostnotal flange** (**vpnr**: Fig. 125) and **dorsal mesopostnotal flange** (**dpnr**: Fig. 125) extend across the mesopostnotum and unite laterally where they are continuous with the anteriorly oriented, well-sclerotized **mesolaterophragma** (**lph2**: Figs 118–120, 122). The mesopostnotum is connected to the mesoscutum via the dorsal mesopostnotal flange and to the metanotum via the ventral mesopostnotal flange, and is weakly sclerotized between the two flanges. The **dorsal mesopostnotal incision*** (**dmpi**: Figs 120, 125) is situated medially on the dorsal margin of the mesopostnotum. The laterophragma is connected anteriorly with the mesosubalare and laterally with the **humeral sclerite of the metanotum** (**hmsc**: Figs 15a, 89, 121, 123–125, 142, 144). The **axillary lever** (**pnap**: Figs 87, 89, 118, 119, 120–123, 125) is located medial to the humeral sclerite. The **second phragma** (**ph2**: Figs 78, 87, 89, 120–122, 125, 142) arises ventrally from the mesopostnotum. The pseudophragma (Ronquist & Nordlander 1989) is absent from all Scelionidae.

Muscles. The ***mesofurco-mesolaterophragmal muscle*** (***fu2-ph2***: Figs 10–12, 109–111, 115, 121) originates from the dorsal surface of the lateral mesofurcal arm just lateral to the origin of the dorsal mesofurco-profurcal muscle and inserts on the mesopostnotal apodeme. The first phragmo-second phragmal muscle is attached to the anterior surface of the second phragma.

Metanotum

Skeletal structures. The **transmetanotal carina** (**tmc**: Figs 17–19, 86, 88, 97, 98, 126, 130, 131, 136, 137) delimits the smooth, concave **supraalar area** (**saa**: Figs 18, 19, 130, 131) anterolaterally on the metanotum. The humeral sclerite is the separated anterior part of the metanotum. The anterior notal wing process is on the humeral sclerite of the metanotum and the posterior notal wing process is on the anterior part of the supraalar area. The usually foveolate transverse **metanotal trough** (**mnt**: Figs 17, 18, 98, 105, 130, 131, 136, 137) medially and anteriorly delimits the elevated **metascutellum** (**msct**: Figs 17–19, 98, 105, 131, 133, 137).

Laterally, the trough curves posteriorly to extend along the posterior margin of the metanotum. The metascutellum may be limited laterally by the **metascutellar carina*** (**mtsr**: Figs 17, 86, 88, 98, 131, 133). The metascutellum is often furnished with one or more **metanotal spines*** (**mnsp**: Figs 17, 18, 88, 97, 98). These usually originate from the middle of the metascutellum or from the metascutellar carina.

Internally, the metanotal trough corresponds to the **internal metanotal ridge*** (**mtnr**: Figs 126, 127, 132, 142, 144). The metanotal ridge bifurcates medially to surround the internal **chamber of the metanotum*** (**chm**: Figs 126, 144, 151), which corresponds to the metascutellum. The **muscle-bearing process of the metanotum** (**mbpm**: Figs 124, 126, 132, 142, 144, 151) is located ventrally on the anterior part of the metanotum.

Muscles. The ***mesoscutello-metanotal muscle*** (***t2-t3***: Figs 9, 81, 87, 89, 92, 120, 125) originates posteriorly from the scutoscutellar ridge and inserts on the dorsal margin of the metanotum above the chamber of the metanotum. The muscle extends dorsally of the dorsal mesopostnotal incision The ***metapleuro-metanotal muscle*** (***pl3-t3***: Figs 14c, 15, 132, 144, 151, 152) is subdivided into two bands, originates from the dorsal surface of the metapleural ridge and inserts on the muscle-bearing process of the metanotum. The ***metanoto-metatrochanteral muscle*** (***t3-tr3***: Figs 13, 15, 67, 143, 145, 146, 151) originates from the humeral sclerite of the metanotum and inserts on the metatrochanteral apodeme sharing a common tendon with the metapleuro-metatrochanteral and metafurco-metatrochanteral muscles.

Metapectal-propodeal complex

Skeletal structures. The metapectus is delimited dorsally from the propodeum by the **metapleural carina** (**mtpc**: Figs 18, 19, 129, 131, 133–140), which extends from just ventral of the **metapleural arm** (**mtam**: Figs 13, 18, 19, 129, 131, 139, 141, 143, 146, 152) to the metacoxal articulation, passing anteroventral to the **propodeal spiracle** (**T1sp** Figs 15, 18, 19, 129, 133, 135–137, 139). The metapleural arm is the anterodorsal extension of the metapleuron and is delimited from it by the anteriormost extension of the propodeum (prespiracular area, see below). The propodeal-metapectal complex is fused with the mesopleuron ventrally in some Teleasinae (Figs 99, 134).

The metapleuron is divided by the sigmoid **metapleural sulcus** (**mtps**: Figs 18, 19, 96, 129, 131, 133, 134, 136–140) into the **dorsal** and **ventral metapleural areas*** (**dmpa**, **vmpa**: Figs 18, 19, 96, 129, 131, 138). It is usually complete and extends from the metapleural arm to the posterior part of the metacoxal articulation some distance ventral to the metapleural carina; internally it corresponds to the **metapleural ridge** (**mprg**: Figs 13, 14c, 15, 132, 144, 149, 152). The **metapleural apodeme** (**mpa**: Figs 13, 132, 141–144, 148, 150, 152) is on the metapleural ridge and corresponds externally to the **metapleural pit** *(**metp**: Figs 18, 19, 96, 131, 133, 139, 140). In some taxa the metapleural ridge is reduced or absent, in which case only the metapleural apodeme is present (Fig. 142).

The **paracoxal sulcus** (**pcxs**: Figs 19, 99, 105, 131, 133, 138, 140) originates dorsally from the metapleural sulcus and extends ventrally along the anterior margin of the metapleuron; internally it corresponds to the **paracoxal ridge** (**pcxr**: Figs 13–15, 67, 132, 141–146, 151). In *Sparasion* and *Archaeoteleia* (Figs 141–144) the paracoxal ridge is continuous with the dorsal, vertical part of the metapleural ridge; in other Scelionidae it diminishes ventral to the metapleural ridge (Figs 142, 143, 145, 146). The posteroventrally extended **metapleural epicoxal sulcus*** (**meps**: Figs 18, 19, 131, 134) and **metapleural epicoxal carina*** (**mpxc**: Figs 18, 19, 94, 96, 99, 134, 140) originate medially from the paracoxal sulcus and delimit the **metapleural triangle** (**mtp**: Figs 19, 96).

The paired **metepisternal depression** (**mtad**: Figs 13, 99, 134, 142–144, 151) is on the anteroventral margin of the metepisternum. The **ventral carina of the metapleuron*** (**vcmp**: Figs 13, 14c, 18, 99, 134, 142–144) separates the metepisternal depression from the **metacoxal depression*** (**mcxd**: Figs 18, 99, 134, 137, 138, 140). The metacoxal foramen is situated in the middle of the metacoxal depression, which accommodates the base of the metacoxa.

The **metafurcal pit** (**fu3p**: Figs 18, 129, 134) is between the metacoxal foramina; internally it corresponds to the base of the **metafurca** (**fu3**: Figs 14a, b, c). The metafurca is Y-shaped, its base situated anteriorly on the **metadiscrimenal lamella** (**dscl3**: Figs 14a, b, c, 104, 145, 147), which extends between the metafurcal pit and the paracoxal ridge. In some Scelionidae the **metadiscrimen** (**dscr3**: Figs 99, 134) is marked by a row of punctures (Fig. 99). In Telenominae, Gryonini, and Baeini the paracoxal ridge does not extend posterior to the lateral metafurcal arms (Fig. 15b, 142) and the metadiscrimenal lamella is square in lateral view (Fig. 14a). In other Scelionidae the metafurca is slanted anteriorly and the paracoxal ridge extends medially to the metafurcal arms (Figs 15a, 141, 143, 144), in which case the metadiscrimenal lamella is triangular in lateral view (Figs 14b). The **metafurcal arm** (**mtfa**: Figs 13, 14c, 15b, 132, 141–144) is bent posteriorly before fusing with the metapleural apodeme. The site of fusion is distinct. The **dorsal** and the **ventral metafurcal lamellae*** (**dmfl**, **vmfl**: Figs 13, 132, 141, 142; =114, 115 *sensu* Ronquist & Nordlander 1989) extend along the metafurcal arm.

The posterior thoracic spiracle (Vilhelmsen 2000a) is apparently absent from Scelionidae. The propodeal spiracle delimits the posterior margin of the narrow, triangular **prespiracular propodeal area*** (**pspp**: Figs 18, 19, 133, 135–137, 139, 140), which separates the metapleural arm from the rest of the metapleuron. The **third phragma** (**ph3**: Figs 13, 15, 128, 132, 141, 143–146, 151, 152) is a low transverse carina that extends along the anterior margin of the propodeum and diminishes medially. The **dorsal propodeal inflection*** (**dpin**: Figs 128) extends along the dorsal margin of the propodeum posterior to the third phragma. The **metapleural wing articulation** (**plwa3**: Figs 124, 128, 141, 146) is on the anterior end of the dorsal propodeal inflection just posterior to the metapleural arm. The usually oblique **lateral propodeal carina** (**lpc**: Figs 15, 18, 19, 129, 131, 133, 135–140) crosses the posterior part of the propodeum and separates the **lateral propodeal area** (**lpar**: Figs 18, 129, 131, 133, 135–137, 140) from the **metasomal depression** (**metd**: Figs 18, 129, 131, 133, 135, 137, 138, 140). The shape, expression, and location of the lateral propodeal carina vary and in some Scelionidae the anterodorsal end of the carina extends over the dorsal margin of the propodeum to form a projection (e.g., *Probaryconus*). The shape and dorsal extension of the metasomal depression correlate with structures on the petiole. In those females having the ovipositor housed within the dorsal protuberance of the metasoma (Austin & Field 1997), the metasomal depression is also extended to receive the enlarged site of attachment of the petiole. The dorsal ends of the lateral propodeal carinae are far from each other in these cases (Fig. 137), whereas the carinae almost fuse dorsally if the petiole is simple. The dorsal margin of the metasomal depression is simple in most Selionidae, but in *Nixonia* the dorsal margin is projected into a median spine (Figs 138, 139). Some Scelionidae have the lateral propodeal carina fused with the metapleural carina (Figs 129, 131). Usually, the lateral propodeal carina is fused with one of the posteriorly oriented oblique carinae that originate from the anterodorsal margin of the propodeum medial to the propodeal spiracle. The number and topology of these posteriorly oriented dorsal carinae vary. The **plica** (**plc**: Figs 18, 19, 136, 140) is a carina that originates just medial of the propodeal spiracle. The plica fuses with the lateral propodeal carina to form the **posterior propodeal projection*** (**ppp**: Figs 18, 19, 136, 140). The plica separates the usually setaceous **plical area** (**pla**: Figs 18, 136, 140) from the lateral propodeal area. The **propodeal tooth** (**prth**: Figs 18, 129, 137, 138) is a distinct projection on the lateral margin of the **propodeal foramen** (**prfo**: Figs 13, 18, 129, 137, 138). The projection serves as the site of attachment of the **anterolateral depression of the petiole*** (**ldpp**: Figs 153, 155) of the metasoma. The propodeal foramen is encircled by the metasomal depression, which is the posterior, depressed area of the propodeum that accommodates the base of the metasoma. The metasomal depression is limited dorsolaterally by the lateral propodeal carina and ventrolaterally by the ventral part of the metapleural carina. The metasomal depression sometimes is continuous with the metacoxal depression (Figs 129, 138), but in most Teleasinae, Telenominae, Gryonini, Baeini, where the propodeal foramen is situated more dorsally, it is separated from the metacoxal depression by the **ventral propodeal carina*** (**vprc**: Figs 18, 134, 137, 140).

Muscles. The ***metapleuro-metabasalare muscle*** (***pl3-ba3***: Figs 14c, 15a, 67) originates from the anterior surface of the ventral part of the paracoxal ridge. The ***metapleuro-third axillary sclerite of the hind wing muscle*** (***pl3-3ax3***: Figs 14c, 104, 143, 144, 151, 152) originates from the anterior surface of the metapleural ridge (Fig. 144) or, if the ridge is reduced, from the anterodorsal part of the metapleuron ventral to the metapleural arm (Figs 134, 151, 152). The metapleuro-metanotal and the ***metapleuro-metasubalar muscles*** (***pl3-sa3***: Figs 14c, 147, 149, 150) originate from the dorsal surface of the metapleural ridge. The ***metacoxo-metasubalar muscle*** (***cx3-sa3***: Figs 13, 150, 152) originates from the lateral margin of the metacoxa, extends posterior to the metapleural ridge, and shares a common tendon with the metapleuro-metasubalar muscle. The ***median metapleuro-metacoxal muscle*** (***pl3-cx3m***: Figs 14c, 15a, b, 145–147, 149) originates from the metadiscrimenal lamella and inserts on the anterolateral margin of the metacoxa. The ***lateral metapleuro-metacoxal muscle*** (***pl3-cx3l***: Figs 13, 14c, 15a, 67, 149, 152) originates from the posterior surface of the paracoxal ridge, from the ventral surface of the metapleural ridge, and from the metapleuron below the ridge and inserts on the lateral margin of the metacoxa anterior to the site of origin of the metacoxo-metasubalar muscle. The posterior margin of the site of origin of the muscle usually corresponds externally to the ventral part of the metapleural carina. The ***metapleuro-metatrochanteral muscle*** (***pl3-tr3***: Figs 13, 15a) originates partly from the ventral surface of the metapleural apodeme, partly from the metapleuron ventrally of the metapleural apodeme. The metanoto-metatrochanteral muscles extend anterior to the metafurcal arm and the metapleural ridge just posterior to the paracoxal ridge. The muscle is absent in ***Sparasion and Nixonia.*** The ***metafurco-metatrochanteral muscle*** (***fu3-tr3***: Figs 13, 15a, 67, 148, 149) originates from the lateral part of the metafurcal arm anterior to the lateral part of the site of origin of the metafurco-metacoxal muscle. The ***metafurco-metacoxal muscle*** (***fu3-cx3m,l***: Figs 13, 15a, b, 67, 148, 151) is subdivided, the lateral band originates from the posterior surface of the ventral metafurcal lamella the median band from metadiscrimenal lamella in most Scelionidae dorsally of the site of origin of the median metapleuro-metacoxal muscle (Fig. 15a). In Telenominae, Gryonini and Baeini the median band originates posterior to the site of origin of the medain metapleuro-metacoxal muscle (15b). The muscle inserts on the posterior margin of the metacoxa. The ***metafurco-mesofurcal muscle*** (***fu3-fu2***: Figs 10, 15a) originates from the anterior surface of the lateral part of the metafurcal arm and inserts on the posterior surface of the lateral mesofurcal arms. The ***metafurco-second abdominal sternal muscle*** (***fu3-S2***: Figs 13, 14c, 104, 145–147, 151, 153–155) originates from the posterior surface of the dorsal metafurcal lamella. In *Sparasion*, the muscle consists of two bands that insert with a common tendon on to the second metasomal sternum. The obliquely oriented ***third phragmo-second phragmal muscle*** (***ph3-ph2***: Fig. 13) originates from the dorsal surface of the third phragma and inserts on the posterior surface of the second phragma. The ***third phragmo-second abdominal tergal muscle*** (***ph3-T2***: Figs 13, 14c, 67, 143, 145–147, 149, 151–155) originates exclusively from the ventral surface of the third phragma in most Scelionidae. The muscle inserts on the dorsal surface of the second abdominal tergite. The ***propodeo-second abdominal tergal muscle*** (***T1-T2***: Figs 13, 152–155) is present only in *Scelio*. The site of origin of the muscle limited anteriorly by the posterior margin of the site of origin of the lateral metapleuro-metacoxal mucle. The ***propodeo-second abdominal sternal muscle*** (***T1-S2***: Figs 13, 14c, 104, 145, 152–155) originates ventral to the third phragma and inserts on the anterodorsal margin of the second abdominal sternite. The anterior margin of the site of origin of the muscle corresponds to the metapleural carina externally. The ***propodeo-first metasomal spiracle muscle*** (***T1-T1sp***: Figs 13, 14c) originates from the ventral part of the metapectal-propodeal complex just dorsal to the posterior end of the metapleural ridge. In *Archaeoteleia*, *Nixonia*, and *Sparasion* the muscle originates from the **dilator muscle apodeme*** (**dma**: Fig. 132), which corresponds to the **posteroventral metapleural pit*** (**pvpp**: Figs 131, 139).

Discussion

Possible exocrine glands

Scelionidae have numerous coriaceous and usually setaceous patches on the body surface. The correlation between some metasomal coriaceous patches, such as the felt fields, and exocrine glands was discussed by Masner & Huggert (1989) for Platygastridae and by Mikó & Masner (*in press*) in Scelionidae. These patches usually have a median porelike structure. The coriaceous microsculpture and associated setae may act as an evaporating surface for the release of glandular products (Noirot & Quennedy 1974; Buckingham & Sharkey 1988, Quicke & Falco 1998), and the median pore could serve as an opening of class III gland cells (Noirot and Quennedy 1974). Many Scelionidae have some coriaceous patches with median porelike openings on the head and mesosoma similar to that found on the metasoma (Fig. 30), *viz*., the frontal, genal, vertex, and postacetabular patches. These patches are distinct only in taxa with a smooth body surface, but their relative location is constant. In most Scelionidae, however, the areas where the patches are located are strongly sculptured, and therefore it is impossible to detect them externally.

Some of the coriaceous areas on the body surface could perhaps serve as enlarged surfaces for muscle attachments. This is seen, for example, in the lateral patches on the metasomal terga (Mikó & Masner, *in press*). We assume that the coriaceous orbital band on the head of Telenominae corresponds with the site of origin of either an anterior extension of the mandibular muscles or the cranio-antennal muscle. To differentiate "gland" patches from "muscle" patches externally requires observation of the presence or absence of median porelike openings, and histological examinations are needed to ascertain the nature of the coriaceous areas on the body surface.

The anterior process of the pronotum (Figs 35, 47) in Teleasinae may also be a cuticular modification around the opening of an exocrine gland. This hypothesis is based on the presence of coriaceous sculpture on the anterior rim of the pronotum below the process, perhaps for better evaporation of gland products, and the lack of any corresponding muscle attachment.

Detailed histological examination of coriaceous and setaceous patches may be a fruitful area for further research because the presence, absence, and structure of exocrine glands and their corresponding external features are important for phylogenetic reconstructions and for better understanding of the biology of Hymenoptera (Billen 1990, Billen & Morgan 1998, Isidoro *et al.* 1996, Buckingham and Sharkey 1988, Smith *et al.* 2001).

Head

All of the extrinsic muscles of the antenna originate from the tentorium in Hymenoptera (Alam 1951, Dhillon 1966, Duncan 1939, Snodgrass 1942, Ronquist & Nordlander 1989, Vilhelmsen 1996). In Scelionidae, one extrinsic muscle of the antenna, the cranio-antennal muscle, originates from the frons. Both the precise site of insertion and the function of this muscle are unknown, but it may be homologous with one of the extrinsic muscles originating from the tentorium in other Hymenoptera. The origin of the muscle may have shifted to the frons due to the extreme low anterior site of origin of the tentorium, but regardless the presence of the cranio-antennal muscle could be an apomorphy for Scelionidae.

In *Archaeoteleia*, the anterior cranio-mandibular muscle originates from the internal surface of the gena, similar to the situation in *Apis* (Snodgrass, 1942) and our own observations of several hymenopteran groups: *Evania, Gasteruption, Helorus, Megaspilus, Galesus, Cotesia,* and Proctotrupidae. The anterior margin of the origin of the anterior cranio-mandibular muscle does not extend beyond the internal shallow ridge corresponding to the malar sulcus in *Archaeoteleia* or the just mentioned non-scelionid hymenopterans. In Scelionidae other than *Archaeoteleia*, the border between the anterior cranio-mandibular and cranio-antennal muscles is anterior to the malar ridge, which we consider as a secondary modification in Scelionidae.

Masner (1976, 1980) considered malar striation to be an important character for the generic classification

of Scelionidae. It seems probable that a less extensive or totally reduced malar striation correlates with less extended origins of the anterior cranio-mandibular and lateral antennal muscles.

In most Scelionidae the pleurostomal fossa, which serves as the posterior mandibular articulation, is on the posterior margin of the oral foramen. The axis of rotation of the mandible extends between the pleurostomal fossa and the anterior pleurostomal condyle, resulting in a transverse biting motion (Fig. 156). In contrast, *Sparasion* and *Tyrannoscelio* have the pleurostomal fossa located more anteriorly, on the lateral margin of the oral foramen. This, together with the more deeply impressed pleurostomal condyle, effectively shifts the axis of rotation so that the mandibles move in a nearly dorsoventral plane (Fig. 157). The movement of the mandible in *Sparasion* is complemented by the unique location of the abductor muscle of the mandible (*cr-mda*). The muscle originates from the lateral wall of the head in most Scelionidae, but on the lateral part of the frons in *Sparasion*. The presence of the frontal ledge in *Sparasion* may be developed for strengthening the frons against the stresses caused by the displaced mandibular abductor.

Scelionidae are highly variable in development of the frontal depression, interantennal process, and associated features. This may, in part, correspond with the development of the cranio-pharyngeal plate muscle. In *Baryconus* the frontal depression is often very deep and its margins carinate (the submedian carinae) and the origin of the cranio-pharyngeal plate muscle is also the most extended. However, the frontal depression receives the antennal scape when it is depressed to the head and therefore may be considered to be functionally homologous with the scrobal depression of some Chalcidoidea (Gibson 1997). Most of the genera generally considered plesiomorphic for the family, such as *Nixonia*, *Plaumannion*, *Huddlestonium*, and *Archaeoscelio*, have an impression on the gena below the eye into which the scape fits.

Different patterns of sclerotization between the occipital and oral foramina were discussed by Vilhelmsen (1999). He assumed that the sclerotization was formed by a hypostomal bridge in the common ancestor of the Cephoidea, Siricoidea, Orussidae and Apocrita. The hypostomal bridge is formed by the fusion of the hypostomae medially, as indicated by continuity of the hypostomae between the maxillary condyles. In *Orussus* and many Apocrita, however, the hypostomal bridge is largely replaced by a postgenal bridge formed by the medially expanded postgenae. In some Apocrita and in *Orussus* a single median sulcus is present on the postgenal bridge. Microtrichia are found on the lateral margin of this sulcus suggesting that it has been formed by the invagination of the dorsal part of the hypostomal bridge.

The condition in Scelionidae resembles that of *Orussus*, in which the median sulcus of the postgenal bridge is indicated by a narrow band of microtrichia (Fig. 31). In these cases the hypostomal sulcus is interrupted medially. We consider therefore the sclerotized area between the oral and occipital foramina as postgenal in origin, and therefore prefer to use the term postgenal pit instead of hypostomal pit for the pit located on the postgenal bridge. In Teleasinae, however, the median sulcus of the postgenal bridge is absent (Figs 30, 32) similar to the condition in *Xiphydria* (Xiphydriidae) and those apocritans where the hypostomal bridge is most distinct. In these taxa the hypostomal bridge is covered with minute microtrichia and is limited laterally from the postgenae by a pair of sulci. The sulci correspond internally to ridges continuous with the tentorium. The hypostomal sulcus is continuous with the sulci laterally delimiting the hypostomal bridge. In Teleasinae, although the sclerotized area between the occipital and oral foramina is delimited by a pair of sulci similar to those in *Xiphydria*, these do not correspond to any internal ridges. Moreover, the postgenal pits, which mark the posterior site of origin of the tentorium, usually are located medial to these sulci, and the hypostomal sulcus in Teleasinae is continuous medially. There are similar sulci delimiting a median area of the postgenal bridge in other Scelionidae having a well-developed median sulcus of the postgenal bridge. On the basis of these observations we conclude that the sclerotized area between the occipital and oral foramina of Teleasinae is indeed the postgenal bridge, and the median sulcus of the postgenal bridge is secondarily reduced.

Masner (1979a, 1983) and Mineo & Villa (1982) described numerous carinae on the posterior surface of the head in Gryonini that are useful for species differentiation and species-group characterizations. Most of these carinae cross or limit the attachment sites of different bands of the posterior cranio-mandibular muscle.

Therefore, they probably serve to reinforce the posterior wall of the head, stabilizing it against stresses caused by contractions of these muscles. Of the terminology proposed, we are reluctant to accept the term hypostomal sulcus *sensu* Masner (1983), which delimits a triangular, impressed area for accommodating the propleura. In Hymenoptera, the hypostomal sulcus dorsally delimits the oral foramen (Chapman 2004, Vilhelmsen 1999). We also reject the term postoccipital sulcus proposed by Mineo & Villa (1982) for the same structure, because the sulci are outside the postocciput. Rather, we suggest the term postgenal sulcus in preference to the terms proposed by Masner, Mineo, and Villa.

The internal apodeme corresponding with the preocellar pit is connected to the brain via an epidermal cell bundle and may act as suspension to stabilize the position of the brain (Isidoro & Bin 1994).

The distance between the postgenal pits and the posterior tentorial pits is correlated with the length of the incorporated part of the anterior tentorial arm (ventral lamella of the tentorium). Usually, the shorter the head the longer the incorporated part and therefore the longer the distance between the posterior and hypostomal tentorial pits.

In Hymenoptera, the anterior tentorial pit generally corresponds with the attachment site of the anterior tentorial arm and is distinctly separated from the pleurostomal condyle (Snodgrass 1942, Ronquist & Nordlander 1989, Gibson 1997, Huber & Sharkey 1993). In these taxa, the clypeus is delimited dorsally by the epistomal sulcus, represented internally by the epistomal ridge, and laterally by the clypeo-pleurostomal line. The anterior tentorial arm originates from the anterior margin of the oral foramen in most Scelionidae, and the inverted U-shaped epistomal ridge extends completely to the oral foramen. Therefore, in Scelionidae the clypeus is delimited only by the epistomal sulcus, and the clypeo-pleurostomal sulcus is absent.

Pronotum

In *Nixonia,* the netrion sulcus extends anterior to the mesothoracic spiracle (Masner 1979: fig. 1, Gibson 1985), whereas in other scelionids it extends to the posterolateral margin of pronotum below the mesothoracic spiracle (Masner 1979: e.g., figs 4–8). Consequently, the mesothoracic spiracle is on the netrion in *Nixonia*, and in other scelionids it is located on the posterodorsal edge of the pronotum, distinctly above the netrion (Gibson 1985).

Masner (1979) suggested that the netrion apodeme might serve for muscle attachment. Gibson (1985) reported that the netrion apodeme lacked muscle attachment and concluded that its main function is to strengthen the lateroventral part of the pronotum, possibly related to the ringlike structure of the pronotum. In Scelionidae, the pronoto-third axillary sclerite of the fore wing muscle originates partly from the netrion (Figs 7, 8: t1-3ax2) as a pronotal flexor of the fore wing, and the netrion apodeme forms the anterior limit of the muscle's attachment site in most species. The same muscle originates entirely from the mesopectus in other hymenopterans, including the closely related Platygastridae. The only taxon other than Scelionidae having a pronotal origin of the flexor of the fore wing is Vanhorniidae. *Sparasion* lacks a netrion apodeme, but the posterior pronotal inflection is located more anteriorly to delimit a narrow posterior area on the pronotum. The pronotal flexor of the fore wing originates from this area.

Gibson (1985) proposed that the posterior pronotal inflection is the reduced prepectus that has fused with the posterior margin of the pronotum. He justified this hypothesis based mainly on the location of occlusor muscle apodeme, which is on the prepectus when this is independent, but on or anterior to the posterior pronotal inflection in a number of Apocrita, including almost all Scelionidae. Although in some scelionid genera the occlusor of the first spiracle originates from the occlusor muscle apodeme anterior to the netrion as reported by Gibson (1985), most lack the occlusor muscle apodeme and the muscle orginates from the anterior surface of the netrion apodeme or from the lateral pronotal area anterior to the netrion apodeme. Following Gibson (1985), the presence of the occlusor muscle apodeme is plesiomorphic and its absence in Scelionidae is the result of secondary loss. The reduction of the occlusor muscle apodeme may be correlated with the development of the netrion apodeme.

Snodgrass (1942) and Alam (1951) reported the presence of a prophragmo-laterocervical muscle in Apocrita. Vilhelmsen (2000b) argued that this muscle is only a secondary subdivision of the pronoto-laterocervical muscle, with its origin shifted from the pronotum to the first phragma. In Scelionidae, the sites of origin of the pronoto-propleural, pronoto-laterocervical, and the pronoto-postoccipital muscles extend along the dorsal margin of the pronotum as well as the first phragma.

Propectus

The propleural arm is well developed in most Hymenoptera, serving as the site of origin of muscles inserting on the protrochanter, mesofurca and pronotum. Two muscle bands insert on the protrochanter in most Apocrita, one originating from the propleural arm and the other from the propleuron (Duncan 1939, Snodgrass 1942, Vilhelmsen 2000b). The mesofurco-propleural arm muscle originates partly from the propleural arm and partly from the "adjacent crest" of the profurcal arm in *Vespula* (Duncan 1939). The propleural arm is reduced in Scelionidae and the sites of origin of the above muscles have been transferred to other propectal areas. The profurco-pronotal muscle of Scelionidae may be homologous with the propleural arm-pronotal muscle of other Hymenoptera because of the relative position of the pronotal site of attachment of the muscle and because the muscle appears to cross over the reduced propleural arm. In Scelionidae, the depressor of the protrochanter originates exclusively from the propleuron. The dorsal mesofurcal retractor of the propectus inserts exclusively on the posterior profurcal lamella in Scelionidae, which may be homologuos with the "adjacent crest" of the profurcal arm (Duncan 1939).

The profurcal bridge is absent from Scelionidae, *Vespula* (Duncan 1939), Mymarommatoidea (Vilhelmsen and Krogmann 2006) and most Chalcidoidea (Krogmann & Vilhelmsen 2006) but is present in *Ibalia* (Ronquist & Nordlander 1989), *Apis* (Snodgrass 1942), *Megalyra*, and *Orthogonalys* (Vilhelmsen 2000b). The bridge is present in Xiphydriidae and Orussidae (Vilhelmsen 2000b) and probably in the apocritan ground plan, but its occurrence is highly variable within Apocrita (Vilhelmsen unpubl.).

Vilhelmsen (2000b) erroneously reported only one profurcal pit in basal Hymenoptera; however, two pits can be observed within a shallow depression on the dorsal part of the prosternum in most Hymenoptera (Vilhelmsen unpubl.), e.g., *Stenobracon* (Alam 1951) *Apis* (Snodgrass 1942) and most Chalcidoidea (Krogmann & Vilhelmsen 2006), as well as Scelionidae. A notable exception is most Cynipoidea (Ronquist & Nordlander 1989; Vilhelmsen unpubl.) which have only one profurcal pit. The deep prosternal incisions separating the basisternum from the furcasternum in Scelionidae have not been observed in any other Hymenoptera (Vilhelmsen unpubl.).

Mesonotum

The tegula is connected to the mesoscutum by membranous connectivae. Due to the minute size of dissected specimens we were not able to determine without histologic examinations whether the depressor of the tegula (Duncan 1939) is present or absent from Scelionidae.

The skaphion is a modification of the anterior part of the pronotum that apparently is not found outside of Scelionidae. Kozlov (1970) considered the presence of the skaphion as the main diagnostic character for the tribe Psilanteridini. Masner (1972) argued against this hypothesis, noting that the skaphion is present in a range of other genera, and that its presence or absence was not well correlated with the understanding of higher classification of scelionids. Therefore, he concluded that the “...skaphion is a character of problematic value” (Masner 1972). The skaphion carina, which delimits the posterior margin of the skaphion, crosses the anterior site of attachment of the first phragmo-second phragmal muscle. Therefore, it may be a structure to strengthen the mesoscutum against the stresses generated by muscle contraction. Such stresses, however, are common to almost all flying insects, and this seems to us to be an unsatisfactory hypothesis to explain the development of this region in only a single family of Apocrita. The possible suggestion that the skaphion is a plesiomorphic feature, perhaps the prescutum found widely in other insects, is similarly unsatisfactory because the skaphion is not present in any of the taxa currently considered to be plesiomorphic.

Scutellar-axillar complex

A vertical and a horizontal carina on the axilla in Scelionidae may be homologous with the axillar carina of basal Hymenoptera. The axillar carina separates the vertical dorsal axillar surface from the horizontal lateral axillar surface (Gibson 1985). In Scelionidae, the horizontal transaxillar carina (tac: Figs 9, 17–19, 75, 77–79, 88, 95, 96) separates a vertical and horizontal area of the axilla, and therefore could be considered as the axillar carina *sensu* Gibson (1985). However, this carina is absent from *Nixonia* (Figs 90, 93) and *Archaeoteleia* (Figs 76, 77); in *Scelio* (Fig. 72) the transaxillar carina seems to be formed secondarily from one of the interspaces between the foveae of the scutoscutellar sulcus. The vertical axillar carina (axc: Figs 9, 17, 18, 76, 77, 79, 88, 90, 91, 93, 95, 96) is well developed in all Scelionidae. It separates an anterior vertical and a posterior partly vertical, partly horizontal area on the axilla. In *Apis* and some other apocritans, mainly in those taxa where the axilla is small, the dorsal axillar area is not only reduced, but is posteriorly or laterally declined. Due to the declination of the dorsal axillar area, the originally horizontal axillar carina then becomes vertical (Gibson 1985). We consider the axillar carina in Scelionidae to be homologous with the axillar carina of other hymenopterans, and thus term the area of the axilla anteriorly delimited by the axillar carina as the lateral axillar area, and the posterior area as the dorsal axillar area. We consider the transaxillar carina to be a new structure in Scelionidae.

Krogmann & Vilhelmsen (2006) proposed the term axillular ridge for an oblique internal ridge corresponding to the axillular carina. A similar internal apodeme, the scutellar bridge is present in Telenominae and Teleasinae. However, this structure does not correspond to the axillular carina nor other external ridges or carinae. We therefore consider it as a strenghtening feature of the mesoscutellum against stresses caused by the contraction of the mesoscutello-metanotal muscle.

The hollow mesoscutellar arm encloses the connection between the reservoir of the dorsal vessel and the wing base. The mesoscutellar arm is well developed in many Hymenoptera. Vilhelmsen and Krogmann (2006) located the mesoscutellar arm in Mymarommatidae, whose lateral part extends to the postalar process (sca: fig. 11). We were not able to detect any hollow structure that could be considered as the mesoscutellar arm in Scelionidae. Externally, the lateral part of the scutellar arm could correspond to the postalar process.

Mesopectus and mesofurca

Gibson (1986) reported the retractor of mesoscutum (Figs 129: pl2-t2c) as present only in Chalcidoidea among Apocrita, but because of its presence in Symphyta hypothesized it as a symplesiomorphy and suggested that the muscle might be found in other apocritans in which the pronotum and mesopleuron were not rigidly connected. He termed the area of the mesopectus serving as site of origin of the retractor of the mesoscutum as the acropleuron. Ronquist & Nordlander (1989) reported a pleuro-notal muscle in *Ibalia* which ends in a pad of rubberlike material similarly to that in Eupelmidae. They noted, however, that the homology is questionable because the muscle in Eupelmidae inserts more anteriorly than in *Ibalia*. Gibson (1993) homologised the prealary sclerite muscle of *Corydalus* and t2-plr2 muscle of *Xyela* with the retractor of the mesoscutum of eupelmids. In Scelionidae, there is also a muscle similar to that in *Ibalia* and *Xyela* inserting on the ventral apodeme of the first phragma. The apodeme is always located anterior to the preaxilla. Although the muscle originates more anteriorly in eupelmids, the preaxilla is also more elongated anteriorly than in Proctotrupoidea *s. l.* or in Cynipoidea, and the muscle originates just anterior to the preaxilla (Gibson 1986: fig. 5). We consider that the muscle reported by Ronquist & Nordlander (1989) in *Ibalia* and that observed in Scelionidae is homologous with the retractor of mesoscutum of *Xyela* and Chalcidoidea. We therefore use the term acropleural apodeme and acropleural sulcus for the apodeme and corresponding external sulcus that serve as the site of origin of the retractor of mesoscutum, or the third mesopleuro-mesonotal muscle (pl2-t2c).

The acetabulum is the anterior, vertical impressed area of the mesopectus limited laterally by the acetabular carina. The acetabular foveae and field (Johnson 1984) are on the anteroventral part of the mesopectus, posterior to the acetabulum; these names were derived on the basis of the proximity of these structures to the

acetabulum. In fact they are not part of the acetabulum, and therefore we prefer to use the adjective postacetabular to refer to them.

Johnson (1984) proposed the term episternal foveae for the sulcus located on the anteroventral part of the mesopectus and used this character for species-group characterizations in *Telenomus*. Some members of other scelionid taxa have similar structures, including Thoronini (Johnson & Masner 2004) and Teleasinae (Mikó & Masner in press). The sulcus corresponds to the mesopleural site of attachment of the mesopleuro-mesobasalare muscle (pl2-ba2) and occurs in most Scelionidae. However, it is usually obscured by the general sculpture of the mesopleuron or is fused with the anterior row of foveae flanking the mesopleural carina. The sulcus is more expressed and separated in taxa having a more extended site of origin of the mesopleuro-mesobasalar muscle. Wharton (2006) revised and homologized some external features of the mesopectus on the basis of muscle attachments in Ichneumonoidea. He redefined the term sternaulus to refer to a sulcus or row of foveae on the mesopleuron corresponding to the mesopleural site of origin of the mesobasalare muscle. Thus, we consider the episternal foveae to be homologous with the sternaulus of Ichneumonoidea and adopt this term for Platygastroidea.

Masner (1976, 1991) and Masner & Huggert (1989) used the term sternaulus for a horizontal carina in *Doddiella* (Scelionidae), and many Platygastridae and Diapriidae. In Platygastridae and Diapriidae, the "sternaulus" *sensu* Masner corresponds with the ventral margin of the site of origin of the anterior and posterior mesopleuro-third axillary sclerite of the fore wing muscles and the second mesopleuro-mesonotal muscle, similar to some Cynipidae. This structure is a functional analogue of the precoxal sulcus of Ichneumonoidea (Wharton 2006). In *Doddiella*, however, the second mesopleuro-mesonotal muscle is rodlike and originates from the pleural apodeme. Furthermore, the ventral margin of the site of origin of the two mesopleuro-third axillary sclerite muscles are not aligned at one level. In *Doddiella*, the sternaulus *sensu* Masner does not correspond to the ventral margin of the origin of these muscles, but may correspond with the mesopectal site of attachment of the indirect elevator of the fore wing (first mesopleuro-mesonotal muscle).

The origin of the mesopleuro-mesofurcal muscle extends along the mesepimeral ridge. The dorsal part of the mesopleural site of attachment of the muscle extends to an internally concave, externally convex area on the dorsal part of the mesopectus, which is internally delimited anteriorly by a more or less well-developed apodeme, the anterior margin of the speculum. The anterior margin of the speculum is homologous with the pleural ridge (PIR: fig. 17G of Snodgrass 1942) in *Apis* and with the second mesopleural apodeme (Pl2A2: fig. 51 of Duncan 1939) in *Vespula*. Externally, the anterior margin of the speculum corresponds with the prespiracular sulcus, considered here homologous with the pleural sulcus (pls2: Fig. 15 of Snodgrass 1942) in *Apis* and the mesopleural suture (pl2s: fig. 42 of Duncan 1939) in *Vespula*. Posteriorly, the site of origin of the mesopleuro-mesofurcal muscle is delimited by the mesepimeral ridge (= k, posterior marginal ridge of mesopleuron: figs 16H, 17B of Snodgrass 1942; = Pl2A3: fig. 53 of Duncan 1939), which corresponds externally to the mesepimeral sulcus (= e, recurrent grove of mesopleuron: fig. 17A of Snodgrass 1942). The internally concave and externally convex area of the mesopleuron, from which the mesopleuro-mesofurcal muscle originates, is called the speculum in Ichneumonidae (Townes 1969) and Cynipoidea (Ronquist & Nordlander 1989), and we have adopted this term for the Scelionidae. On the basis of muscle attachments, the anterior margin of the speculum is the only internal apodeme in Apocrita which may be considered homologous with a part of the mesopleural ridge. The ridge is well developed in most non-apocritan Hymenoptera, where it extends between the pleural wing process and the mesocoxal articulation; a fully developed mesopleural ridge is absent from all Apocrita except a few Chalcidoidea (Krogmann & Vilhelmsen 2006; Vilhelmsen unpubl.).

In most scelionids the anterior margin of the speculum is reduced ventrally, and the pleural apodeme, if present, is separated from it. In the *Psix* group of genera of Telenominae, however, the anterior margin of the speculum extends ventrally to the mesocoxal articulation and is indicated externally by the transpleural sulcus (Fig. 105). These structures could be easily considered as homologous with the mesopleural ridge and sulcus. The anterior margin of the speculum is distinctly separated from the pleural apodeme in most Scelionidae.

The fusion of the pleural apodeme and the anterior margin of the speculum appears to be unique for the *Trissolcus* and *Telenomus* groups of genera of Telenominae. The anterior margin of the speculum begins at the posterodorsal edge of the mesopleuron, which corresponds to the subalar pit in Scelionidae. This condition is similar to that in *Vespula*, and therefore we use the term subalar pit (Duncan 1939) instead of posterior subalar pit (Ronquist & Nordlander 1989).

Gibson (1999) discussed the putative evolution of the mesotrochanteral depressor muscles in Hymenoptera. He stated that the muscle originates partly from the mesofurca (fu_2-tr_2) and partly from the mesopleuron (pl_2-tr_2) in Evaniidae, Pelecinidae, Proctotrupidae and Vanhorniidae, but exclusively from the mesopleuron in Scelionidae. This condition was considered as the end stage of a transformation series in which the tergal part of the depressor muscle is lost and the furcal part transferred to the pleuron. In those Hymenoptera taxa with only a furcal depressor of the mesotrochanter, the mesofurcal depressor of the mesotrochanter is usually subdivided into a lateral and a median muscle band (figs 47–49, Gibson 1985). The single depressor muscle of the mesotrochanter in most Scelionidae appears to originate from the surface of the speculum (Gibson 1985, 1999), however, as mentioned above, the speculum is obscured entirely by the origin of the mesopleuro-mesofurcal muscle in all Apocrita. Therefore, the pleural depressor of the mesotrochanter seems to originate from the internal surface of the muscle pad of the mesopleural-mesofurcal muscle (Figs. 10–12, 112, 114). In fact, the membranous anterior extension of the mesofurca serves as the site of origin of both muscles. The anterior extension of the mesofurca is twisted posterodorsally, therefore the originally ventrally located lateral mesofurco-mesotrochanteral muscle originates exclusively from its internal (median) surface, while the originally dorsally located mesopleuro-mesofurcal muscle attaches to its external (lateral) surface (Figs 10–12, 108–115). This condition is widely distributed in Apocrita having a pleural depressor of the mesotrochanter *sensu* Gibson (1985, 1999). The lateral band of the depressor of the mesotrochanteral muscle has no pleural origin in Evaniidae, Pelecinidae, Proctotrupidae and Vanhorniidae, but as in Scelionidae originates only from the internal (median) surface of the posterodorsally twisted anterior extension of the mesofurca. We assume that the lateral band of the muscle of these taxa, which was incorrectly considered by Gibson as originating from the pleuron, is homologous with the lateral band of the secondary subdivided furcal depressor of the mesotrochanter of Heloridae, Gasteruptidae and Aulacidae. Therefore, we use the term lateral furcal depressor of mesotrochanter (lateral mesofurco-mesotrochanteral muscle) instead of pleural depressor of mesotrochanter *sensu* Gibson (1985, 1999). In some Scelionidae genera, *Nixonia, Sparasion, Gryon, Idris* and *Archaeoteleia,* both the lateral and the median bands of the furcal depressor of the mesotrochanter are present. This observation is in contrast to Gibson (1985), who observed only the presence of the lateral furcal depressor in Scelionidae examined by him.

Gibson (1985) reported that there is no pleural depressor of the mesotrochanter in Platygastridae and proposed two possible explanations for this: (i) the depressor of the mesotrochanter was lost and its function was taken over by one of the coxal muscles or (ii) it is present, but because of the minute size of platygastrids it is difficult to locate. Our dissections show the presence of the lateral furcal depressor of the mesotrochanter in Platygastridae, and that it appears to originate from the interior surface of the speculum similar to that in Scelionidae and other Hymenoptera. The attachment site of the mesopleuro-mesofurcal muscle is also extended anteriorly lining the interior surface of the speculum as in Scelionidae. A rod-like muscle inserts on a tendon from the mesocoxa and originates on the speculum with an extended origin; we consider this to be the lateral furcal depressor of the mesotrochanter in platygastrids. Since the median furcal depressor of the mesotrochanter is present in some Scelionidae, its absence cannot be an autapomorphy of Platygastroidea, but its ocurrence might be informative within the superfamily. The presence of the lateral furcal depressor in both Scelionidae and Platygastridae indicates that this trait might indicate close relationship between Platygastroidea and one or more of the other taxa possessing it (Evaniidae, Pelecinidae, Proctotrupidae, and Vanhornidae), as suggested by Gibson (1985).

The mesepimeral ridge, and therefore the corresponding mesepimeral sulcus are epimeral in origin on the

basis of the site of origin of the mesopecto-mesofurcal muscle (Ronquist & Nordlander 1989). We therefore do not support the use of the term mesepimeron for the posteriorly delimited area of the mesopectus (e.g., Masner 1979). The postepimeral foveae *sensu* Johnson & Masner (1985) extends on the mesepimeron, and therefore we prefer to use the term mesepimeral sulcus.

Flexors of the hind wing originate exclusively from the metapleuron in most Hymenoptera (Alam 1951, Duncan 1939, Ronquist & Nordlander 1989, Snodgrass 1942, Vilhelmsen 2000a). Gibson (1986) reported that the flexor of the hind wing (pl2-3ax3) originates from the mesopleuron posterior to the mesepimeral ridge in Eupelmidae. Heraty *et al.* (1994) hypothesized that the mesopleural flexor of the hind wing in Eupelmidae could be homologous with the furcal-basalar muscle of some basal Hymenoptera. The flexor of the hind wing originates partly from the posterior mesepimeral area of the mesopectus and partly from the metapectus in *Nixonia*, *Sparasion*, and *Scelio*, but in other scelionids appears to originate exclusively from the mesopectus similar to Eupelmidae. The muscle clearly inserts into the third axillary sclerite of the hind wing. The mesopleural origin of the first flexor of the hind wing is not unique for Scelionidae and Eupelmidae. The muscle originates at least partly from the mesopleuron also in *Helorus*, *Proctotrupes*, and *Vanhornia*. In those taxa having the mesopleural band of the flexor of the hind wing, the posterior mesepimeral area is well developed. In taxa with the flexor of the hind wing originating only from the metapleuron the mesepimeral ridge usually extends just anterior to the posterior mesepimeral inflection and the posterior mesepimeral area is usually very narrow and inflected. Therefore, we believe that the posterior mesepimeral area of the mesopectus is serially homologues with the netrion and is associated with the transfer of the flexor of hind wing from the metapectus to the mesopectus. In *Apis*, *Proctotrupes*, *Trichopria*, and *Andricus* the mesosubalare muscle originates from the mesocoxa as in Scelionidae. In Chalcidoidea, the muscle originates from the mesopectus.

Metanotum

The term dorsellum is widely used in apocritan taxonomy (e.g., Gibson 1997, Graham 1969, Johnson 1984, Masner & Garcia 2002, Yoder 2004). Ronquist & Nordlander (1989) hypothesized that the dorsellum is homologous with the metascutellum of basal Hymenoptera. Later, Ronquist (1995) reverted to the term dorsellum because of uncertainty whether the structure is serially homologous with the mesoscutellum. Krogmann & Vilhelmsen (2006) synonymyzed the term dorsellum with the metascutellum without explanation. In winged insects, the meso- and metascutellum accommodate circulatory organs connected to the posterior wing veins via the hollow scutellar arms, facilitating circulation of haemolymph through the wings (Krenn & Pass 1994, Vilhelmsen 2000a). The dorsal vessel in the metanotum of Orussidae does not extend to the metascutellum and the scutellar arms are solid (Vilhelmsen 2000a). Vilhelmsen (2000a) hypothesized that this condition may be correlated with the reduced hind wing venation of the family; this is possibly also the reason for the difficulties in identifying functional mesoscutellar arms in Scelionidae (see above). We assume that because of the reduced hind wing venation of most Apocrita the dorsal vessel is also reduced. The internal metanotal ridge bifurcates medially delimiting the internal chamber of the metanotum in Scelionidae (Figs 126, 127), which corresponds externally with a median, elevated area of the metanotum. This internal chamber is connected to a ventral hollow ridge, which extends along the ventral margin of the metanotum (sca: Figs 126, 127, 132). This condition is similar to that of basal Hymenoptera, where a median chamberlike structure, which corresponds to the metascutellum, is located on the metanotum and is connected with the wing base via the hollow scutellar arm. We assume that the hollow ventral ridge of the scelionid metanotum could be homologous with the scutellar arm and the median elevated area of the metanotum with the metascutellum of basal Hymenoptera. Therefore we use the term metascutellum in preference to dorsellum.

Duncan (1939) reported the presence of an independent, partly or entirely separated sclerite connecting to the anterior margin of the metanotum and bearing the anterior notal wing process. No independent sclerite of the metanotum was reported in basal Hymenoptera (Dhillon 1966, Vilhelmsen 2000a). Ronquist & Nordlander (1989) also did not find any independent sclerite of the metanotum. They assumed that the supraalar

area of the Cynipoidea, which bears the anterior notal wing process, could be homologous with the humeral sclerite that is fused secondarily to the metanotum. In Scelionidae, the humeral sclerite is distinctly separated from the metanotum and is connected to the first axillary sclerite of the hind wing similar to that in *Vespula* (Duncan 1939), *Apis* (Snodgrass 1942), and *Stenobracon* (Alam 1951) and other apocritans except Cynipoidea (Vilhelmsen & Mikó unpublished).

Daly (1963) reported presence of the metanoto-metatrochanteral muscle in *Andricus, Chalcis, Sirex*, and *Xyela*, and that this muscle shares its attachment on the metanotum with the t_3-pl_3 muscle in *Andricus*. Vilhelmsen (2000a) homologized the latter muscle with the median metapleuro-metanotal muscle. The muscle inserts on the humeral sclerite in *Pseudofoenus*, *Pristaulacus*, and *Evaniella* (present observations). The metanoto-metatrochanteral muscle shares its insertion site on the metatrochanter with the metafurco-metatrochanteral muscle, and its origin on the supraalar area with the metapleuro-metanotal muscle in *Andricus* (reported also by Daly 1963). On the basis of the site of metanotal attachment (supraalar area = humeral sclerite), we agree with Vilhelmsen (2000a) that the t_3-pl_3 muscle (Daly 1963) of *Andricus* is homologous with the median metapleuro-metanotal muscle of basal Hymenoptera and Evanoidea. Although in Scelionidae the metanoto-metatrochanteral muscle also originates from the humeral sclerite, it inserts on the metatrochanter via a common tendon with the metafurco-metatrochanteral and the metapleuro-metatrochanteral muscle. The median metapleuro-metanotal muscle is absent. We assume that the median metapleuro-metanotal muscle is secondarily reduced in Scelionidae and consider the metapleuro-metatrochanteral muscle as a secondary subdivision of the metafurco-metatrochanteral muscle.

Metapectal-propodeal complex

The term epimetrum was proposed by Mineo & Caleca (1992) for a "strongly narrowed vertical and smooth strip, located between the meso and metapleuron" (Figs 1, 2: Mineo & Caleca 1992). On the basis of dissection of *Dyscritobaeus* specimens, the epimetrum is the anterior part of the metapleuron delimited by the fused paracoxal and metapleural sulci. This condition is similar to that in *Sparasion* or *Archaeoteleia*. Therefore we consider the epimetrum to be homologous with the anteriorly delimited area of the metapleuron of other Scelionidae.

Vilhelmsen (2000a) concluded that the metapleural ridge and the corresponding metapleural sulcus mark the site of fusion between the metapleuron and the propodeum, and thus the posterior metepimeron is totally reduced in Apocrita. In Scelionidae, however, the metapleural carina usually marks the border between the sites of origin of propodeal and metapleural muscles. A similar carina extends from the metapleural wing articulation to the coxal articulation in *Ibalia* (Ronquist & Nordlander 1989), *Stenobracon* (Alam 1951), *Proctotrupes*, and *Helorus* (present observations). It is difficult to decide whether the metapleural area delimited dorsally by the metapleural carina and ventrally by the metapleural sulcus is homologous with the metepimeron of basal Hymenoptera or is a secondary extension of the metapleuron.

Vilhelmsen (2000a, 2003) considered the anteriorly located metafurca on the metadiscrimenal lamella to be an autapomorphy for Hymenoptera. The metafurcal pit is usually on or close to the posterior end of the metadiscrimen and, therefore, the base of the metafurca is located on the posterior part of the metadiscrimenal lamella. However the metafurca is slanted anteriorly and the paracoxal ridge extends posteriorly in most Hymenoptera. Therefore, the metafurcal arms originate anteriorly from the metadiscrimen and the metadiscrimenal lamella is triangular in lateral view (Fig. 14b). This condition occurs in most Scelionidae; however, the paracoxal ridge does not extend to the metafurcal arm in Telenomiane, *Idris* and *Gryon* (Figs 14a, 145). Because the former condition occurs in basal Hymenoptera, we consider the posterior site of origin of the metafurcal arms to be a secondary modification.

Four muscles originating from the propodeal-metapectal complex insert on the petiole in Scelionidae. Two of them are clearly homologous with muscles 32 and 35 of basal Hymenoptera (Vilhelmsen 2000a). The other two muscles occur in *Vespula* (Duncan 1939) and *Apis* (Snodgrass 1943). Vilhelmsen (2000a) did not

homologize the propodeo-second metasomal tergal muscle with any propodeal muscle of basal Hymenoptera. He also hypothesized that the propodeo-second metasomal sternal muscle could be the secondary subdivision of the metafurco-second abdominal sternal muscle.

Acknowledgments

We thank J. Heraty (University of California, Riverside), F. Bin (University of Perugia, Perugia) and S. Csősz (Hungarian Natural History Museum) for contributing specimens important to this study; G. A. P. Gibson, L. Krogmann, G. Melika and M. Földvári for revising an earlier version and making valuable comments. This work was supported in part by the National Science Foundation under grant No. DEB-0614764 to N.F.J, OTKA T049183 and Bolyai scholarship to Z.P., and Synthesys DK-TAF2316, High-Lat and CanaCol Foundation grant to I.M.

References

Alam, S.M. (1951) The skeleto-muscular mechanism of *Stenobracon deesae* Cameron (Braconidae, Hymenoptera) - An ectoparasite of sugarcane and juar borers of India. Part I. Head and thorax. *Aligarh Muslim University Publications (Zoological Series) on Indian Insect Types*, 3, 1–174.

Austin, A.D. & Field, S.A. (1997) The ovipositor system of scelionid and platygastrid wasps (Hymenoptera: Platygastroidea): comparative morphology and phylogenetic implications. *Invertebrate Taxonomy*, 11, 1–87.

Austin, A.D, Johnson, N.F. & Dowton, M. (2005) Systematics, evolution and biology of scelionid and platygastrid wasps. *Annual Review of Entomology*, 50, 553–582.

Billen J. (1990) Phylogenetic aspects of exocrine gland development in the Formicidae. In: Veeresh, G.K., Mallik, B. & Viraktamath, C.A. (Eds), Social Insects and the Environment. Oxford & IBH Publishing Co, New Delhi, pp. 317–318.

Billen J. & Morgan E.D. (1998) Pheromone communication in social insects - sources and secretions. In : Vander Meer, R.K., Breed, M.D., Espelie, K.E. & Winston, M.L. (Eds), *Pheromone Communication in Social Insects : Ants, Wasps, Bees, and Termites.* Westview Press, Boulder, Oxford, pp. 3–33.

Bin , F. & Dessart, P. (1983) Cephalic pits in Proctotrupoidea, Scelionidae and Ceraphronoidea (Hymenoptera). *Redia* 66, 563–575.

Bostik Findey (2001) Technical data sheet Blu Tack. Available from: *http://www.bostikfindley.com.au/pdf/datasheet/bostik_blu_tack.pdf* (30. November 2006)

Bucher, G.E. (1948) The anatomy of *Monodontomerus dentipes*. *Canadian Journal of Research*, 26(D), 230–281.

Buckingham, G.R. & Sharkey, M.J. (1988) Abdominal exocrine glands in Braconidae (Hymenoptera). In: Gupta, V. (Ed), Advances in Parasitic Hymenoptera Research. E.J. Brill, Leiden/New York, pp. 199–242.

Chapman, R.F. (Reginald Frederic) (2004) The insects structure and function / R.F. Chapman. 4th ed. Cambridge University Press, Cambridge, 770pp.

Daly, H.V. (1963) Close-packed and fibrillar muscles of the Hymenoptera. *Annals of the Entomological Society of America*, 56, 295–306.

Dhillon, S.S. (1966) Morphology and biology of *Athalia proxima*. *Aligarh Muslim University Publications (Zoological Series) on Indian Insect Types*, 7, 1–170.

Duncan, C.D. (1939) A Contribution to the biology of North American vespine wasps. *Stanford University Publications University Series Biological Science*, 8, 1–272.

Gibson, G.A.P. (1985) Some pro- and mesothoracic structures important for phylogenetic analysis of Hymenoptera, with a review of some terms used for structures. *The Canadian Entomologist*, 117, 1395–1443.

Gibson, G.A.P. (1986) Mesothoracic skeletomusculature and mechanics of flight and jumping in Eupelminae (Hymenoptera, Chalcidoidea: Eupelmidae). *The Canadian Entomologist*, 118(7), 691–728.

Gibson, G.A.P. (1993) Groundplan structure and homology of the pleuron in Hymenoptera based on a comparison of the skeletomusculature of Xyelidae (Hymenoptera) and Raphidiidae (Neuroptera). *Memoirs of the Entomological Society of Canada*, 165, 165–187.

Gibson, G.A.P. (1997) Chapter 2. Morphology and Terminology. In: Gibson, G.A.P., J.T. Huber and J.B. Woolley (Eds.), *Annotated Keys to the Genera of Nearctic Chalcidoidea (Hymenoptera).* National Research Council Canada, NRC Research Press, Ottawa, pp. 16–44.

Gibson, G.A.P. (1999) Sister-group relationships of the Platygastroidea and Chalcidoidea (Hymenoptera) - an alternative hypothesis to Rasnitsyn (1988). *Zoologica Scripta* 28(1–2), 125–138.
Gordh, G. & Headrick, D.H. (2001) *A Dictionary of Entomology.* CABI Publishing Oxon/New York, 1032 pp.
Graham, M.W.R. de V. (1969) The Pteromalidae of north-western Europe (Hymenoptera: Chalcidoidea). *Bulletin of the British Museum (Natural History) Entomology Supplement,* 16, 1–908.
Hadley, A. (2006) CombineZ5. Available from: *http://www.hadleyweb.pwp.blueyonder.co.uk/CZ5/combinez5.htm* (30. November 2006)
Heraty, J.M., Darling, D.C. & Woolley, J.B (1994) Phylogenetic implications of the mesofurca and the mesopostnotum in Hymenoptera. *Journal of Hymenoptera Research,* 3, 241–277.
Huber, J.T. & Sharkey, M.J. (1993) Structure, Chapter 3. In: Goulet, H. & Huber, J.T. (Eds), Hymenoptera of the world and identification guide of families. Agriculture Canada Research Branch Monograph no. 1894E, Ottawa, pp. 14–59.
Isidoro, N. & Bin, F. (1994) Fine structure of the preocellar pit in *Trissolcus basalis* (Woll.) (Hymenoptera: Scelionidae). *International Journal of Insect Morphology and Embryology,* 23(3), 189–196.
Isidoro, N., Bin, F., Colazza, S. & Vinson, S.B. (1996) Morphology of antennal gustatory sensilla and glands in some parasitoid Hymenoptera with hypothesis on their role in sex and host recognition. *Journal of Hymenoptera Research,* 5, 206–239.
Johnson, N.F. (1984) Systematics of Nearctic *Telenomus*: classification and revisions of the *podisi* and *phymatae* species groups (Hymenoptera: Scelionidae). *Bulletin of the Ohio Biological Survey,* 6(3), 1–113.
Johnson, N.F. (1996) Revision of world species of *Paratelenomus* Dodd (Hymenoptera: Scelionidae). *The Canadian Entomologist,* 128, 273–291.
Johnson, N.F. & Masner, L. (1985) Revision of the genus *Psix* Kozlov and Lê (Hymenoptera: Scelionidae). *Systematic Entomology,* 10, 33–58.
Johnson, N. F. & Masner, L. (2004) The genus *Thoron* Haliday (Hymenoptera: Scelionidae), egg–parasitoids of water-scorpions (Hemiptera: Nepidae), with key to world species. *American Museum Novitates,* 3452, 1–16.
Kozlov, M.A. (1970) [Supergeneric groups of the Proctotrupoidea (Hymenoptera).] *Entomologicheskoye Obozreniye*, 49, 115–127.
Krenn, H.W. & Pass, G. (1994) Morphological diversity and phylogenetic analysis of wing circulatory organs in insects, part I: non Holometabola. *Zoology,* 98, 7–22. [In Russian]
Krogmann, L. & Vilhelmsen, L. (2006) Phylogenetic implications of the mesosomal skeleton in Chalcidoidea (Hymenoptera: Apocrita) – tree searches in a jungle of homoplasy. *Invertebrate Systematics,* 20, 615-674.
Masner, L. (1972) The classification and interrelationships of Thoronini (Hym.: Proctotrupoidea, Scelionidae). *The Canadian Entomologist,* 104, 833–849.
Masner, L. (1976) Revisionary notes and keys to world genera of Scelionidae (Hymenoptera: Proctotrupoidea). *Memoirs of the Entomological Society of Canada*, 97, 1–87.
Masner, L. (1979a) The *variicornis*-group of *Gryon* Haliday (Hymenoptera: Scelionidae). *The Canadian Entomologist,* 111, 791–805.
Masner, L. (1979b) Pleural morphology in scelionid wasps (Hymenoptera, Scelionidae) — an aid to higher classification. *The Canadian Entomologist,* 111, 1079–1087.
Masner, L. (1980) Key to genera of Scelionidae of the Holarctic region, with descriptions of new genera and species (Hymenoptera: Proctotrupoidea). *Memoirs of the Entomological Society of Canada*, 113, 1–54.
Masner, L. (1983) A revision of *Gryon* Haliday in North America (Hymenoptera: Proctotrupoidea: Scelionidae). *The Canadian Entomologist,* 115, 123–174.
Masner, L. (1991) Revision of *Spilomicrus* in North America north of Mexico (Hymenoptera, Proctotrupoidea, Diapriidae). *The Canadian Entomologist,* 123, 107–177
Masner, L. & Denis, J. (1996) The Nearctic species of *Idris* Foerster. Part I: the *melleus*-group (Hymenoptera: Scelionidae). *The Canadian Entomologist,* 128, 85–114.
Masner, L. & Garcia R., J.L. (2002) The genera of Diapriinae (Hymenoptera: Diapriidae) in the World. *Bulletin of the American Museum of Natural History,* 268, 1–138.
Masner, L. & Huggert, L. (1989) World review and keys to genera of the subfamily Inostemmatinae with reassignment of the taxa to the Platygastrinae and Sceliotrachelinae (Hymenoptera: Platygastridae). *Memoirs of the Entomological Society of Canada*, 147, 1–214.
Mikó, I. & Masner, L. (submitted) World revision of *Xenomerus* Walker (Hymenoptera: Scelionidae). *Zootaxa.*
Mineo, G. & Villa, L. (1982) The morphology of the back of the head of Gryonini (Hym. Proctotrupoidea, Scelionidae). *Estratto dal Bollettino del Laboratorio di Entomologia Agraria "Filippo Silvestri" di Portici,* 39, 133–162.
Mineo, G. & Caleca, V. (1992) New characters in Gryonini (Hymenoptera: Scelionidae). *Phytophaga,* 4, 11–16.
Noirot, C. & Quennedy, A. (1974) Fine structure of insect epidermal glands. *Annual Review of Entomology,* 19, 60–80.
Quicke, D.L.J. & Falco, J.V. (1998) A putative pheromone gland associated modification of the hind tibia in *Vipio moneilemae* (Hymenoptera: Braconidae: Braconinae). *Journal of Hymenoptera Research,* 7, 118–121.

Rasnitsyn, A.P. (1988) An outline of the evolution of the hymenopterous insects (order Vespida). *Oriental Insects*, 22, 115–145.
Richards, O.W. (1977) Hymenoptera. Introduction and keys to families. *Handbooks for the Identification of British Insects*, 6(1), 1–100.
Ronquist, F. (1995) Phylogeny and classification of the Liopteridae, an archaic group of cynipoid wasps (Hymenoptera). *Entomologica Scandinavica Supplement*, 46, 1–74.
Ronquist, F. & Nordlander, G. (1989) Skeletal morphology of an archaic cynipoid, *Ibalia rufipes* (Hymenoptera: Ibaliidae). *Entomologica Scandinavica Supplement*, 33, 1–60.
Smith, A.R., O'Donnell, S. & Jeanne, R.L. (2001) Correlated evolution of colony defence and social structure: A comparative analysis in eusocial wasps (Hymenoptera: Vespidae). *Evolutionary Ecology Research*, 3, 331–344.
Snodgrass, R.E. (1935) *Principles of Insect Morphology.* McGraw-Hill Book Company, New York. 667 pp.
Snodgrass, R.E. (1942) The skeleto-muscular mechanisms of the honey bee. *Smithsonian Miscellaneous Collections*, 28(1–2), 1–120.
Torre-Bueno, J.R. de la. (1989) *The Torre-Bueno Glossary of Entomology.* New York Entomological Society, New York. 840 pp.
Townes, H. (1969) Genera of Ichneumonidae, Part 1. *Memoirs of the American Entomological Institute*, 11, 1–300.
Vilhelmsen L. (1996) The preoral cavity of lower Hymenoptera (Insecta): comparative morphology and phylogenetic significance. *Zoologica Scripta*, 25, 143–170.
Vilhelmsen, L. (1999) The occipital region in the basal Hymenoptera (Insecta): a reappraisal. *Zoologica Scripta*, 28, 75–85.
Vilhelmsen, L. (2000a) Before the wasp-waist: Comparative anatomy and phylogenetic implications of the skeleto-musculature of the thoraco-abdominal boundary region in basal Hymenoptera (Insecta). *Zoomorphology*, 119, 185–221.
Vilhelmsen, L. (2000b) Cervical and prothoracic skeleto-musculature in the basal Hymenoptera (Insecta): Comparative anatomy and phylogenetic implications. *Zoologischer Anzeiger*, 239, 105–138.
Vilhelmsen, L. (2003) Towards a consensus: latest results from simultaneous analysis of the basal hymenopteran lineages. *Entomologische Abhandlungen*, 61, 162–163.
Vilhelmsen, L. & Krogmann, L. (2006) Skeletal anatomy of the mesosoma of *Palaeomymar anomalum* (Blood & Kryger, 1922) (Hymenoptera: Mymarommatidae). *Journal of Hymenoptera Research*, 15, 290-306.
Wharton, R.A. (2006) The species of *Sternaulopius* Fischer (Hymenoptera: Braconidae, Opiinae) and the braconid sternaulus. *Journal of Hymenoptera Research*, 15(2), 317–347.
Yoder, M.J. (2004) Revision of the North American species of the genus *Entomacis* (Hymenoptera: Diapriidae). *The Canadian Entomologist*, 136, 323 – 405.

Appendix

abbreviation	term	figures	reference	synonyms
aal	antero-admedian line	16, 17, 69, 75, 80	Ronquist & Nordlander 1989	
ac	acetabular carina	10, 11, 12, 16, 35, 74, 94, 96, 99, 100, 134	Johnson 1984	
acra	acropleural apodeme*	12, 71, 101, 106		
act	acetabulum	10, 11, 16, 35	Richards 1977	=procoxal depression *sensu* Krogmann & Vilhelmsen 2006
adi	antero-dorsal incision of mesopleuron*	12, 76, 100		
amsp	anterior margin of the speculum*	10, 12, 101, 103, 104, 106, 112		=pleural ridge *sensu* Snodgrass 1942; =second mesopleural apodeme *sensu* Duncan 1939
anem	anterior extension of meso-furca*	10, 12, 108, 112–115		
anfo	antennal foramen	1a, b	Ronquist & Nordlander 1989	= toruli *sensu* Masner 1980, Yoder 2004
anwp	anterior notal wing process	9, 17, 18, 75, 77, 79	Gibson 1985	
aoc	anterior ocellus	1b	Masner 1980	
apfb	anterior process of the mesofurcal bridge	10, 117	Duncan 1939	
aph1	ventral apodeme of the first phragma*	9, 66, 71, 73		= 55 *sensu* Ronquist & Nord-lander 1989
app	anterior process of the pro-sternum	7, 8, 35, 37, 45	Duncan 1939	
apr	anterior process of the pronotum*	35, 47		
aprl	anterior profurcal lamella	5, 7, 8, 39, 40, 44	modified after Vilhelm-sen & Krogmann 2006	= a6 *sensu* Vilhelmsen 2000b; = inner process of first furcal arm *sensu* Duncan 1939
arp	anterior rim of pronotum	16, 19, 48, 56	Ronquist & Nordlander 1989	
asc	antennal scrobe	1a, 23, 25	Ronquist & Nordlander 1989	= speculum *sensu* Masner & Denis 1996
asu	acropleural sulcus	19, 76, 94, 96, 97, 100, 105, 107	Gibson 1986	
atp	anterior tentorial pit	28	Ronquist & Nordlander 1989	
ats	postacetabular sulcus*	16, 19, 35, 94, 96, 99, 100, 134		= acetabular foveae *sensu* Johnson 1984
auc	axillular carina	9, 17–19, 78, 86, 93, 95, 96	Gibson 1985	
axc	axillar carina	9, 17, 18, 76, 77, 79, 88, 90, 91, 93, 95, 96	Gibson 1985	
axu	axillula	9, 17–19, 74, 78, 79	Gibson 1985	
ba2	mesobasalare	10, 12, 76, 101	Gibson 1985	
bstr	basisternum	6–8, 37, 38, 41, 45	Snodgrass 1942	
chm	chamber of the metanotum*	126, 144, 151		
cly	clypeus	1a, 23, 25	Masner 1980	

..... continued on the next page

Appendix (continued)

abbreviation	term	figures	reference	synonyms
cpa	cervical pronotal area*	16, 19, 49, 56, 59, 61		
crva	cervical apodeme	6, 7, 42, 44, 46	Vilhelmsen 2000b	
ctk	central keel	1a, 23, 25	Masner 1980	
cvpr	cervical prominence	6, 7, 16, 35	Ronquist & Nordlander 1989	
daa	dorsal axillar area	9, 17–19, 76, 77, 79, 88, 90, 93, 95, 96	Ronquist & Nordlander 1989	
dip	dorsal incision of the propleuron*	6		
dipr	dorsal incision of the pronotum*	48–50		
dma	dilator muscle apodeme*	132		= peg like invagination *sensu* Duncan 1939
dmfl	dorsal metafurcal lamella*	13, 132, 141		
dmi	dorsal mesopleural inflection	10, 94, 103, 108		= mesepimeral inflection *sensu* Ronquist & Nordlander 1989
dmpa	dorsal metapleural area*	18, 19, 96, 129, 131, 138		
dmpi	dorsal mesopostnotal incision*	120, 125		
dpa	dorsal pronotal area*	3, 16, 19, 39, 48, 49, 56, 105		
dpi	dorsal pronotal inflection	4, 50, 52–54, 60	Ronquist & Nordlander 1989	
dpin	dorsal propodeal inflection*	128		
dpl	dorsal propleural area*	5, 7, 40		
dpnr	dorsal mesopostnotal flange	125	Ronquist & Nordlander 1989	
dprl	dorsal profurcal lamella	5, 7, 8, 37, 41, 45	Vilhelmsen 2000b	
dscl2	mesodiscrimenal lamella	12, 104	Krogmann & Vilhelmsen 2006	
dscl3	metadiscrimenal lamella	14a, b, c, 104, 145, 147	Krogmann & Vilhelmsen 2006	
dscr2	mesodiscrimen	134	modified after Ronquist & Nordlander 1989	=mesodiscrimenal line *sensu* Krogmann & Vilhelmsen 2006
dscr3	metadiscrimen	99, 134	modified after Ronquist & Nordlander 1989	=metadiscrimenal line sensu Krogmann & Vilhelmsen 2006
epax	anterior extension of the preaxilla*	48, 75		
epc	epomial carina	3, 16, 19, 48, 49, 51, 56, 61	Masner 1980	
epl	epicoxal lobe*	5, 16, 19, 35		
epsr	epistomal ridge	1b, 34	Ronquist & Nordlander 1989	
fas	facial striae*	1a, 23, 25		
fdp	frontal depression	22, 24	Masner 1980	
fed	femoral depression	19, 74, 94, 96, 97, 99, 100, 105, 107	Gibson 1997	= mesopleural depression *sensu* Masner 1979b
fld	frontal ledge	21	Masner 1980	

..... *continued on the next page*

Appendix (continued)

abbreviation	term	figures	reference	synonyms
fos	fossa	2, 30	Masner 1983	
frb	mesofurcal bridge	10, 11, 108–110, 113, 116, 117	Heraty *et al.* 1994	
fro	frons	1a	Huber & Sharkey 1993	= upper face *sensu* Gibson 1997
frp	frontal patch*	1a, 23		
fu1a	profurcal arm	5, 7, 8, 40, 41, 45	Vilhelmsen 2000b	
fu1p	profurcal pit	8, 37, 38, 41, 45	Vilhelmsen 2000b	
fu2	mesofurca	11, 12, 108–110, 113	Ronquist & Nordlander 1989	
fu2p	mesofurcal pit	12, 99, 134	Ronquist & Nordlander 1989	
fu3	metafurca	14a, b, c, 15	Vilhelmsen 2000a	
fu3p	metafurcal pit	18, 129, 134	Ronquist & Nordlander 1989	
fust	furcasternum	6–8, 37, 41, 45	Snodgrass 1942	
gen	gena	1a, 2	Huber & Sharkey 1993	
gnp	genal patch*	2, 30		
hmsc	humeral sclerite of the metanotum	15a, 89, 121, 123–125, 142, 144	Duncan 1939	= independent sclerite *sensu* Snodgrass 1942, = X *sensu* Bucher 1948
hy	hypostoma	2, 31	Ronquist & Nordlander 1989	
hyc	hyperoccipital carina	2	Masner 1979a	
hys	hypostomal sulcus	2, 30, 31	Vilhelmsen 1999	
hyst	hypostomal tooth*	2, 26, 30, 32		
iap	interantennal process	1a, 20, 21, 26	Masner 1980	
ics	interocellar space	1b	Masner 1980	
laa	lateral axillar area	9, 17, 19, 76, 77, 79, 88, 90, 93, 95, 96	Ronquist & Nordlander 1989	=lateral panel *sensu* Krogmann & Vilhelmsen 2006
lapa	anterior extension of lateral axillar area*	9, 67, 79, 85, 87, 89, 90, 91–93, 121, 123		
lapr	lateral articular process*	7, 8, 37		
lbp	lateral basisternal projection*	6–8, 37, 38, 41, 45		
lbr	labrum	1b, 26, 28	Gordh & Headrick 2001	
lbrs	labral setae	1a, 26	Yoder 2004	
lcp	longitudinal carina of the propleuron*	5, 36		=ventrolateral carina *sensu* Krogmann & Vilhelmsen
ldl	longitudinal line of the dorsal profurcal lamella*	5, 7, 8, 45		
ldpp	anterolateral depression of the petiole*	153, 155		
lmfa	lateral mesofurcal arm	10–12, 108–110, 113, 115	Heraty *et al.* 1994	
lmms	lateral margin of mesoscutum*	9, 17		
lmsp	lateral mesoscutal spine*	74, 75, 94, 95		
loc	lateral ocellus	1b, 156, 157	Masner 1980	

..... continued on the next page

Appendix (continued)

abbreviation	term	figures	reference	synonyms
lpa	lateral pronotal area*	16, 19, 49, 56, 59, 61		
lpal	lateral propleural area*	5, 7, 8, 36		
lpar	lateral propodeal area	18, 129, 131, 133, 135–137, 140	Ronquist 1995	
lpc	lateral propodeal carina	15, 18, 19, 129, 131, 133, 135, 136–39, 140	Ronquist & Nordlander 1989	
lph2	mesolaterophragma	118–120, 122	Heraty *et al.* 1994	
maa	mandibular adductor muscle apodeme	2, 21	Ronquist & Nordlander 1989	
mas	malar sulcus	1a, 23, 25	Gibson 1997	
maxl	maxilla	2, 31	Ronquist & Nordlander 1989	
mbpm	muscle bearing process of the metanotum	124, 126, 132, 142, 144, 151	Duncan 1939	= lever of the metanotal ramus *sensu* Alam 1951
mc	mesopleural carina	19, 36, 94, 96, 97, 99	Masner 1979b	
mcp	mesocoxal depression*	10, 99, 134		
mcxd	metacoxal depression	18, 99, 134, 137, 138, 140		
mdb	mandible	1a, 21, 156, 157	Gordh & Headrick 2001	
meer	mesepimeral ridge	10–12, 106–115	Ronquist & Nordlander 1989	=posterior marginal ridge of mesopleuron *sensu* Snodgrass 1942; =third mesopleural apodeme *sensu* Duncan 1939
mees	mesepimeral sulcus*	19, 36, 74, 94, 96, 97, 100, 105, 107, 136		= postepimeral foveae *sensu* Johnson and Masner 1985; =recurrent grove of mesopleuron *sensu* Snodgrass 1939
mepi	posterior mesepimeral inflection	11, 12, 106, 108–110, 112–115	Ronquist & Nordlander 1989	
meps	metapleural epicoxal sulcus*	18, 19, 131, 134,		
mes	mesoleural epicoxal sulcus*	16, 19, 96, 99, 100, 134		
metd	metasomal depression*	18, 129, 131, 133, 135, 137, 138, 140		= median propodeal area *sensu* Ronquist 1995
metp	metapleural pit*	18, 19, 96, 131, 133, 139, 140	Krogmann & Vilhelmsen 2006	
mlr	malar region	1a	Masner 1980	
mml	median mesoscutal line	17, 18, 82, 83	Gibson 1985	=median mesoscutal sulcus *sensu* Krogmann & Vilhelmsen 2006
mnsp	metanotal spine*	17, 18, 88, 97, 98		
mnt	metanotal trough	17, 18, 98, 105, 130, 131, 136, 137	Ronquist & Nordlander 1989	
mpa	metapleural apodeme	13, 15, 132, 141–144, 148, 150, 152	Vilhelmsen 2000a	
mprg	metapleural ridge	13, 14c, 15, 132, 144, 149, 152	Vilhelmsen 2000a	
mpxc	metapleural epicoxal carina*	18, 19, 94, 96, 99, 134, 140		

..... *continued on the next page*

Appendix (continued)

abbreviation	term	figures	reference	synonyms
msct	metascutellum	17–19, 98, 105, 131, 133, 137	Vilhelmsen 2000a	= dorsellum *sensu* Gibson 1997, Masner 1980, Ronquist 1995, Yoder 2004
mshs	mesoscutal humeral sulcus	9, 17–19, 72, 75, 83, 84	modified after Masner 1991	
mspb	median sulcus of the post-genal bridge*	2, 31		=conjunction line *sensu* Mineo & Villa 1982; =hypostomal line *sensu* Masner 1983
mtad	metepisternal depression	13, 14c, 99, 134, 142–144, 151	Vilhelmsen 2000a	
mtam	metapleural arm	13, 18, 19, 129, 131, 139, 141, 143, 146, 152	Vilhelmsen 2000a	
mtfa	metafurcal arm	13, 14c, 15, 132, 141–144	Vilhelmsen 2000a	
mtnr	internal metanotal ridge*	126, 127, 132, 142, 144		
mtp	metapleural triangle	19, 96	Johnson 1996	
mtpc	metapleural carina	18, 19, 129, 131, 133–140	Johnson 1984	
mtps	metapleural sulcus	18, 19, 96, 129, 131, 133, 134, 136–140	Vilhelmsen 2000a	
mtsr	metascutellar carina*	86, 88, 98, 131, 133		
nea	netrion apodeme	4, 50, 52, 53, 57, 58, 64, 65	Gibson 1985	
nes	netrion sulcus	3, 16, 49, 51	Masner 1979b	
net	netrion	3, 16, 19, 35, 36, 48, 49, 51, 96, 97, 105	Masner 1979b	
not	notauli	9, 17–19, 75, 80, 82, 83, 84		
obb	orbital band	22	Johnson 1984	
obc	orbital carina	1a, 25	Johnson & Masner 1985	
occ	occipital carina	2, 30, 32, 33	Masner 1980	
ocf	occipital foramen	2	Vilhelmsen 1999	
ocp	occiput	2	Gibson 1997	
ocy	occipital condyle	2, 30	Vilhelmsen 1999	
oma	occlusor muscle apodeme	50, 52, 58, 59	Gibson 1985	
orf	oral foramen	156, 157	Ronquist & Nordlander 1989	
pa	pleural apodeme*	10, 12, 64, 65, 67, 101–104, 106, 118		= pleural apophysis *sensu* Snodgrass 1942; = mesopleural apophysis *sensu* Alam 1951, Dhillon 1966
pap	postalar process	9, 17–19, 75, 77, 78, 84, 86–92, 123, 124	Ronquist & Nordlander 1989	=posterior wing process
papc	postacetabular patch*	19, 35, 96, 100, 134		= acetabular field *sensu* Johnson 1984
pax	preaxilla	9, 17, 19, 72, 74–79	Gibson 1985	
pcs	propleural cervical sulcus*	5, 16, 19, 35, 36		
pcxr	paracoxal ridge	13, 14c, 15, 67, 132, 141–146, 151	Vilhelmsen 2000a	
pcxs	paracoxal sulcus	19, 99, 105, 131, 133, 138, 140	Vilhelmsen 2000a	

..... continued on the next page

Appendix (continued)

abbreviation	term	figures	reference	synonyms
pdem	posterodorsal edge of the mesopleuron*	10–12, 101, 103, 106, 108–110, 113, 115		
pdep	posterodorsal edge of pronotum*	4, 48, 52–54, 97, 105		
pep	posterior extension of preaxilla*	9, 17, 85, 123		
pes	propleural epicoxal sulcus*	5, 16, 19, 35		
pg	postgena	2	Gibson 1997	
pgb	postgenal bridge	2, 30–32	Vilhelmsen 1999	
pgp	postgenal pit*	2, 30, 32		= hypostomal pit *sensu* Bin & Dessart 1983
ph1	first phragma	9, 66, 68–72, 78, 122	Ronquist & Nordlander 1989	
ph2	second phragma	78, 87, 89, 120–122, 125, 142, 144	Ronquist & Nordlander 1989	
ph3	third phragma	13, 15, 128, 132, 141, 143–146, 151, 152	Ronquist & Nordlander 1989	
pla	plical area	18, 136, 140	Gibson 1997	
plc	plica	18, 19, 136, 140	Gibson 1997	
plsf	pleurostomal fossa	2, 26, 28	Ronquist & Nordlander 1989	
plsr	pleurostomal ridge	1b, 34	Ronquist & Nordlander 1989	
plwa3	metapleural wing articulation	15, 124, 128, 141, 146	Duncan 1939	
pmma	posterior mesepimeral area*	19, 36, 74, 96, 97, 100		= mesepimeron *sensu* Masner 1979b
pnap	axillary lever	87, 89, 118, 119, 120–123, 125	Heraty *et al.* 1994	
pnwp	posterior notal wing process	9, 17, 77, 90, 91, 93	Gibson 1986	
pooc	postocciput	2	Ronquist & Nordlander 1989	
pos	postgenal sulcus*	2, 30, 32		=postoccipital sulcus *sensu* Mineo & Villa 1982, =hypostomal sulcus *sensu* Masner 1983
pp	pleural pit	19, 94, 96, 97, 100, 107	Masner 1979b	
ppa	propleural arm	5, 40, 41	Ronquist & Nordlander 1989	
ppi	posterior pronotal inflection	4, 48, 50, 52–55, 60, 62	Gibson 1985	
ppp	posterior propodeal projection*	18, 19, 136, 140		
pprl	posterior profurcal lamella	5, 8, 40, 44, 45	modified after Vilhelmsen 2000b	
ppsu	posterior pronotal sulcus*	35, 56, 96		
prcs	pronotal cervical sulcus*	3, 16, 19, 48, 56, 61, 105		
prfo	propodeal foramen	13, 18, 129, 137, 138	Vilhelmsen 2000a	
prp	preocellar pit	1a, 20	Bin and Dessart 1983	

..... *continued on the next page*

Appendix (continued)

abbreviation	term	figures	reference	synonyms
prsl	parapsidal line	9, 17, 18, 75, 77, 82, 84	Gibson 1985	
prth	propodeal tooth	18, 129, 137, 138	Duncan 1939	
psc	parascutal carina	9, 17, 18, 72, 74–79	Gibson 1985	
pscy	pleurostomal condydle	1b, 26, 28	Ronquist & Nordlander 1989	
psin	prosternal incision*	7, 8, 37, 38, 41, 45		
pspp	prespiracular propodeal area	18, 19, 133, 135–137, 139?, 140	not prespiracular area *sensu* Ronquist 1995	
pss	pronotal suprahumeral sulcus*	3, 16, 19, 36, 48, 49, 56, 105		
pssu	prespecular sulcus*	19, 74, 94, 96, 97, 105		
psu	posterior mesoscutellar sulcus*	9, 17–19, 84, 86, 88, 90		
ptp	posterior tentorial pit	1b, 2, 30, 32	Bin & Dessart 1983	
pvpp	posteroventral metapleural pit*	131, 138, 139	= peg like invagination *sensu* Duncan 1939	
pxc	preaxillar carina*	9, 17, 18, 76, 78, 79		
saa	supraalar area	18, 19, 130, 131	Ronquist & Nordlander 1989	= semidetached sclerite *sensu* Snodgrass 1942, = metanotal segments *sensu* Duncan 1939, = metanotal ramus *sensu* Alam 1951)
sapi	subalar pit	10, 11, 19, 36, 74, 76, 94, 96, 100, 105	Duncan 1939	
sbc	submedian carina	1a, 24	Johnson & Masner 1985	
sca	metascutellar arm	126, 127	Krogmann & Vilhelmsen 2006	
scbr	scutellar bridge*	87, 89		
scu	mesoscutellum	9, 17–19, 75, 83–88, 90	Snodgrass 1942	
shms	mesoscutal suprahumeral sulcus	9, 16, 17, 19, 72, 75, 83, 84	modified after Masner 1991	
sk	skaphion	9, 16, 17, 19, 80, 81	Masner 1972	
skpc	skaphion carina*	9, 16, 17, 80, 81		
sp2	mesothoracic spiracle	4, 19, 48, 52, 60, 61	Duncan 1985	
spec	speculum	19, 36, 74, 94, 96, 97, 100, 105	Ronquist & Nordlander 1989	=upper mesepimeron sensu Gibson 1986; Krogmann & Vilhelmsen 2006
ssr	scutoscutellar ridge	85, 87, 89, 91, 92	Krogmann & Vilhelmsen 2006	
sss	scutoscutellar sulcus	9, 17–19, 72, 74, 75, 78, 83, 84, 86, 90, 95	Gibson 1985	
str	sternaulus	16, 19, 96, 134	Wharton 2006	= episternal foveae *sensu* Johnson 1984, not sternaulus *sensu* Masner 1976, 1991, Masner and Huggert 1989
T1sp	propodeal spiracle	15, 18, 19, 129, 133, 135–137, 139	Duncan 1939	

..... *continued on the next page*

Appendix (continued)

abbreviation	term	figures	reference	synonyms
tac	transaxillar carina*	9, 17–19, 75, 77–79, 88, 95, 96		
tbr	tentorial bridge	2, 29	Ronquist & Nordlander 1989	
tga	tegula	16, 19, 74, 76, 97	Snodgrass 1942	
tmc	transmetanotal carina	17–19, 86, 88, 97, 98, 126, 130, 131, 136, 137	Duncan 1939	
tntr	tentorium	1b, 27, 29	Duncan 1939	
tps	transpleural sulcus	19, 105	Johnson & Masner 1985	
trt	torular triangle*	1a, 23, 25		
tsa	transscutal articulation	9, 17–19, 72, 74, 75, 78, 83, 84, 86, 90	Gibson 1985	
valm	vertical apodemal lobe of the mesoscutellum*	9, 85, 87, 92, 93, 120		
vbp	ventral bridge of the pronotum	3, 16, 35, 49, 50, 56, 57, 59–61		=venter *sensu* Gibson 1985
vcmp	ventral carina of the metapleuron*	13, 14c, 18, 99, 134, 142–144		
vgp	ventral edge of propleuron*	7, 8, 35, 37		
vla	ventral lamella*	1b, 27, 29		
vmfl	ventral metafurcal lamella*	13, 132, 141, 142		
vmpa	ventral metapleural area*	18, 19, 96, 129, 131, 138		
vpa	ventral propleural area*	5, 7, 8, 36		
vpl	ventral profurcal lamella*	5, 7, 8, 40, 41, 45		
vplc	ventral mesopleural carina*	10, 12, 16, 19, 96, 99, 100, 134		
vpnr	ventral mesopostnotal flange	125	Ronquist & Nordlander 1989	
vprc	ventral propodeal carina*	18, 134, 137, 140		
vpt	vertex patch*	1a		
vrcl	vertical ridge of the clypeus*	1b, 34		
vrtm	vertical lobe of mesoscutum*	9, 69, 70, 72		
vrx	vertex	2	Huber & Sharkey 1997	
vvl	ventral vertical lobe of the propleuron*	7, 8, 37, 38, 41, 45		

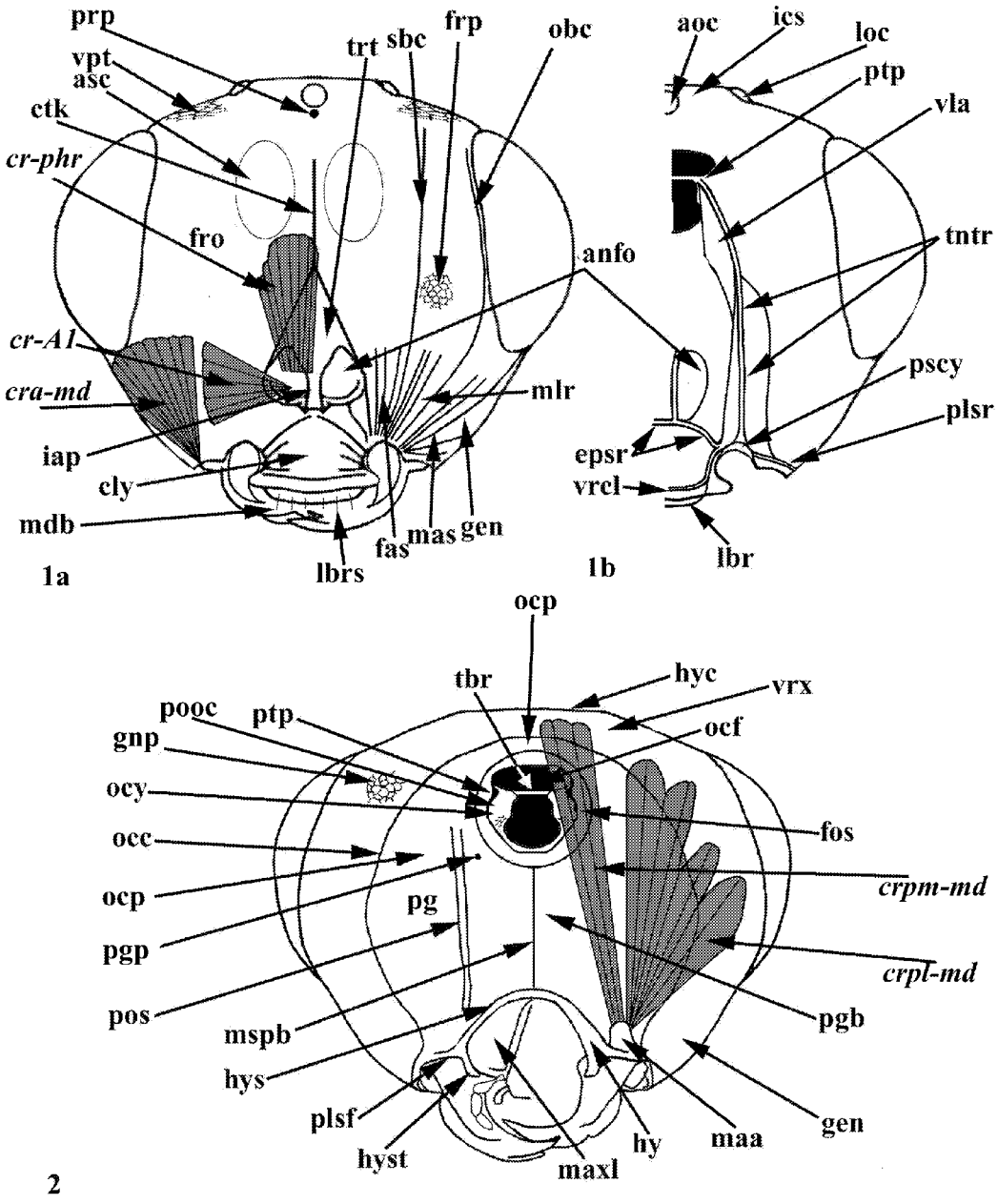

FIGURES 1, 2. Generalized scelionid, head. 1, anterior view (a=external, b=internal); 2, posterior view.

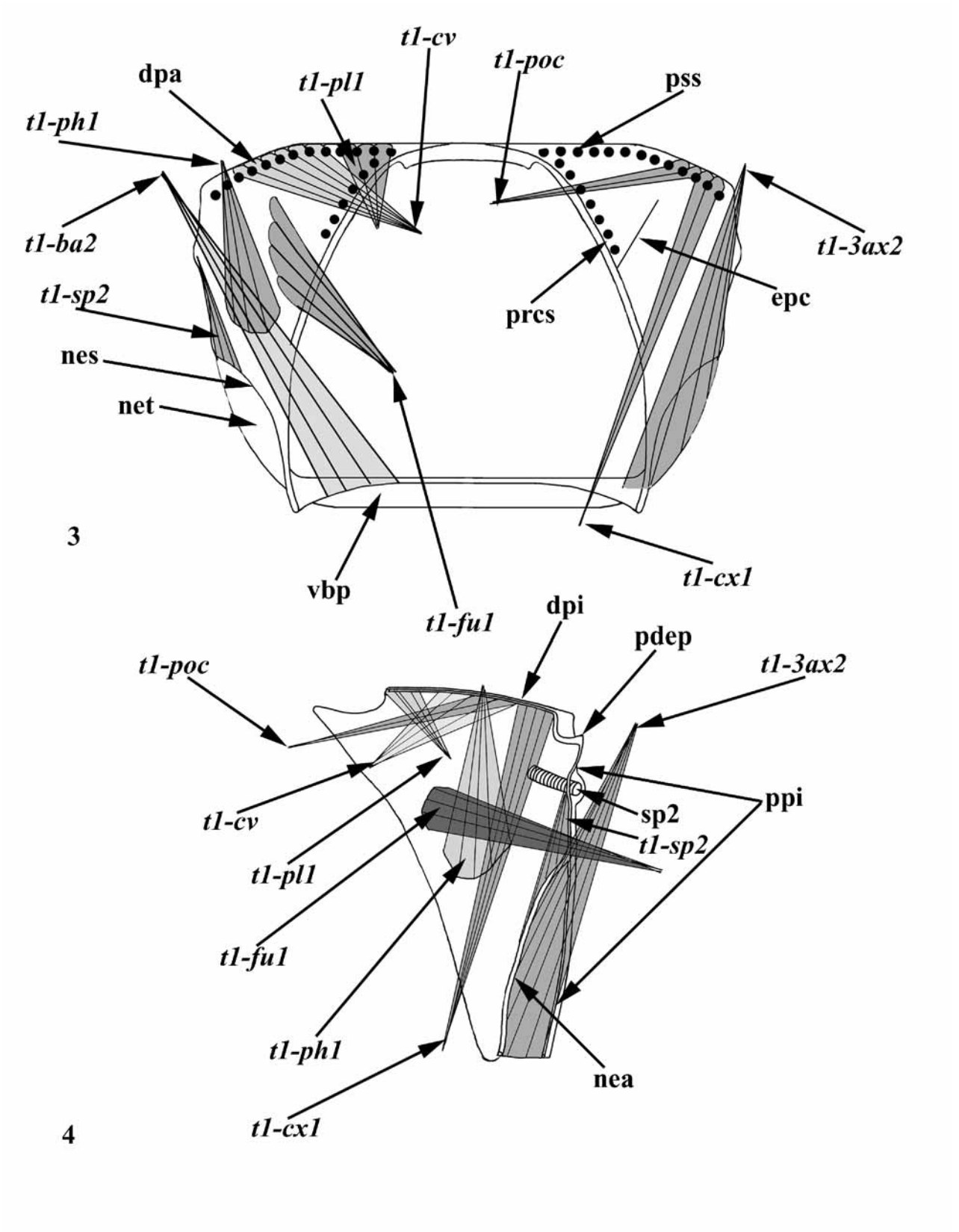

FIGURES 3, 4. Generalized scelionid, pronotum. 3, anterior view; 4, median view.

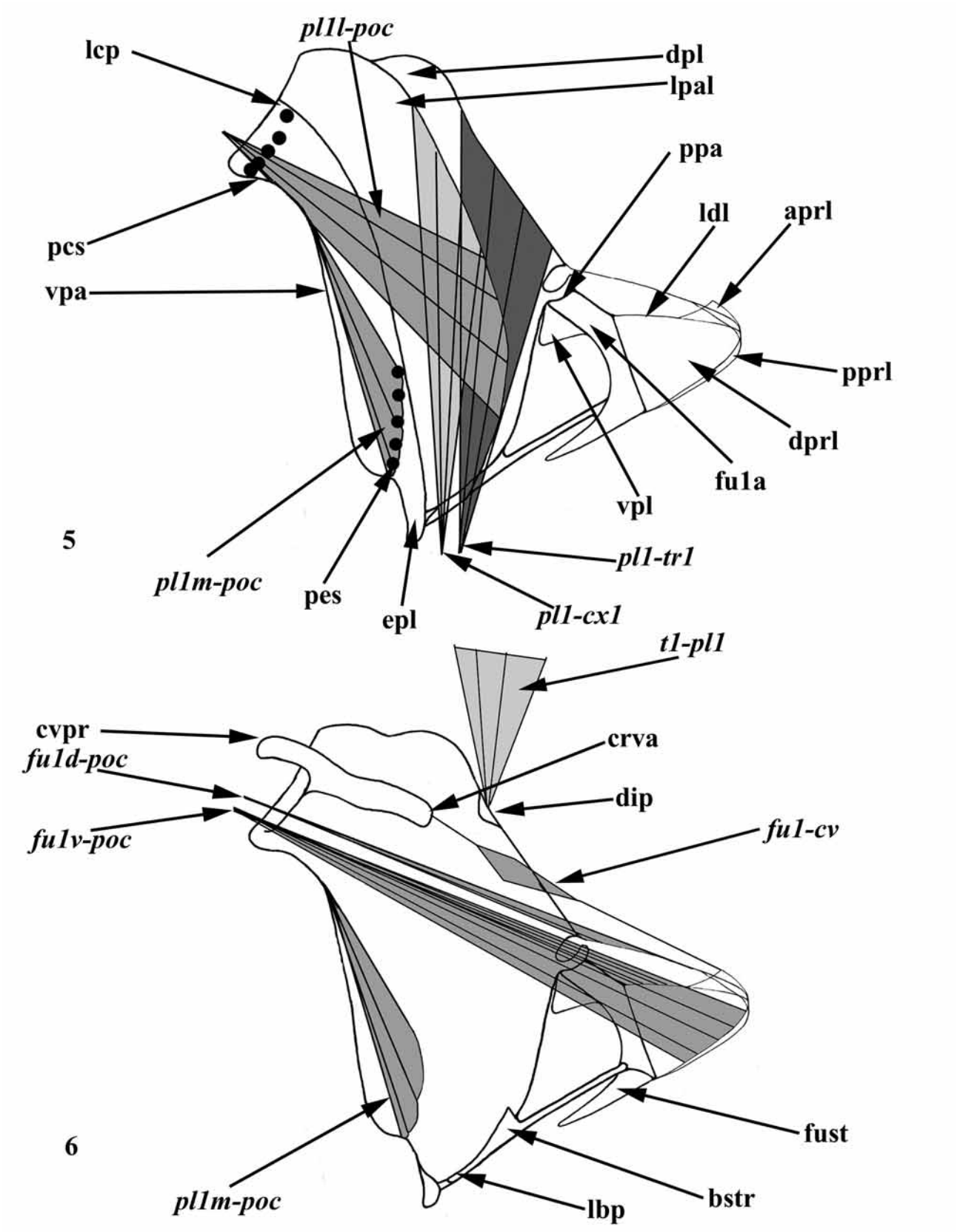

FIGURES 5, 6. Generalized scelionid, propectus. 5, lateral view; 6, median view.

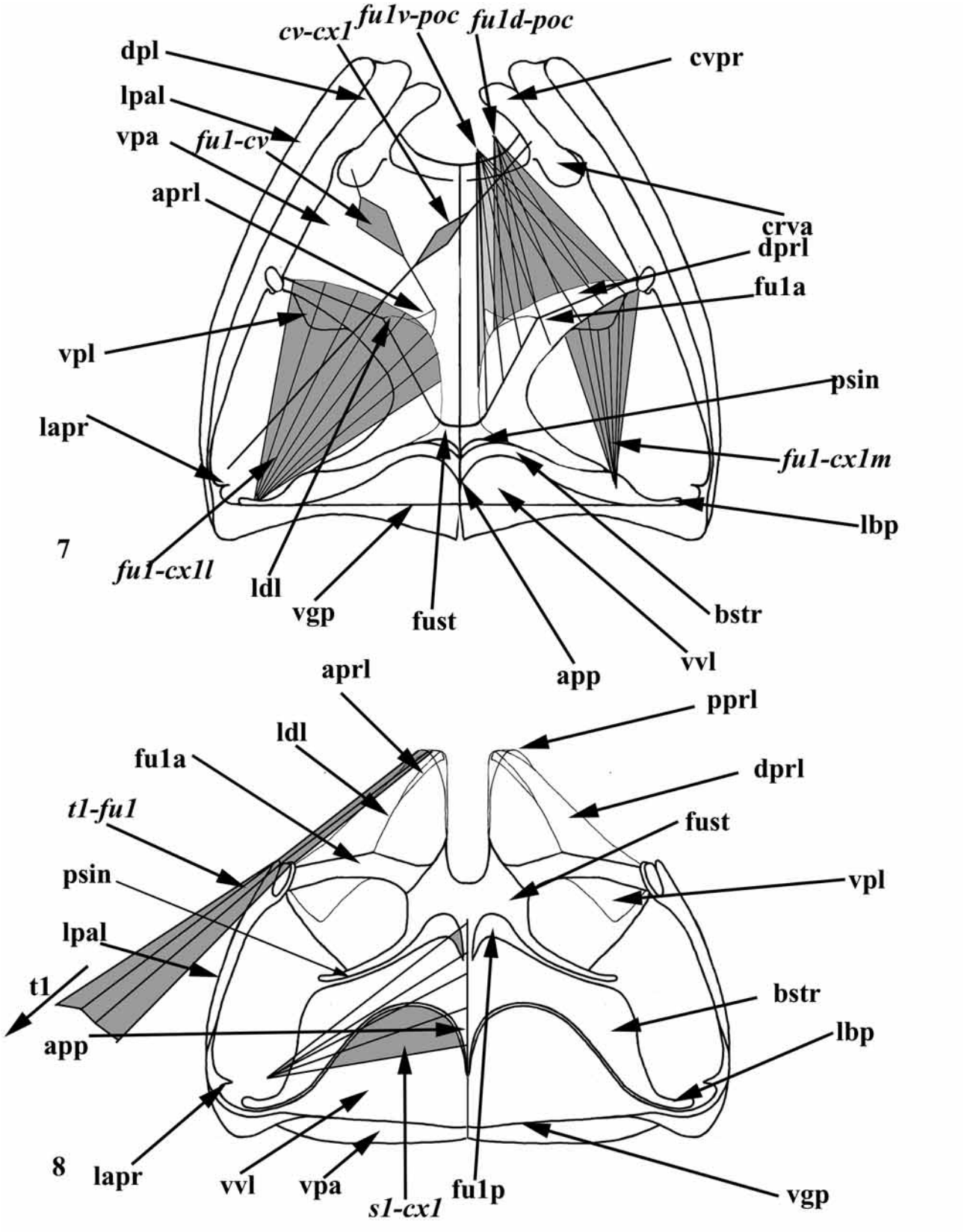

FIGURES 7, 8. Generalized scelionid, propectus. 7, posterior view; 8, ventral view.

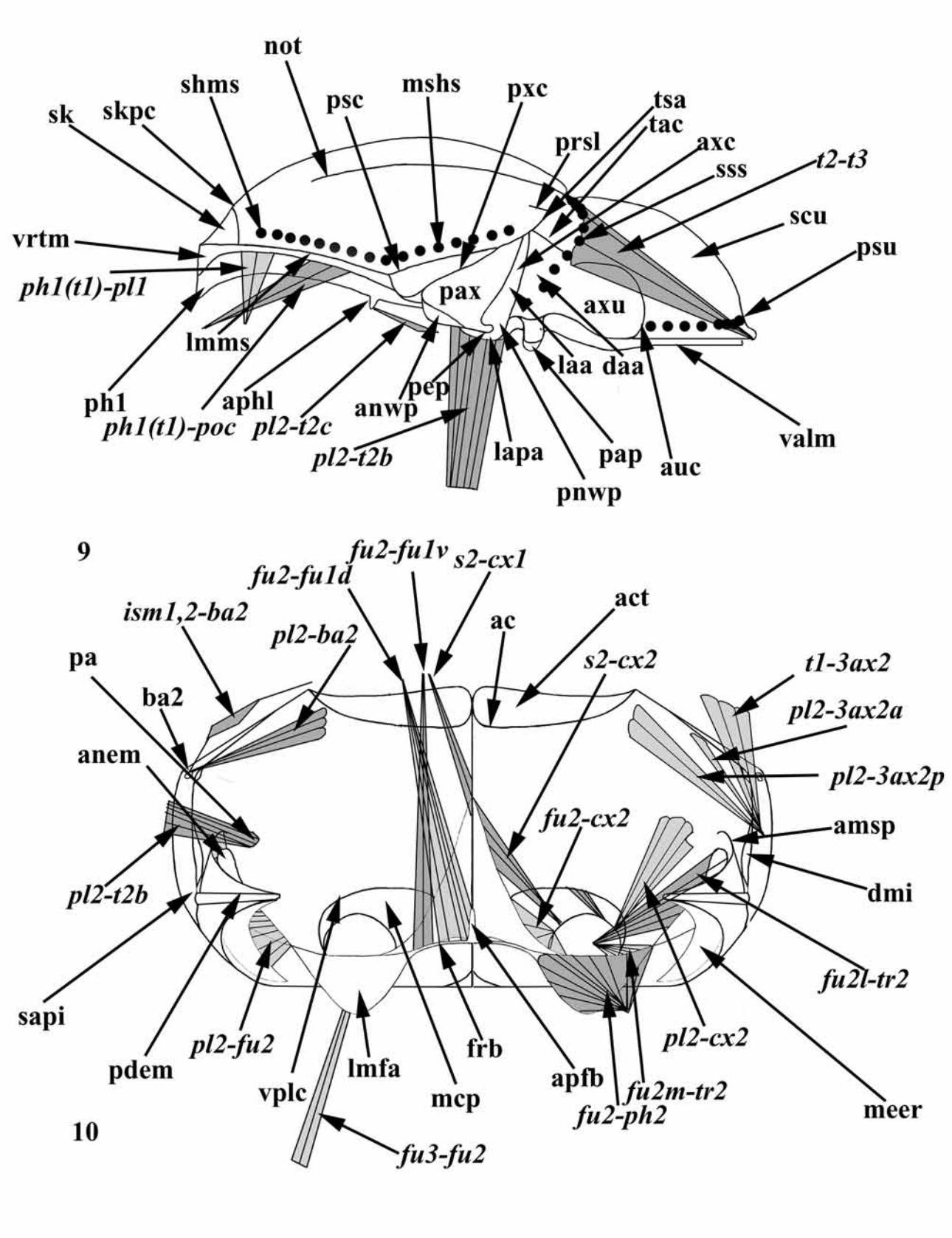

FIGURES 9, 10. Generalized scelionid. 9, mesonotum, lateral view; 10, mesopectus, dorsal view.

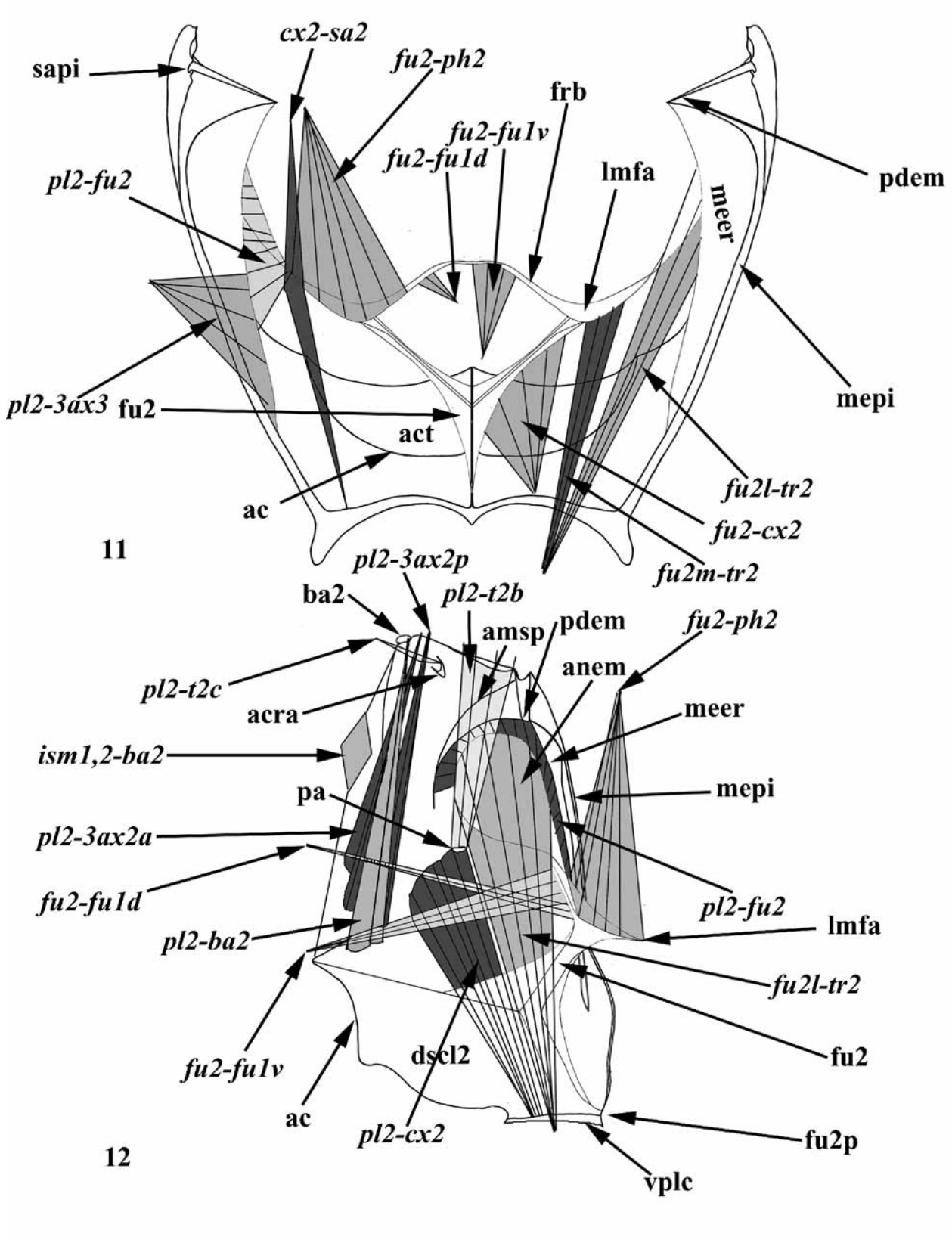

FIGURES 11, 12. Generalized scelionid, mesopectus. 11, posterior view; 12, median view.

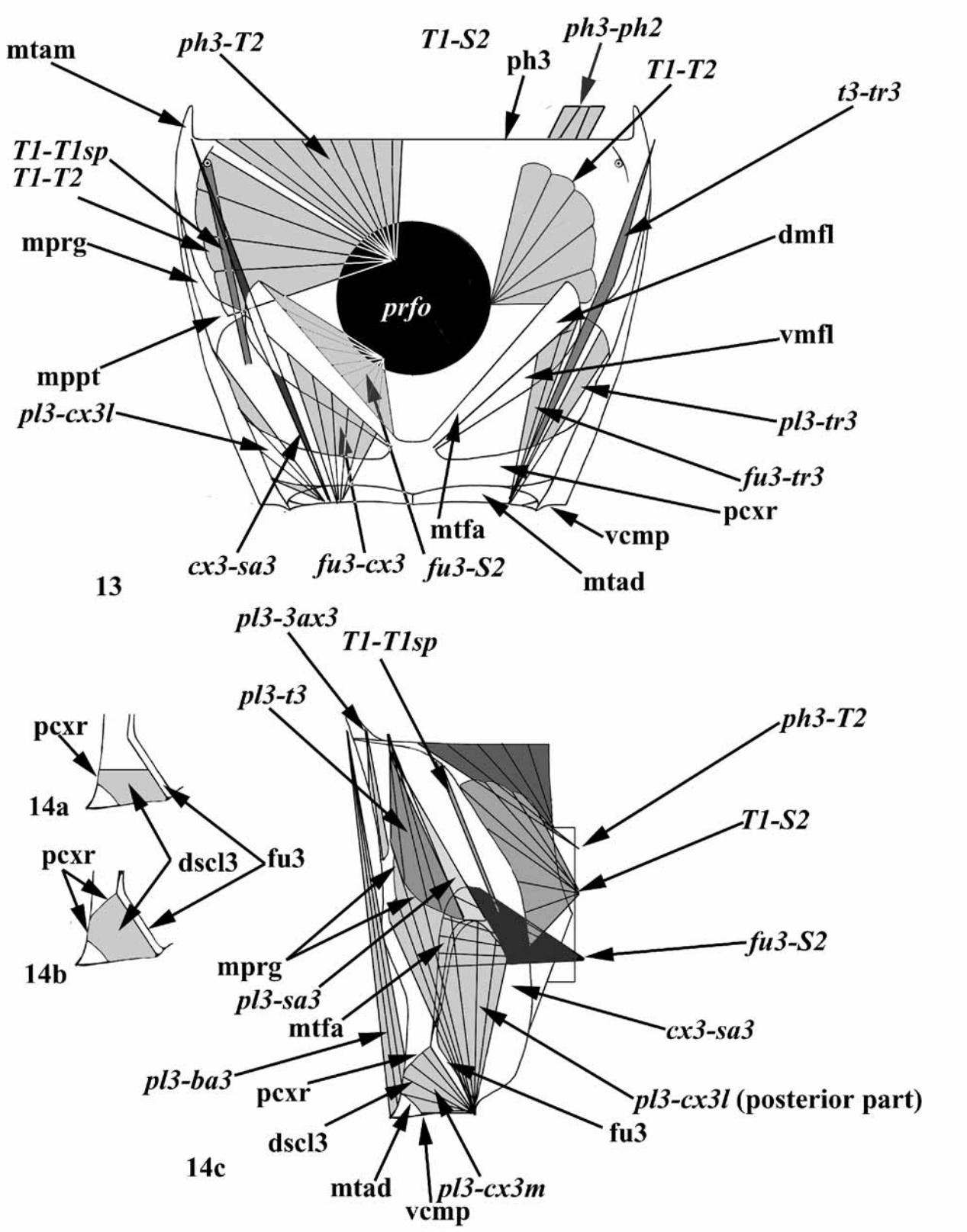

FIGURES 13, 14. Generalized scelionid. 13, metapectal-propodeal complex, anterior view; 14a, b, discrimenal lamella and paracoxal ridge, median view; 14c, metapectal-propodeal complex median view.

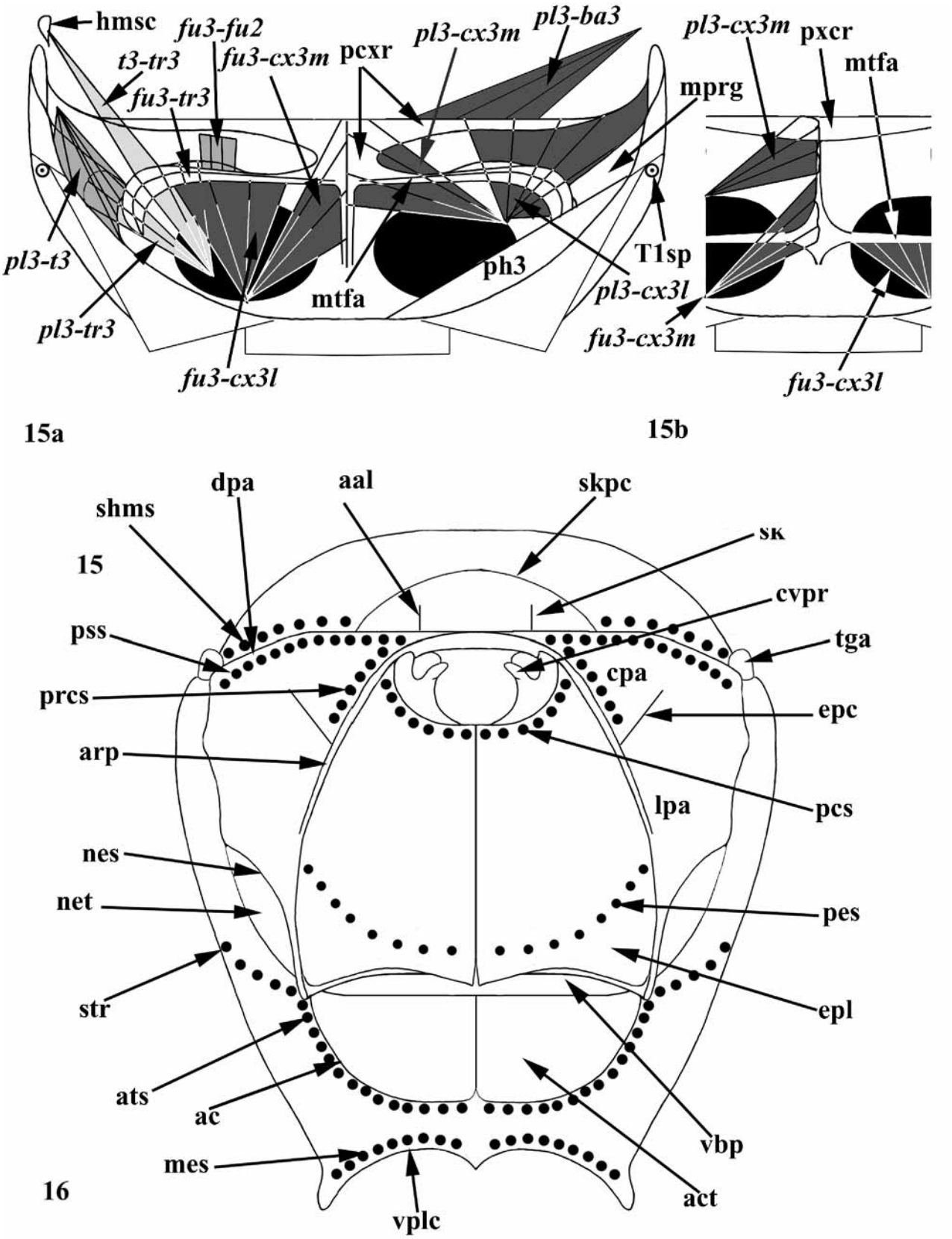

FIGURES 15, 16. Generalized scelionid. 15a, b, metapectal-propodeal complex dorsal view; 16, mesosoma, anterior view.

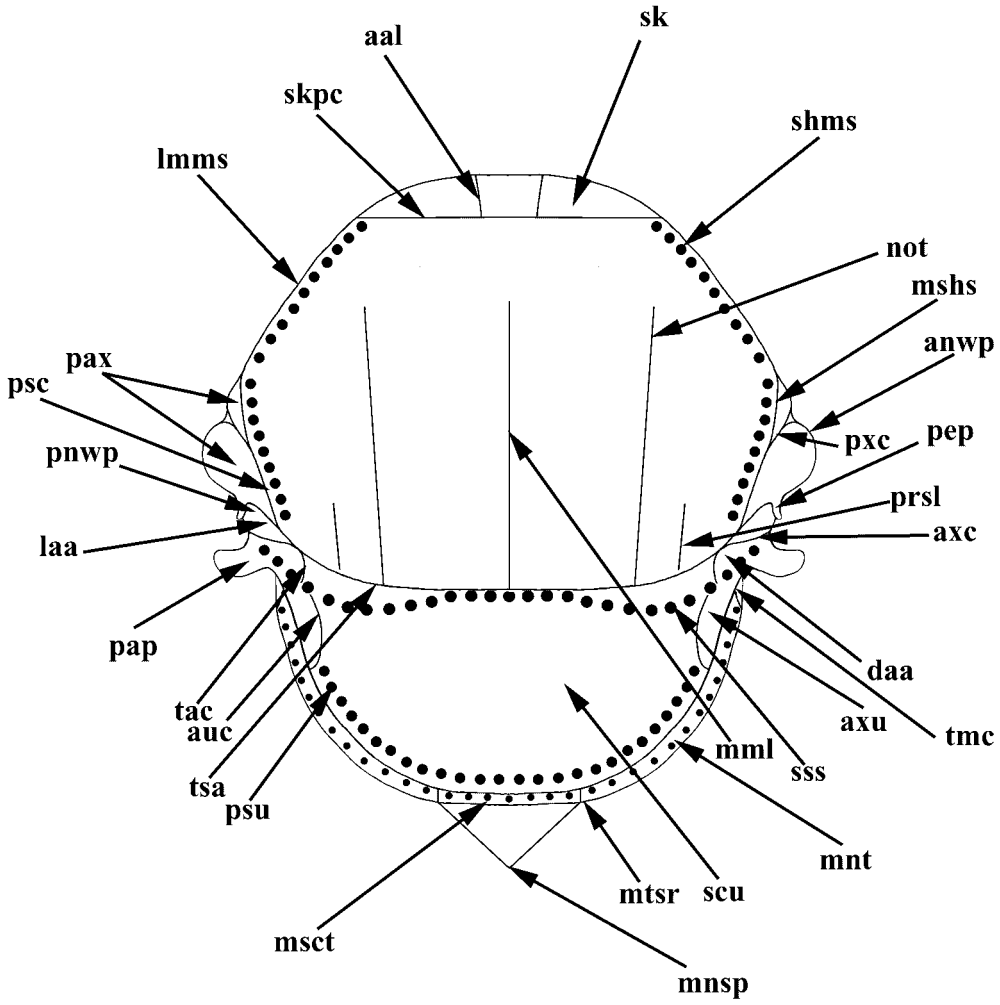

FIGURE 17. Generalized scelionid, mesonotum dorsal view.

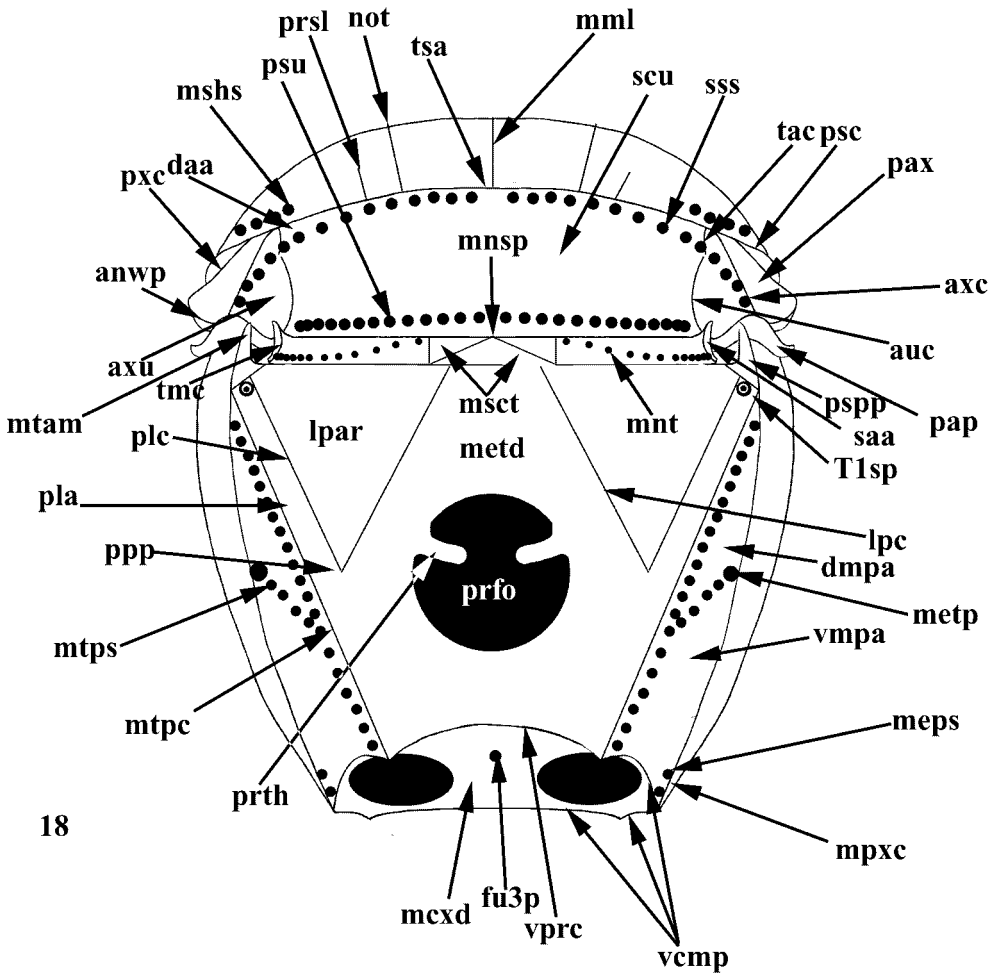

FIGURE 18. Generalized scelionid, mesosoma, posterior view.

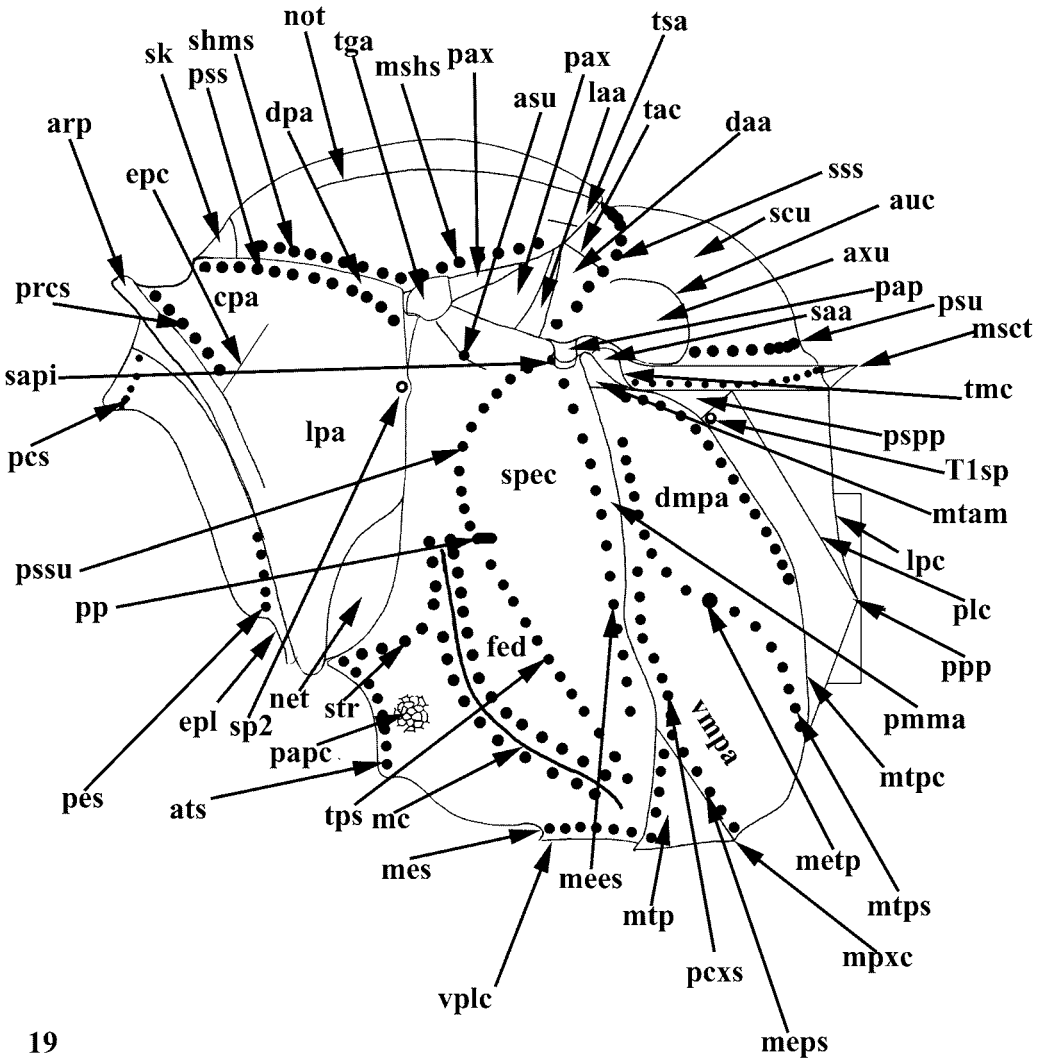

FIGURE 19. Generalized scelionid, mesosoma, lateral view.

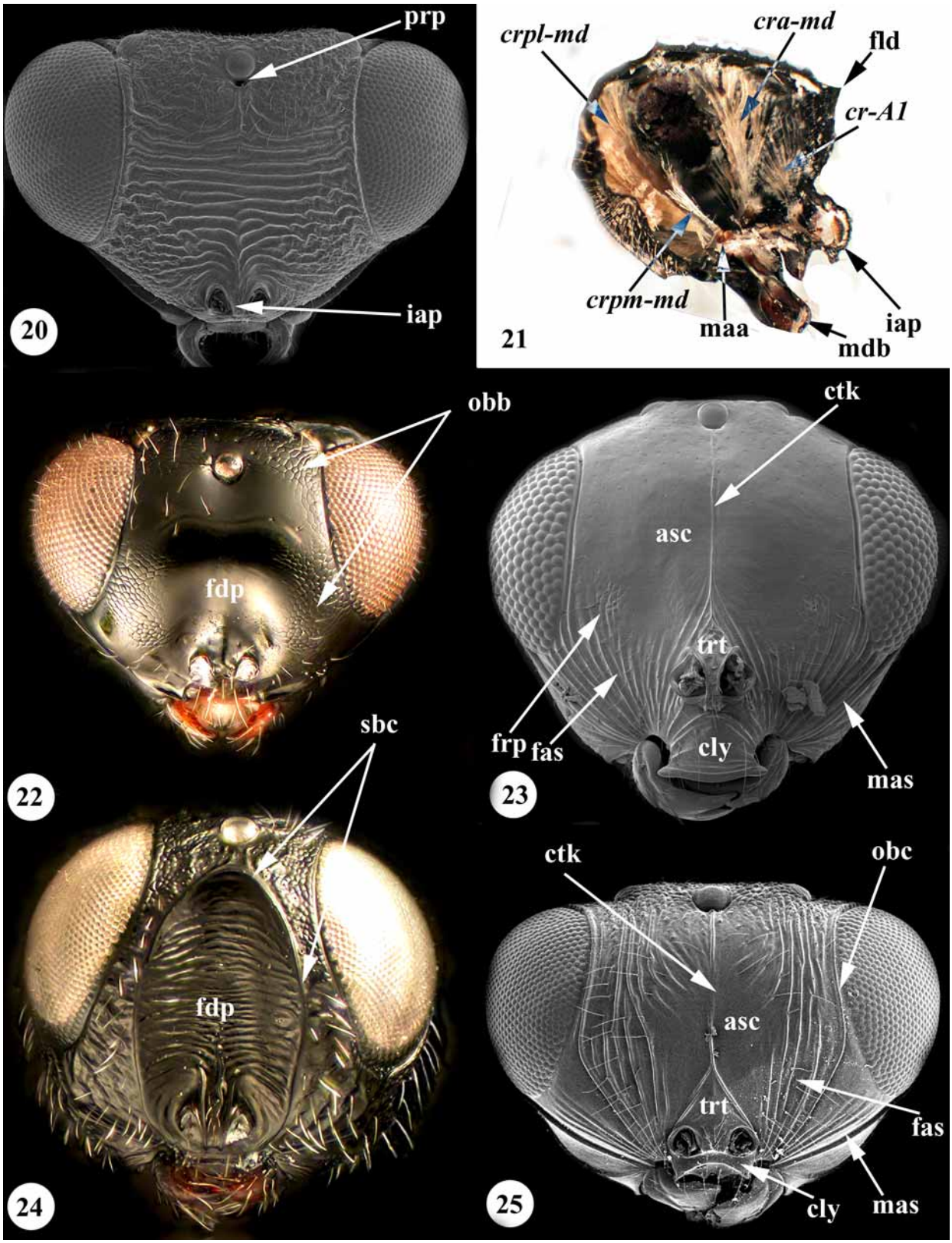

FIGURES 20–25. 20, *Gryon* sp., head, anterior view; 21, *Sparasion sp.*, head, sagittal section; 22, *Telenomus heydeni*, head, anterior view; 23, *Trimorus sp.*, head, anterior view; 24, *Baryconus sp.*, head, anterior view; 25, *Psix sp.*, head, anterior view.

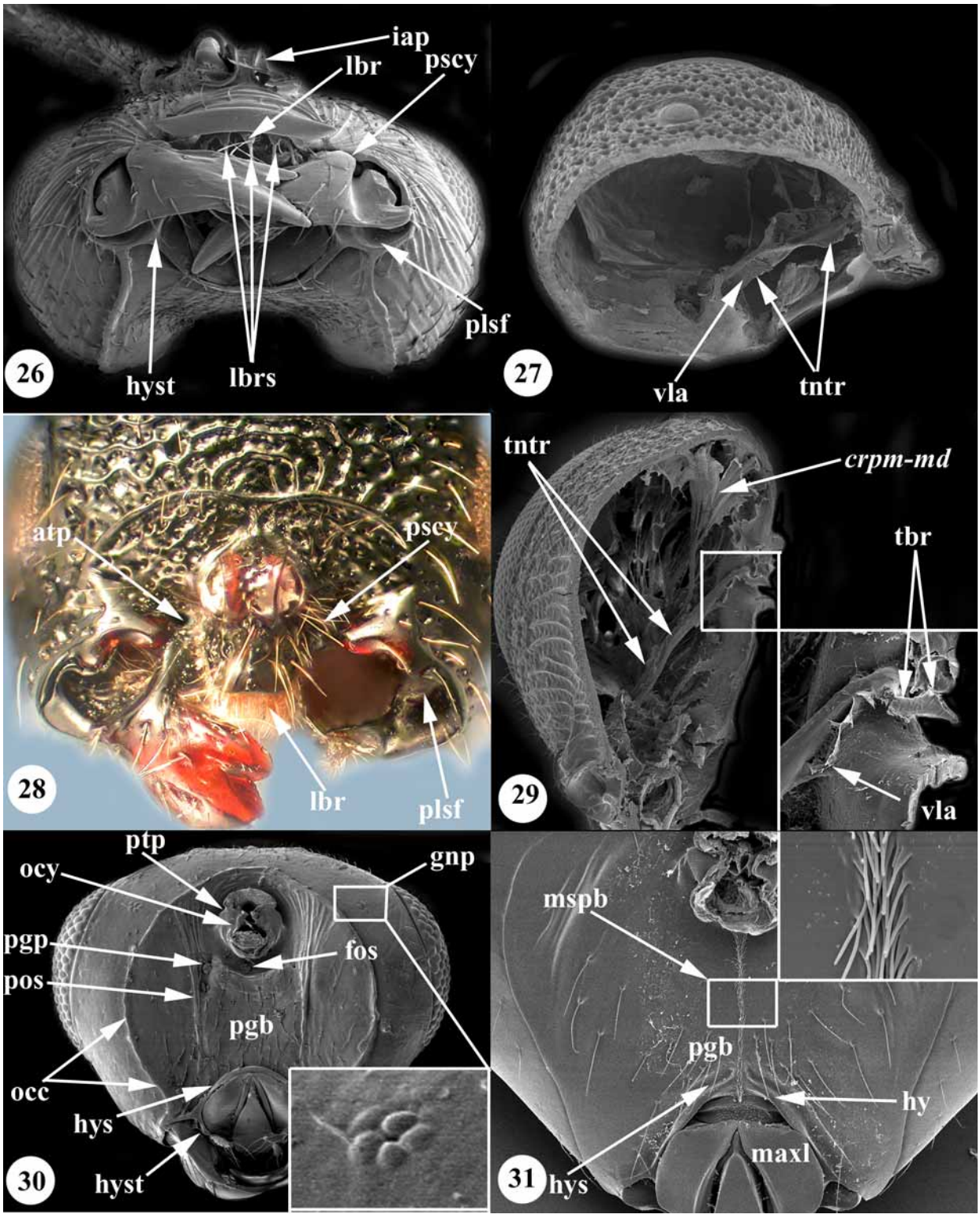

FIGURES 26–31. 26, *Trimorus bohemicus*, head, ventral view; 27, *Nixonia sp.*, head, sagittal section, anterolateral view; 28, *Sparasion sp.*, oral foramen, anteroventral view; 29, *Gryon sp.*, head, sagittal section, anterolateral view; 30, *Trimorus sp.*, head, posterior view; 31, *Telenomus heydeni*, head, posterior view.

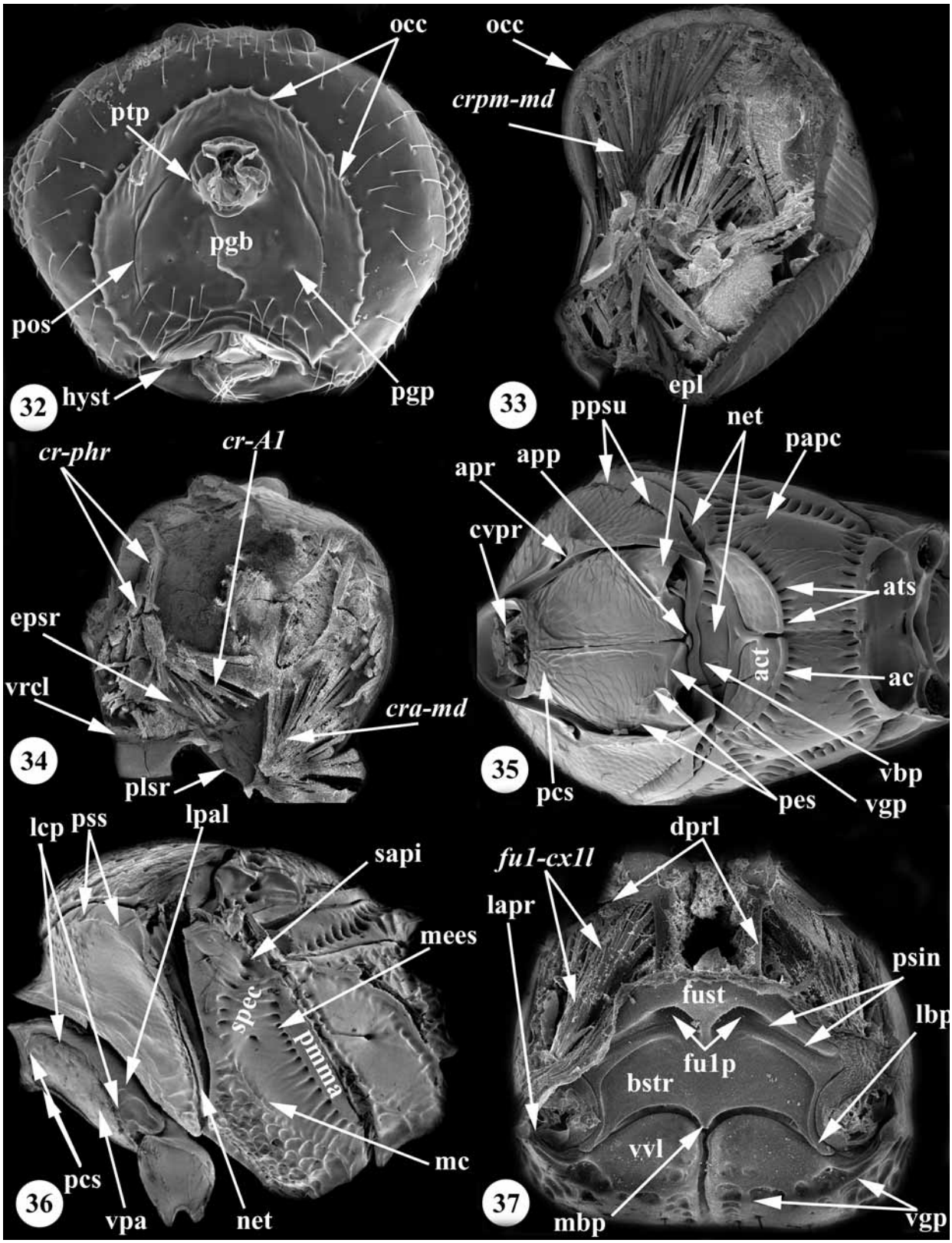

FIGURES 32–37. 32, *Trimorus sp.*, head, posterior view; 33, *Baryconus sp.*, head, sagittal section, anterolateral view; 34, *Archaeoteleia sp.*, head, transverse section, posterior view; 35, *Trimorus flavipes*, mesosoma, anteroventral view; 36, *Trimorus arenicola*, mesosoma, lateral view; 37, *Scelio sp.*, propectus, ventral view.

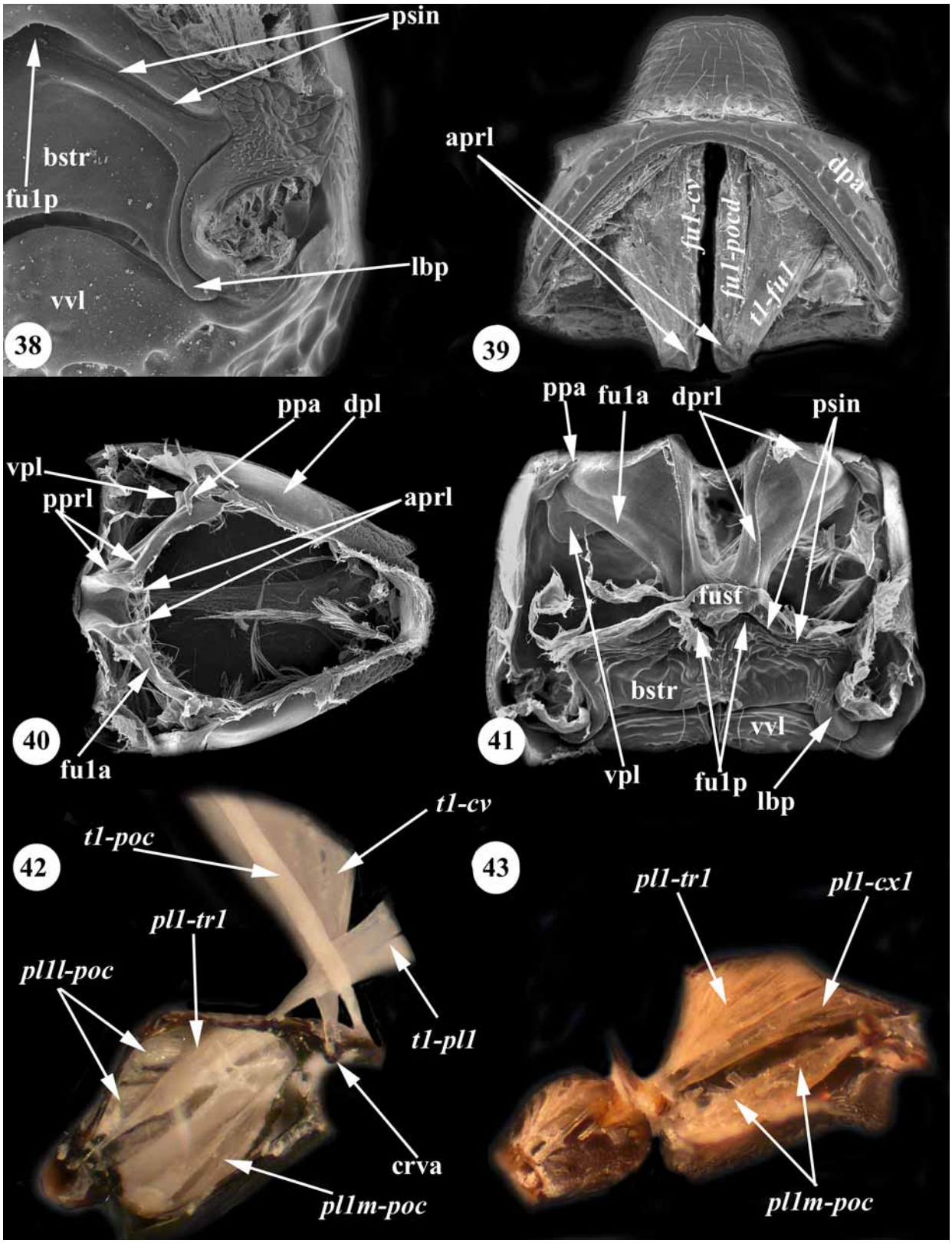

FIGURES 38–43. 38, *Scelio sp.*, prothorax, posteroventral view; 39, *Scelio sp.*, prothorax, dorsal view; 40, *Archaeoteleia sp.*, prothorax, posterodorsal view; 41, *Archaeoteleia sp.*, prothorax, posteroventral view; 42, *Telenomus sp.*, propleuron, median view; 43, *Sparasion sp.*, propleuron, median view.

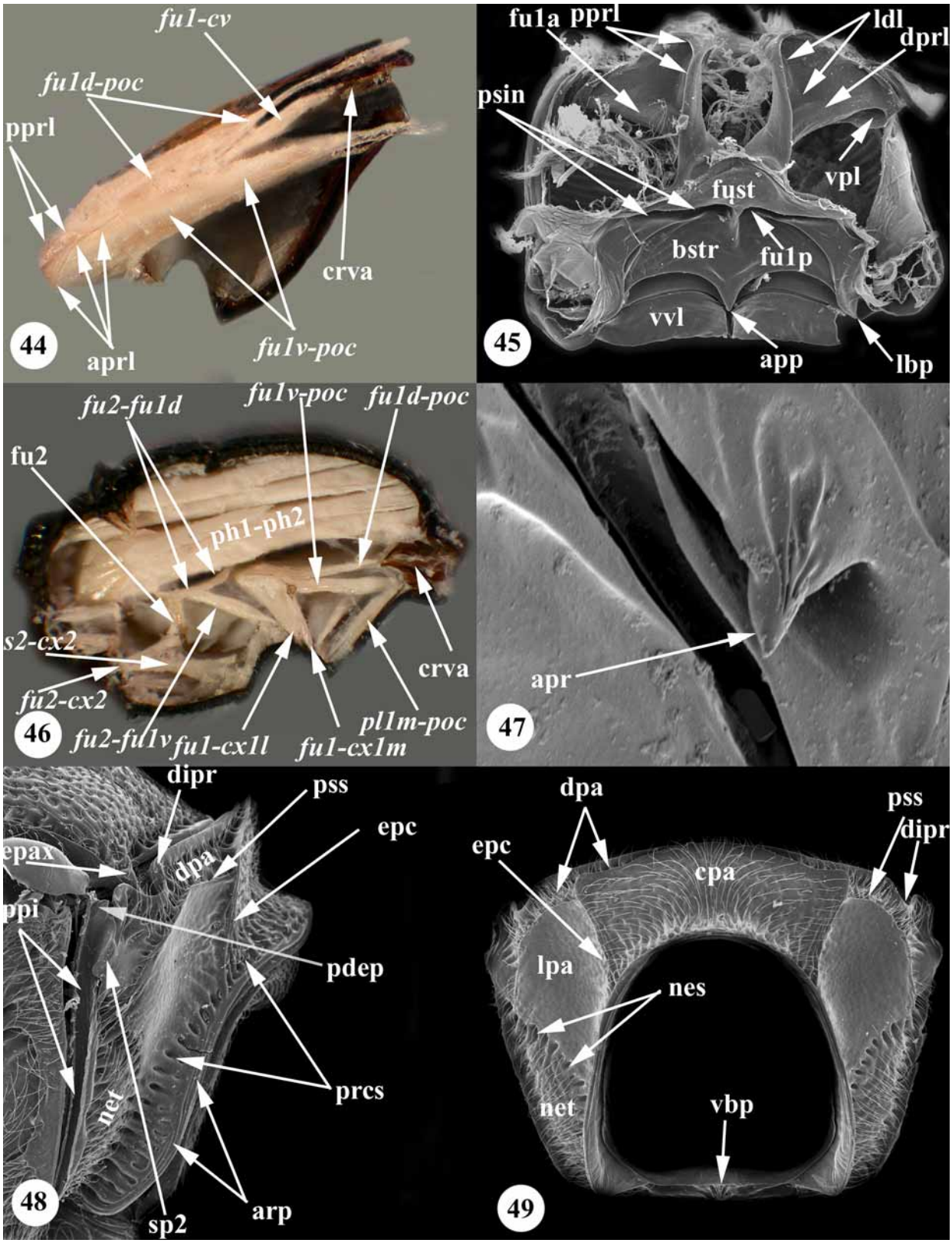

FIGURES 44–49. 44, *Scelio sp.*, propectus, median view; 45, *Telenomus sp.*, propectus, posteroventral view; 46, *Baryconus sp.*, mesosoma, sagittal section, lateral view; 47, *Trimorus flavipes*, anterior process of the pronotum, anterolateral view; 48, *Archaeoteleia sp.*, pronotum, lateral view; 49, *Archaeoteleia sp.*, pronotum, anterior view.

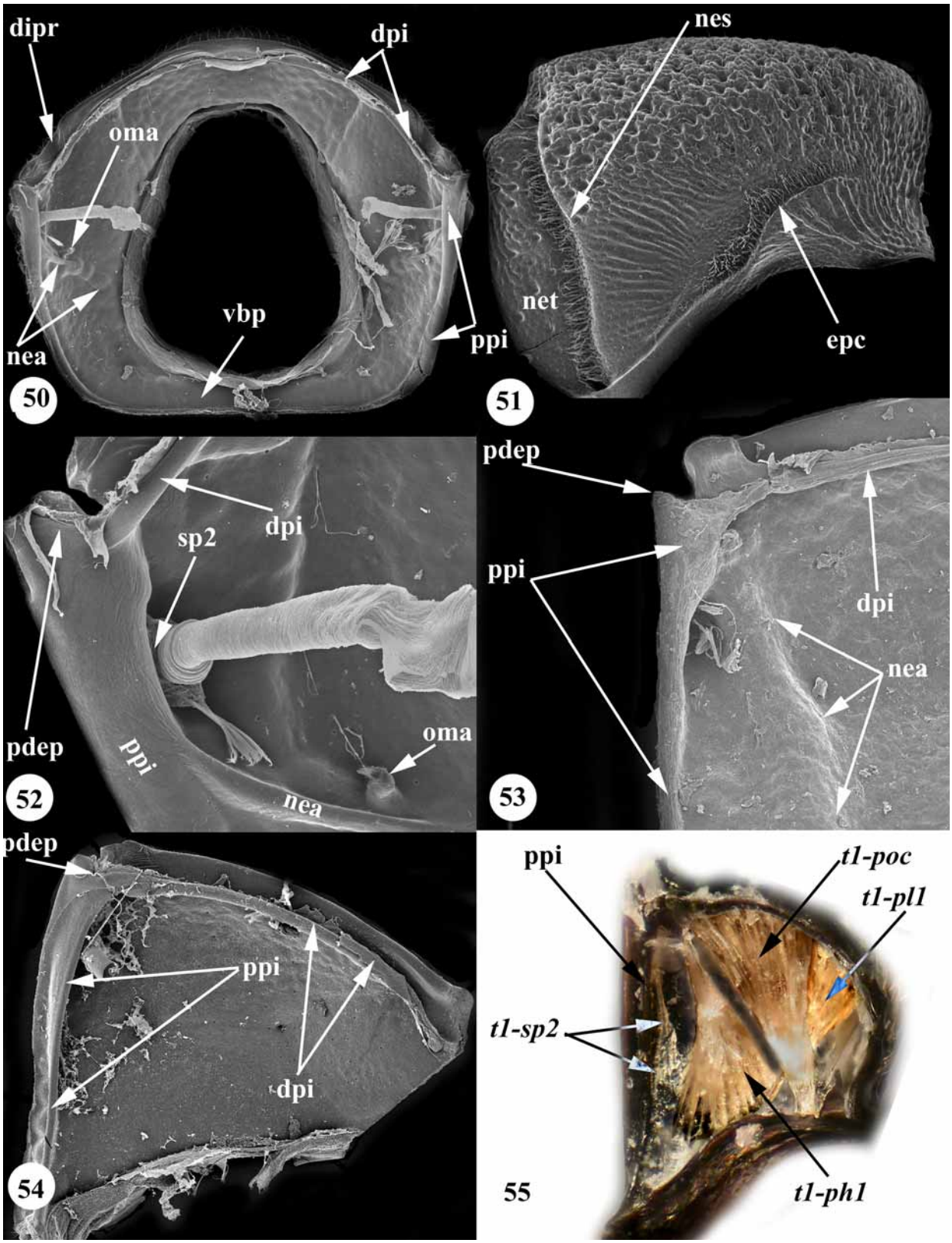

FIGURES 50–55. 50, *Archaeoteleia sp.*, pronotum, posterior view; 51, *Nixonia sp.*, pronotum, lateral view; 52, *Archaeoteleia sp.*, pronotum, posteromedian view; 53, *Nixonia sp.*, pronotum, posteromedian view; 54, *Sparasion sp.*, pronotum, median view; 55, *Sparasion sp.*, pronotum, median view.

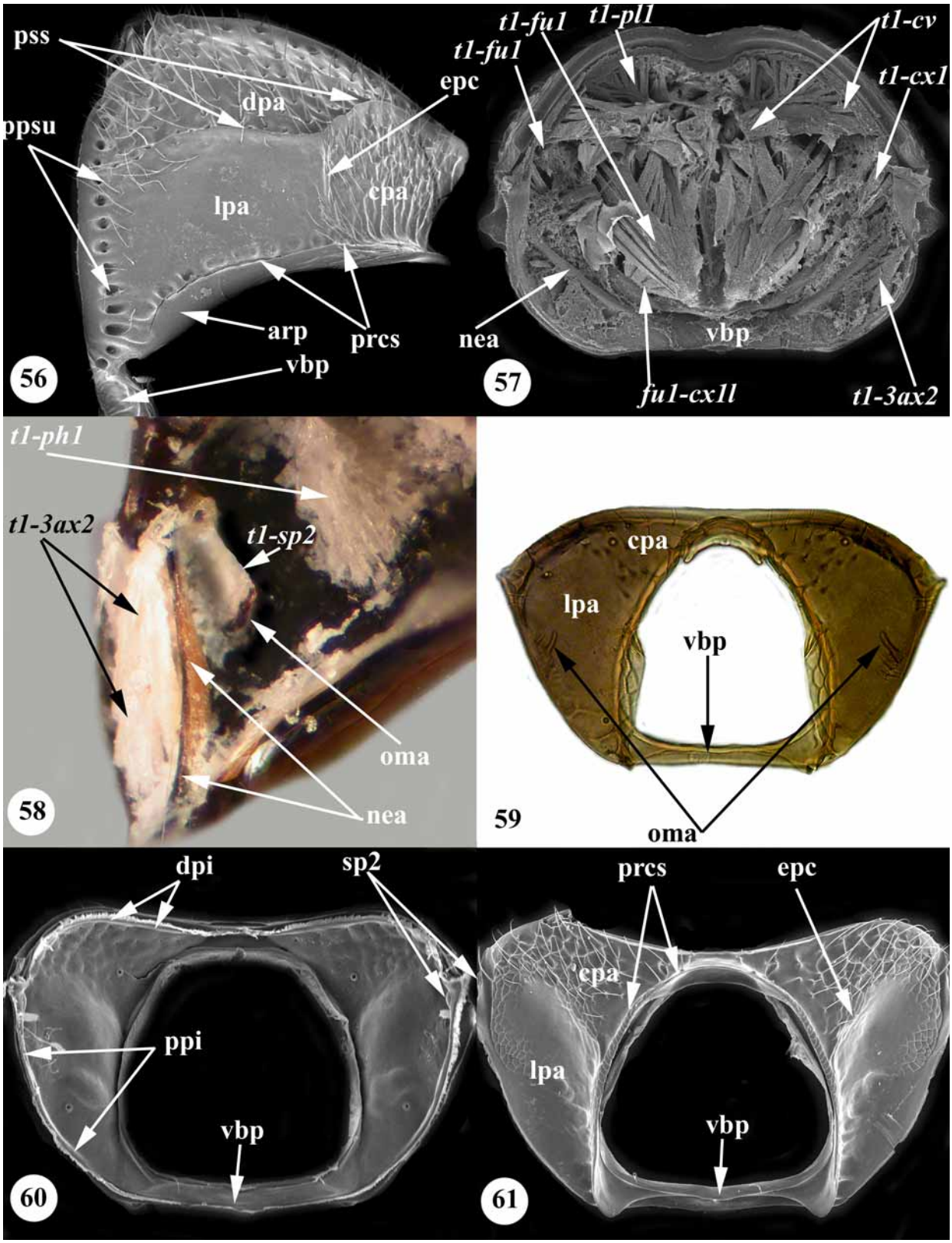

FIGURES 56–61. 56, *Sparasion sp.*, pronotum, lateral view; 57, *Scelio sp.*, propectus and pronotum, posterodorsal view; 58, *Scelio sp.*, pronotum, median view; 59; *Trimorus sp.*, pronotum, anterior view; 60, *Telenomus sp.*, pronotum, posterior view; 61, *Telenomus sp.*, pronotum, anterior view.

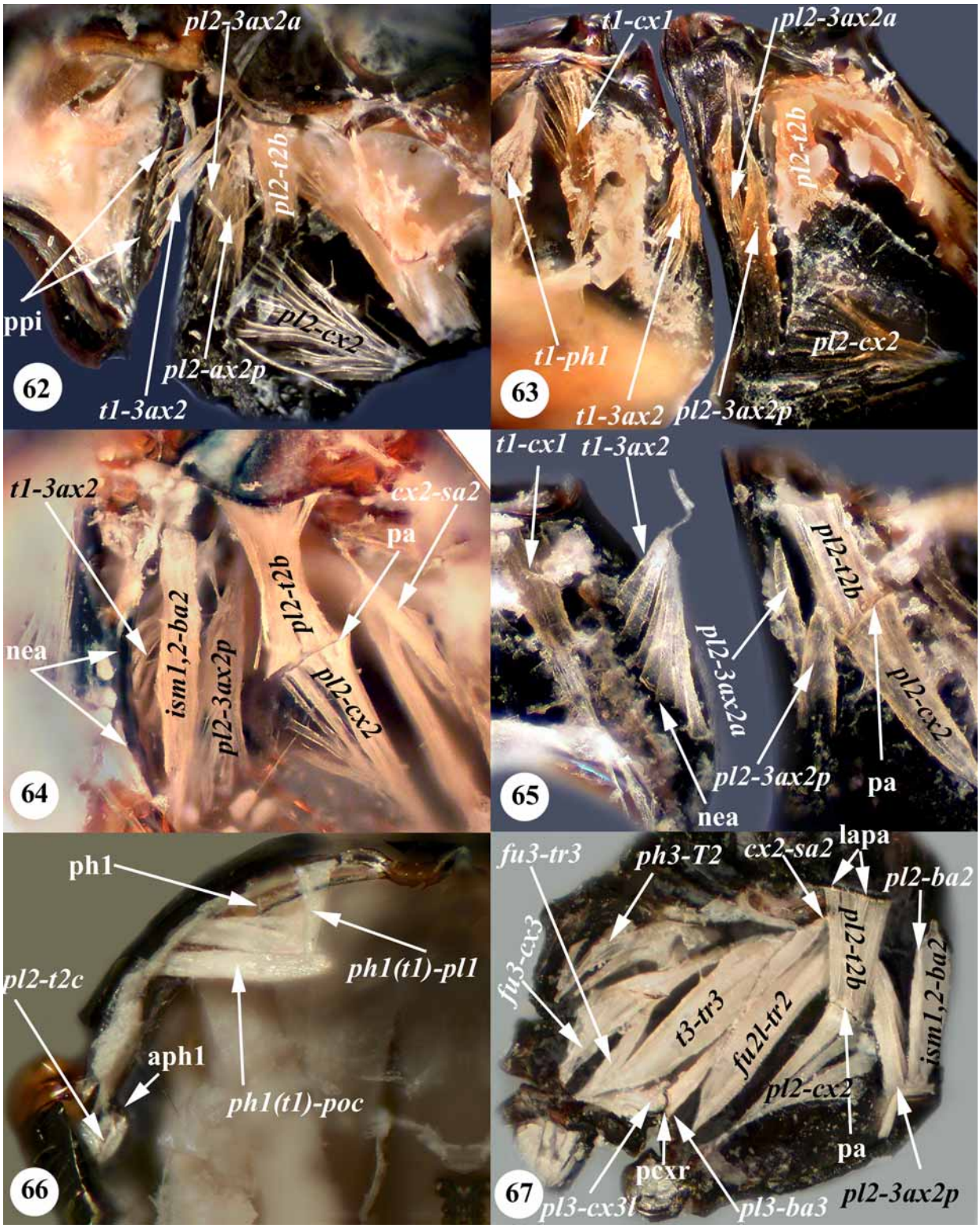

FIGURES 62–67. 62, *Sparasion sp.*, mesosoma, sagittal section, lateral view; 63, *Nixonia sp.*, mesosoma, sagittal section, lateral view; 64, *Neoscelio sp.*, mesosoma, sagittal section, lateral view; 65, *Teleas lamellatus*, mesosoma, sagittal section, lateral view; 66, *Baryconus sp.*, mesosoma, anterolateral view, pronotum and propectus removed; 67, *Baryconus sp.*, mesosoma, sagittal section, lateral view.

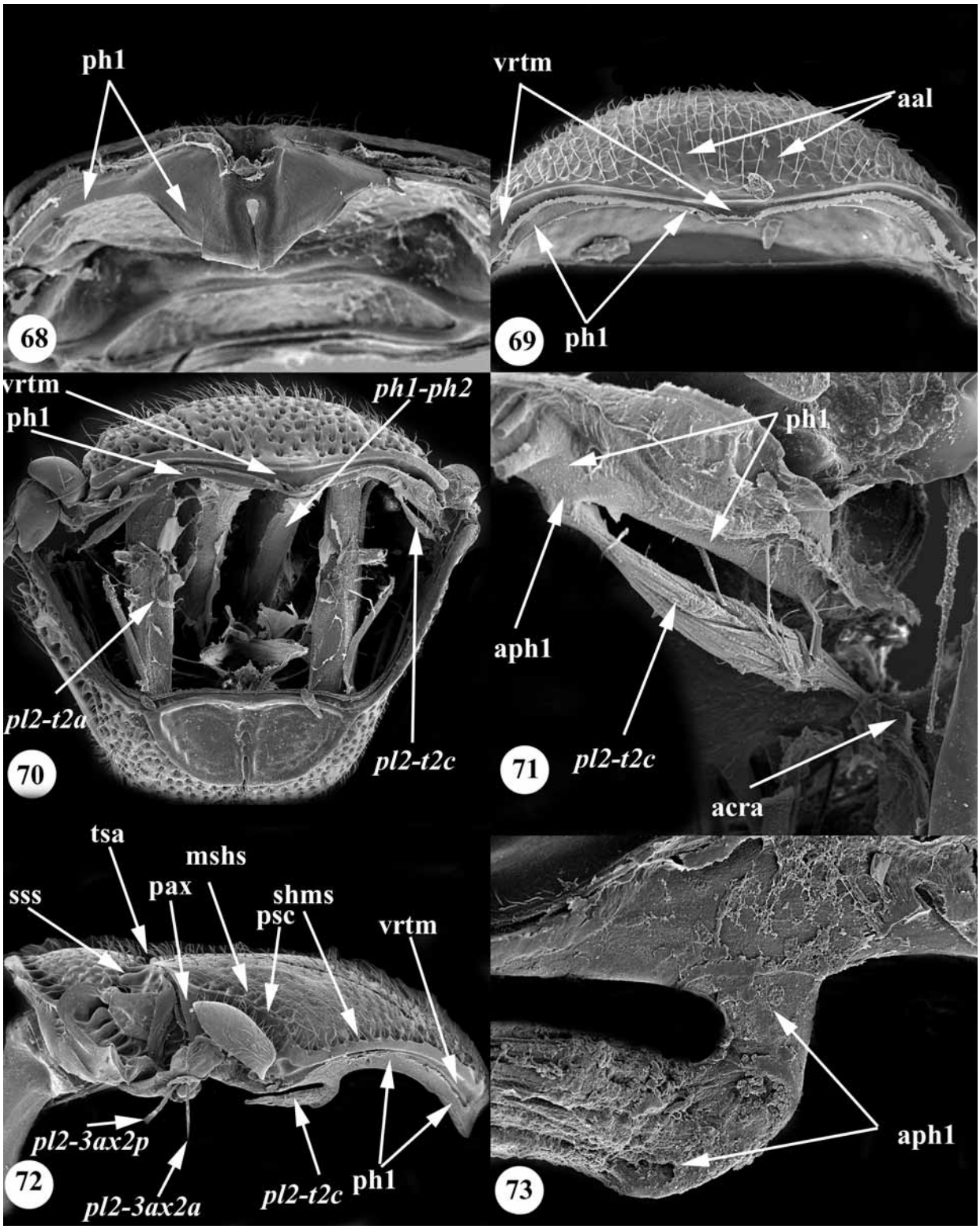

FIGURES 68–73. 68, *Sparasion sp.*, mesoscutum and first phragma, anterior view; 69, *Telenomus sp.*, mesoscutum and first phragma, anterior view; 70, *Trichoteleia sp.*, mesosoma, antero-lateral view, pronotum and propectus removed; 71, *Trichoteleia* sp., mesoscutum and mesopleuron, anteromedian view; 72, *Calliscelio sp.*, mesonotum and second phragma, lateral view; 73, *Calliscelio sp.*, ventral apodeme of the first phragma, lateral view.

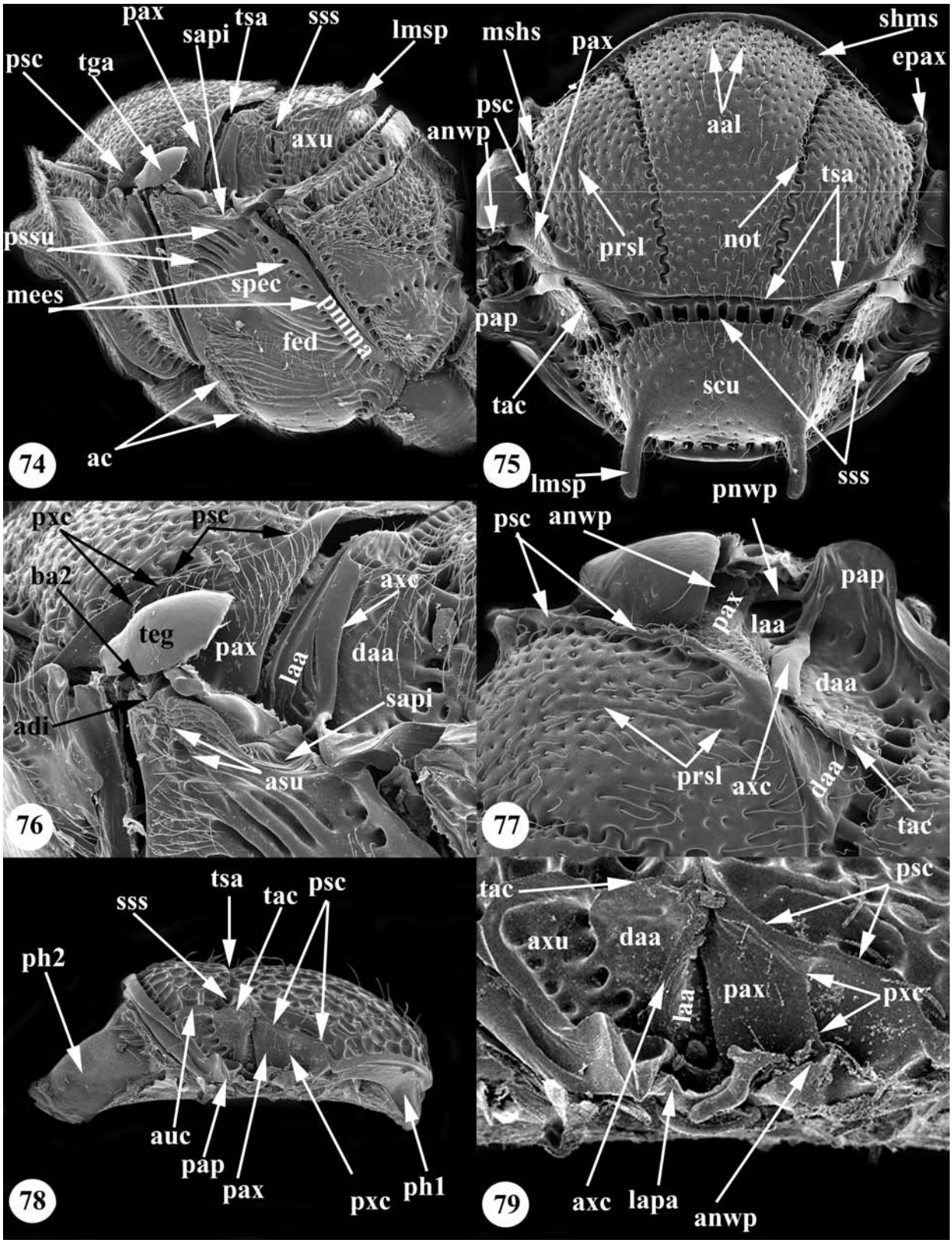

FIGURES 74–79. 74, *Archaeoteleia sp.*, mesosoma, lateral view; 75, *Archaeoteleia sp.*, mesonotum, dorsal view; 76, *Archaeoteleia sp.*, mesosoma, lateral view; 77, *Archaeoteleia sp.*, mesonotum, dorsal view; 78, *Scelio sp.*, mesonotum and second phragma, lateral view; 79, *Scelio sp.*, axilla, axillula and preaxilla, lateral view.

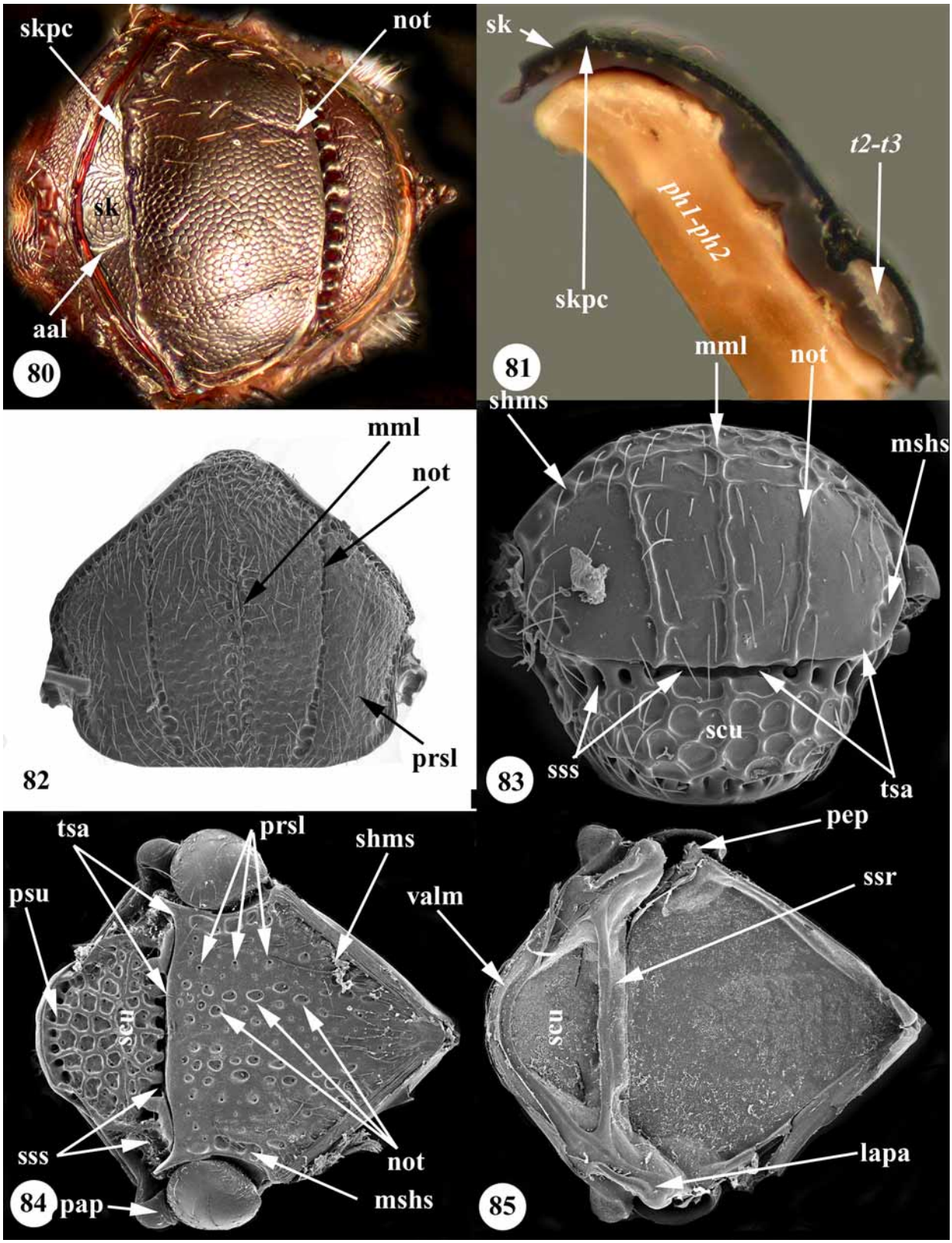

FIGURES 80–85. 80, *Psilanteris sp.*, mesosoma, dorsal view; 81, *Psilanteris sp.*, mesosoma, sagittal section, lateral view, pronotum, pro-, mesopectus, metanotum and metapectal-propodeal complex removed; 82, *Baryconus sp.*, mesoscutum, dorsal view, 83, Teleasinae *n. gen.*, mesonotum, dorsal view; 84, *Sparasion sp.*, mesonotum, dorsal view; 85, *Sparasion sp.*, mesonotum, ventral view.

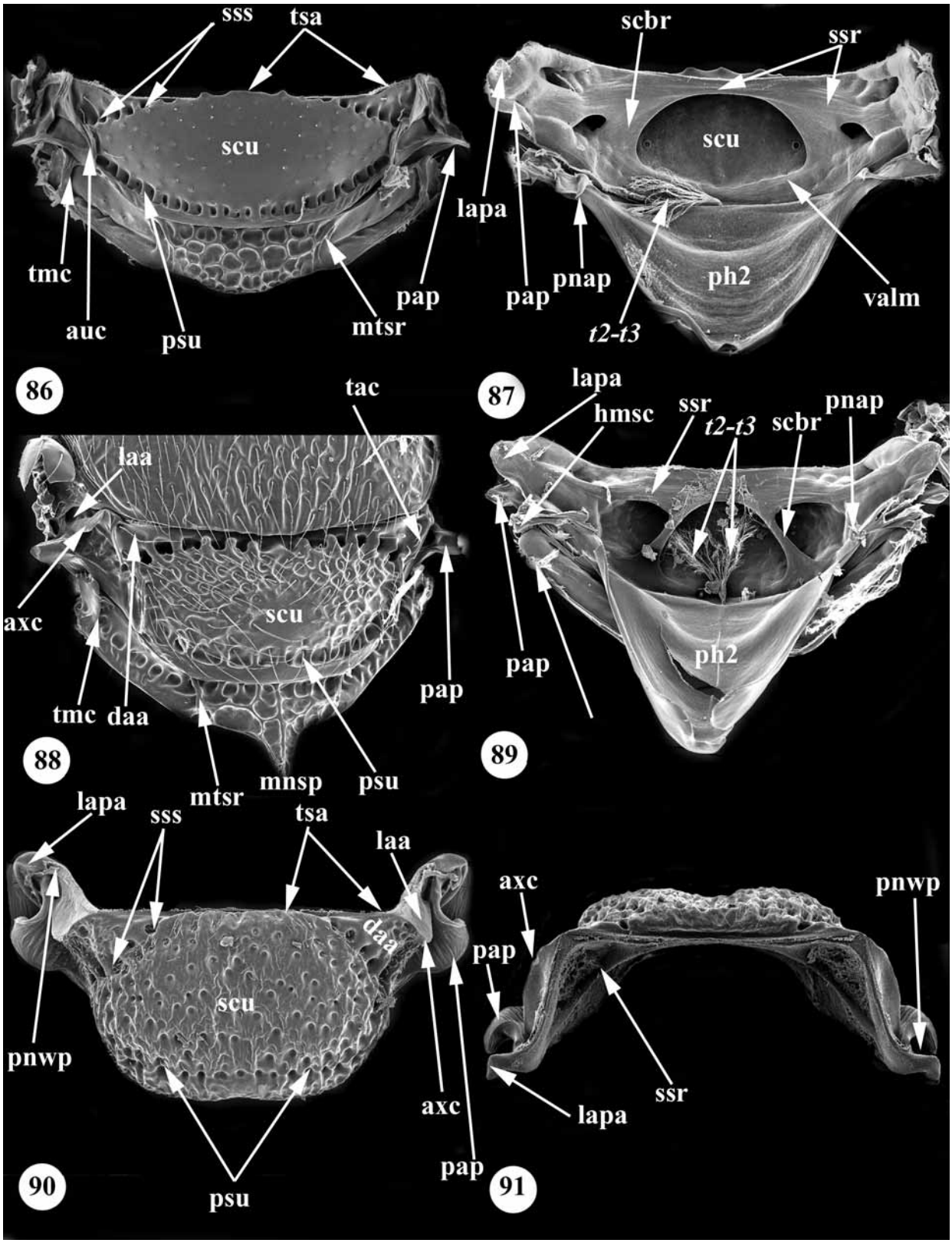

FIGURES 86–91, 86, *Telenomus sp.*, mesoscutellum and metanotum, dorsal view; 87, *Telenomus sp.*, mesoscutellum, mesopostnotum and metanotum, ventral view; 88, *Trimorus sp.*, mesoscutellum and metanotum, dorsal view; 89, *Trimorus sp*., mesoscutellum, mesopostnotum and metanotum, ventral view; 90, *Nixonia sp.*, mesoscutellum, dorsal view; 91, *Nixonia sp.*, mesoscutellum, anterior view.

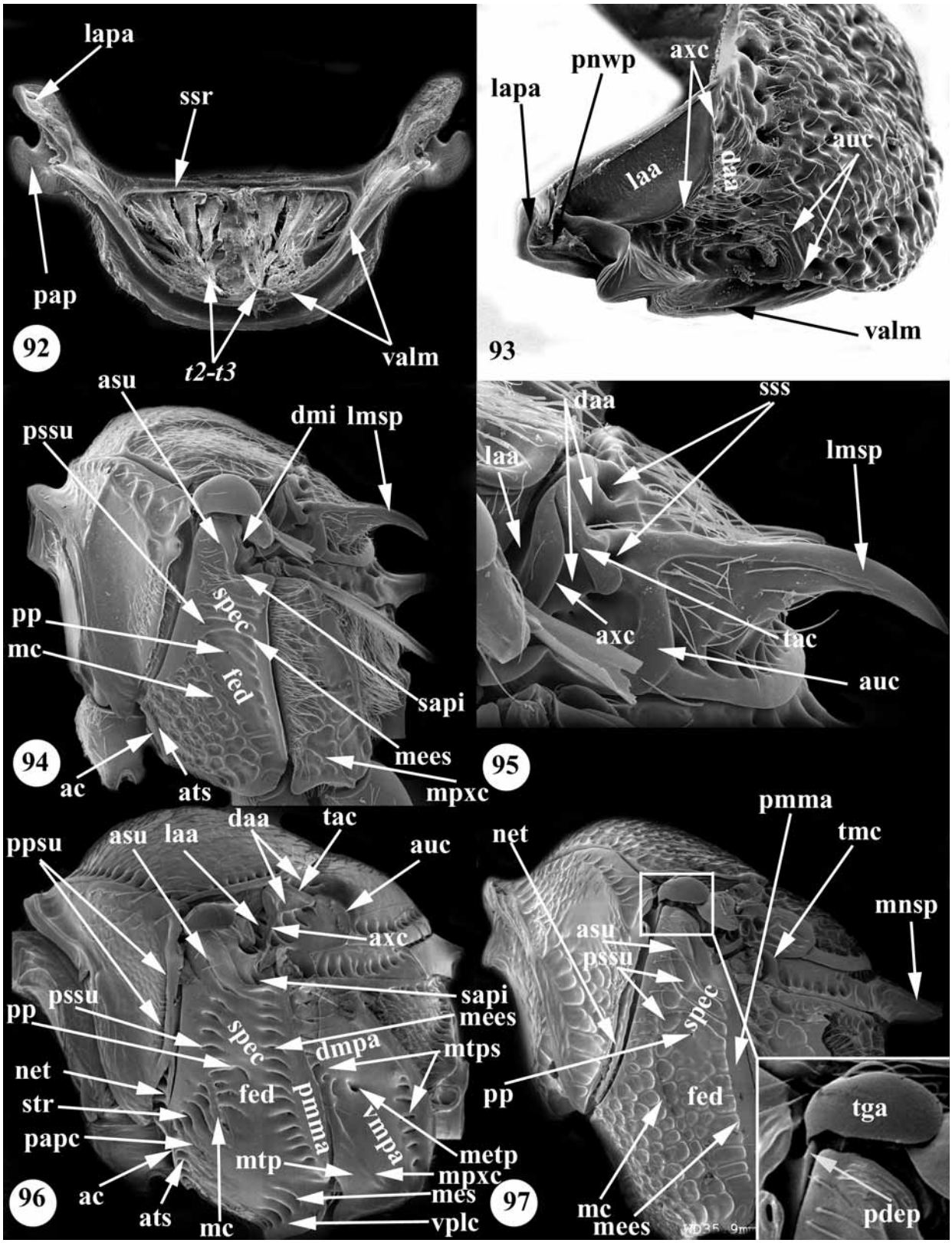

FIGURES 92–97. 92, *Nixonia sp.*, mesoscutellum, ventral view; 93, *Nixonia sp.*, mesoscutellum, dorsolateral view; 94, *Gryonoides sp.*, mesosoma, lateral view; 95, *Gryonoides sp.*, mesoscutellum, lateral view; 96, *Trimorus flavipes*, mesosoma, lateral view; 97, *Trimorus puncticollis*, mesosoma, lateral view.

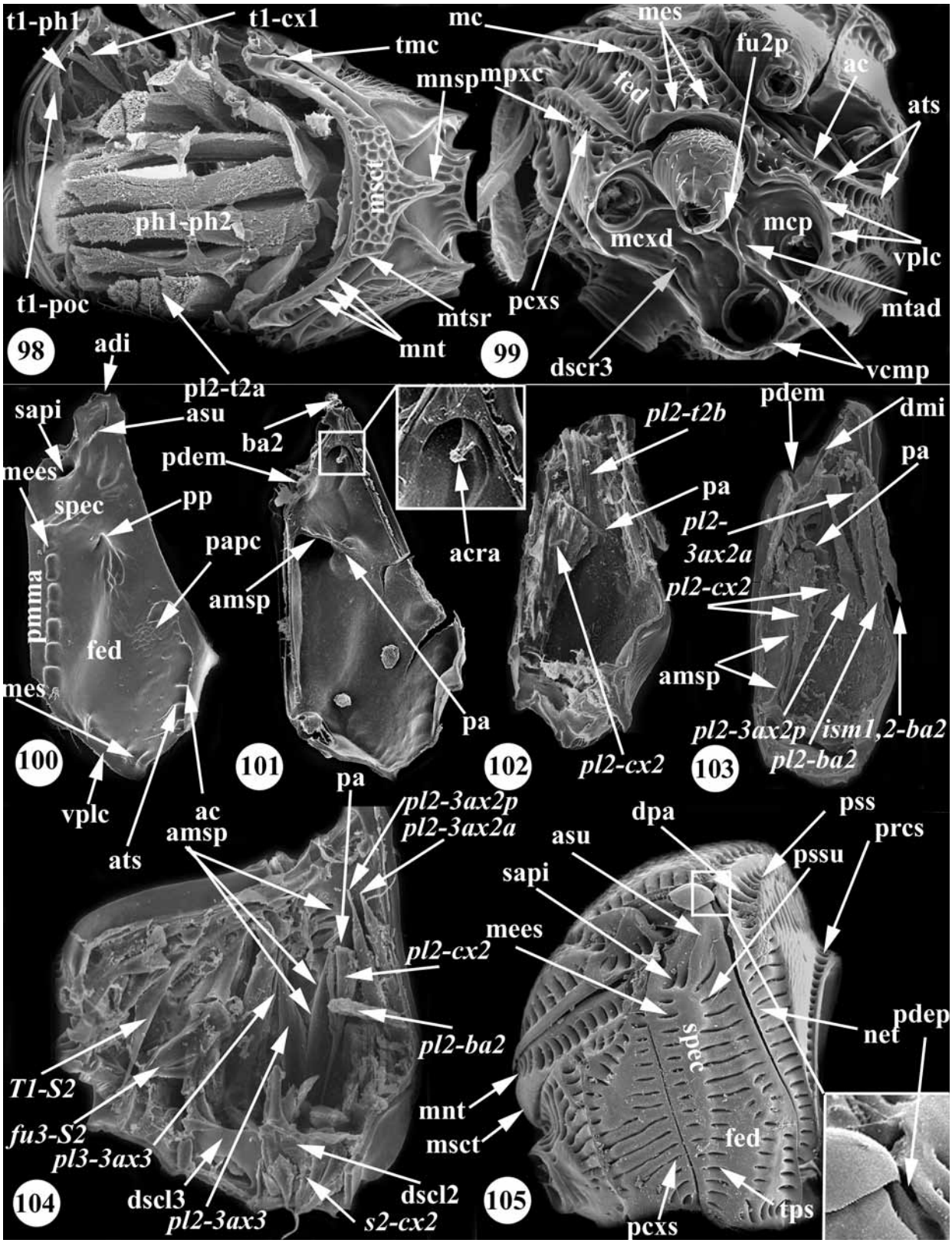

FIGURES 98–105. 98, *Trimorus sp.*, mesosoma, dorsal view, mesonotum removed; 99, *Trimorus hungaricus*, mesosoma, ventral view; 100, *Telenomus sp.*, mesopectus, lateral view; 101, *Telenomus sp.*, mesopectus, median view; 102, *Trissolcus sp.*, mesopectus, median view; 103, *Psix sp.*, mesopectus, median view; 104, *Paratelenomus sp.*, mesosoma, median view; 104, *Paratelenomus sp.*, mesosoma, lateral view.

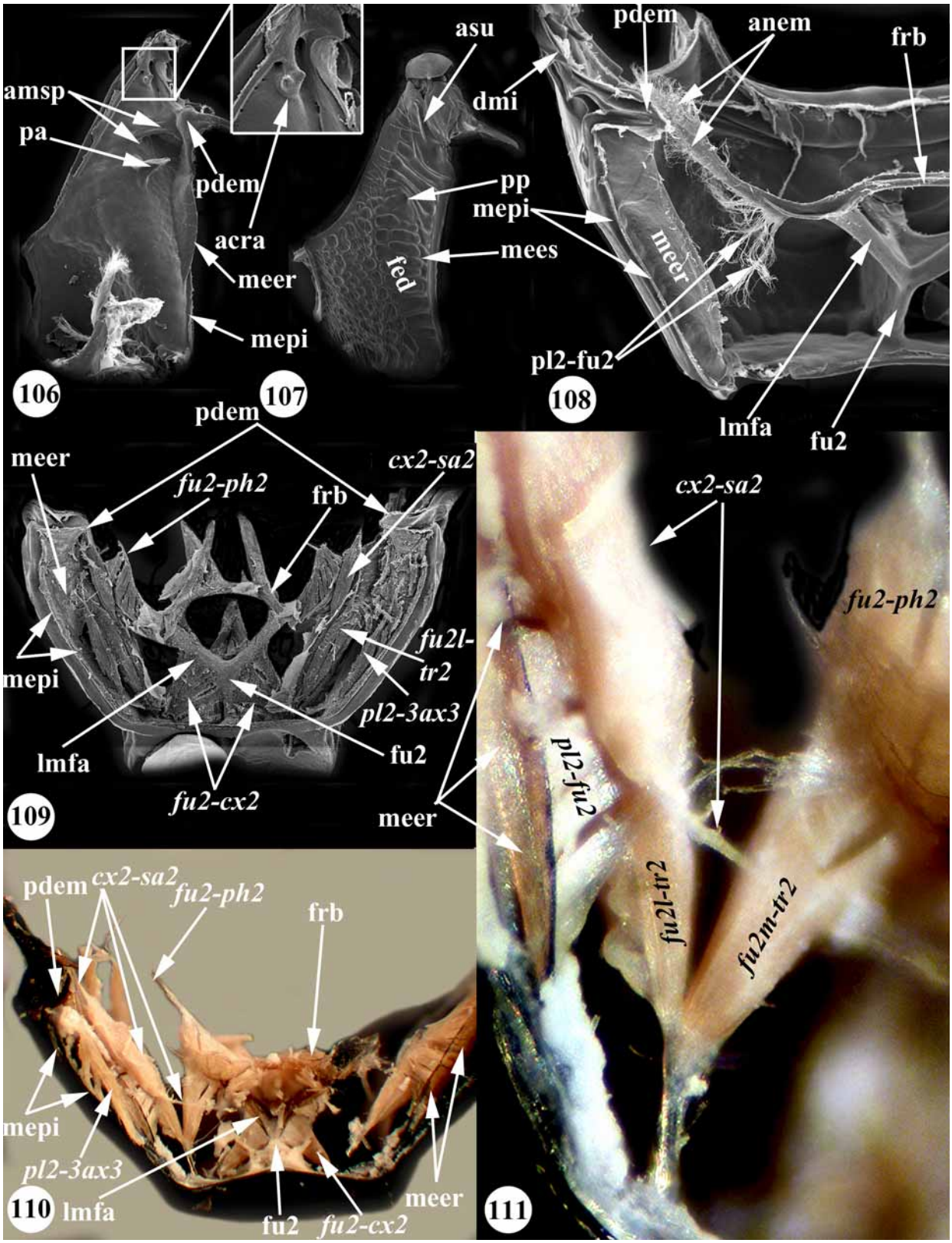

FIGURES 106–111. 106, *Trimorus varicornis*, mesopleuron, median view; 107, *Trimorus varicornis*, mesopleuron, lateral view; 108, *Archaeoteleia sp.*, mesopectus, posterior view, mesonotum, metanotum, mesopostnotum and metapectal-propodeal complex removed; 109, *Baryconus sp.*, mesopectus, posterior view, mesonotum, metanotum, mesopostnotum and metapectal-propodeal complex removed; 110, *Nixonia sp.*, mesopectus, posterior view, mesonotum, metanotum, mesopostnotum and metapectal-propodeal complex removed; 111, *Nixonia sp.*, mesopectus, posterior view, mesonotum, metanotum, mesopostnotum and metapectal-propodeal complex removed.

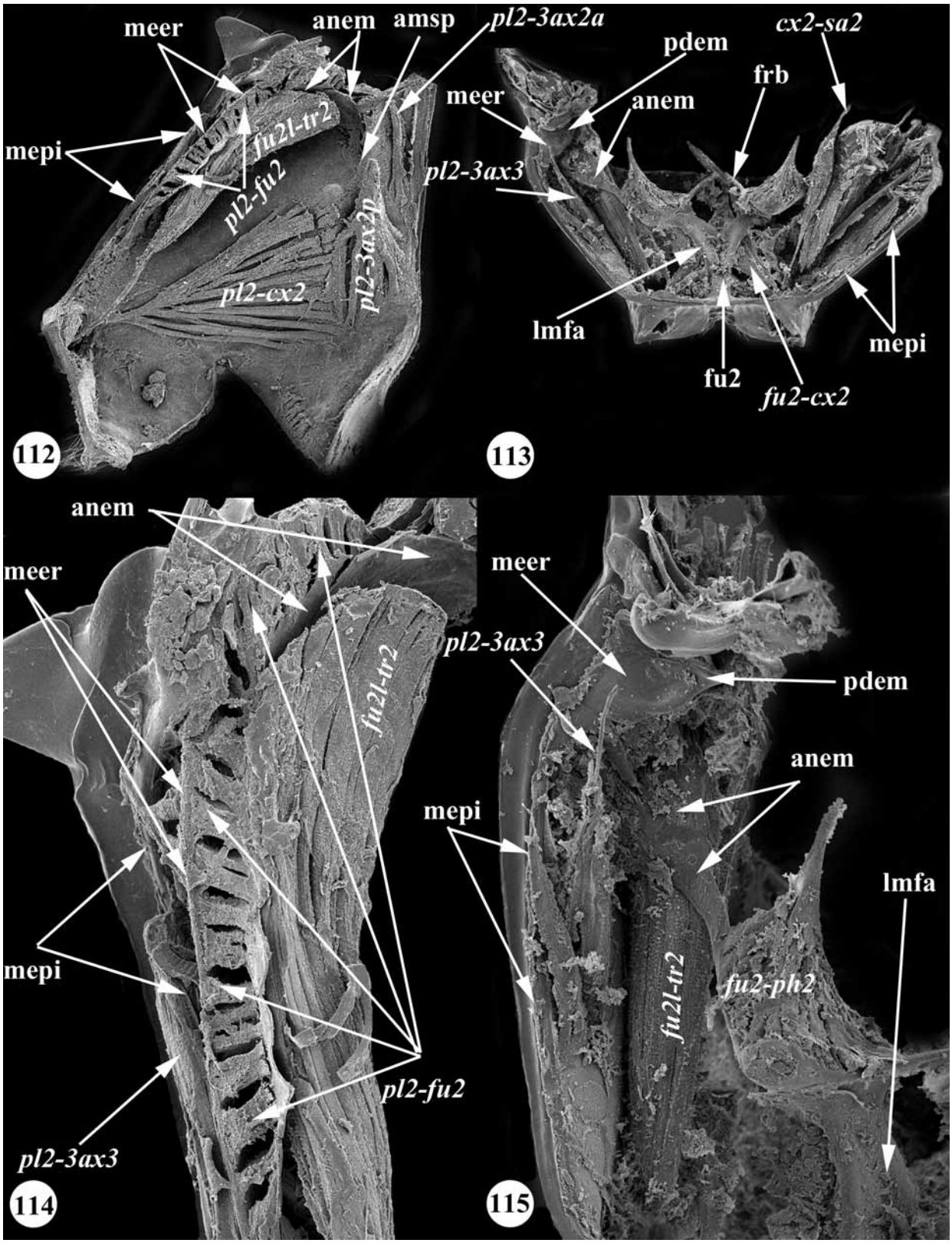

FIGURES 112–115. 112, 114, *Sparasion sp.*, mesopleuron, median view; 113, 115, *Scelio sp.*, mesopectus, posterior view, mesonotum, metanotum, mesopostnotum and metapectal-propodeal complex removed.

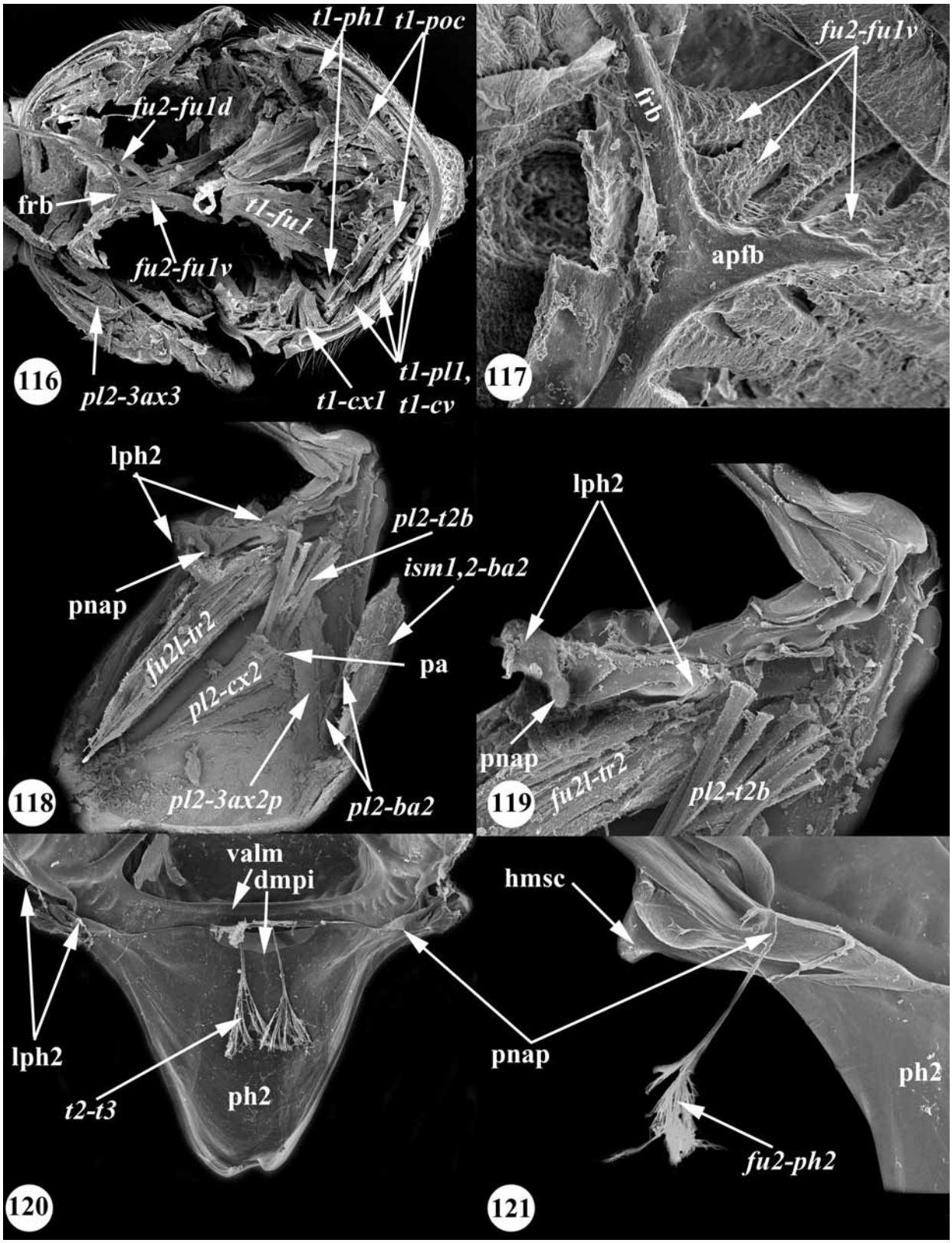

FIGURES 116–121. 116, *Calliscelio sp.*, mesosoma, dorsal view, mesonotum, metanotum, mesopostnotum and metapectal-propodeal complex removed; 117, *Calliscelio sp.*, anterior process of the mesofurcal bridge with ventral mesofurco-profurcal muscle, dorsal view; 118, Scelio sp., mesopleuron and mesolaterophragma, median view; 119, *Scelio sp.*, mesolaterophragma, median view; 120, *Archaeoteleia sp.*, mesoscutellum and mesopostnotum with second phragma, anteroventral view; 121, *Archaeoteleia sp.*, mesolaterophragma, and humeral sclerite, anteroventral view.

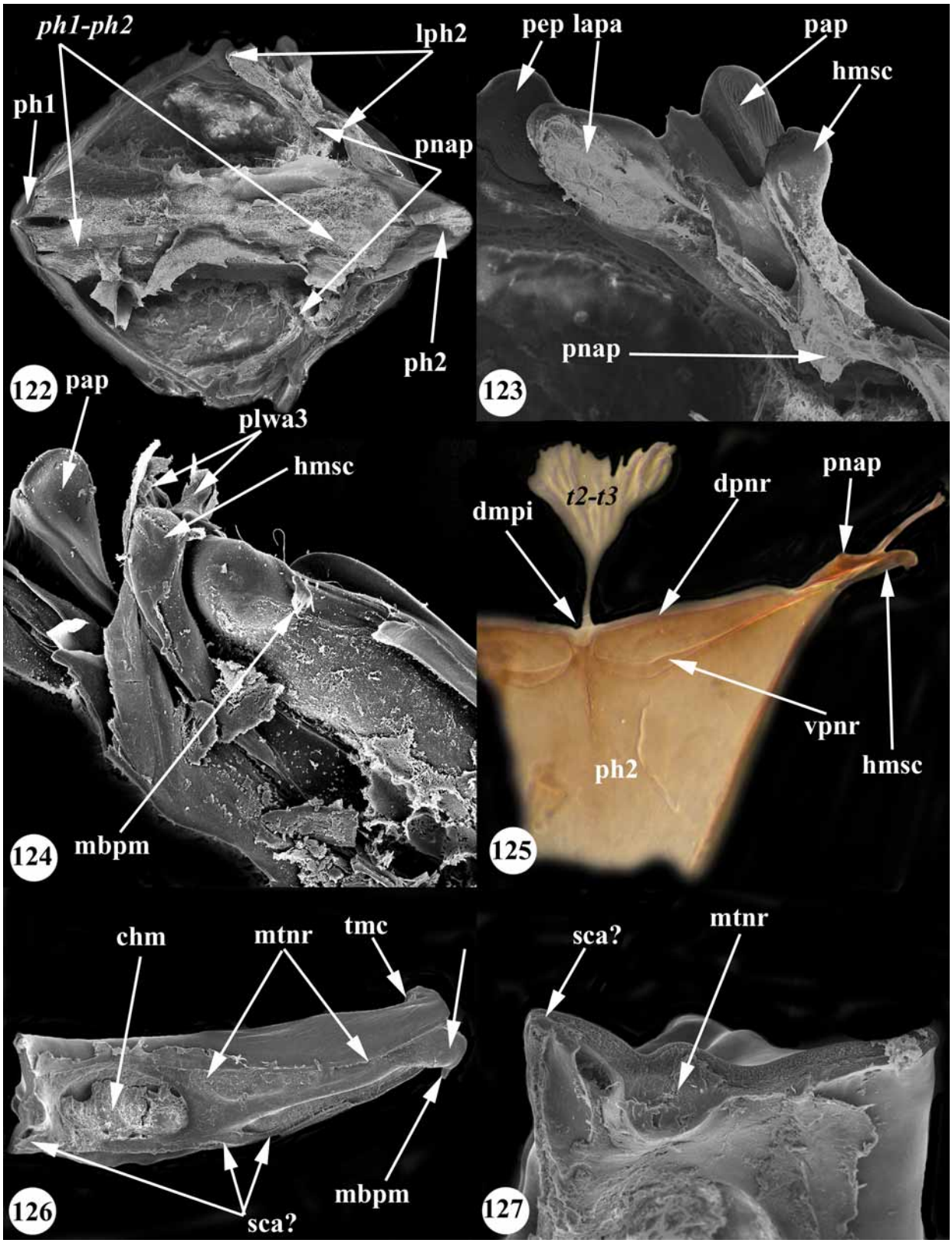

FIGURES 122–127. 122, *Scelio sp.*, mesonotum and mesopostnotum with second phragma, ventral view; 123, *Scelio sp.* mesonotum, mesolaterophragma and humeral sclerite, ventral view; 124, *Baryconus sp.*, mesonotum, mesolaterophragma, humeral sclerite and metanotum, ventral view; 125, *Trimorus sp.*, mesopostnotum with second phragma and humeral sclerite, anterior view; 126, *Sparasion sp.*, metanotum, anterolateral view; 127, *Sparasion sp.*, submedian sagittal section of metanotum, lateral view.

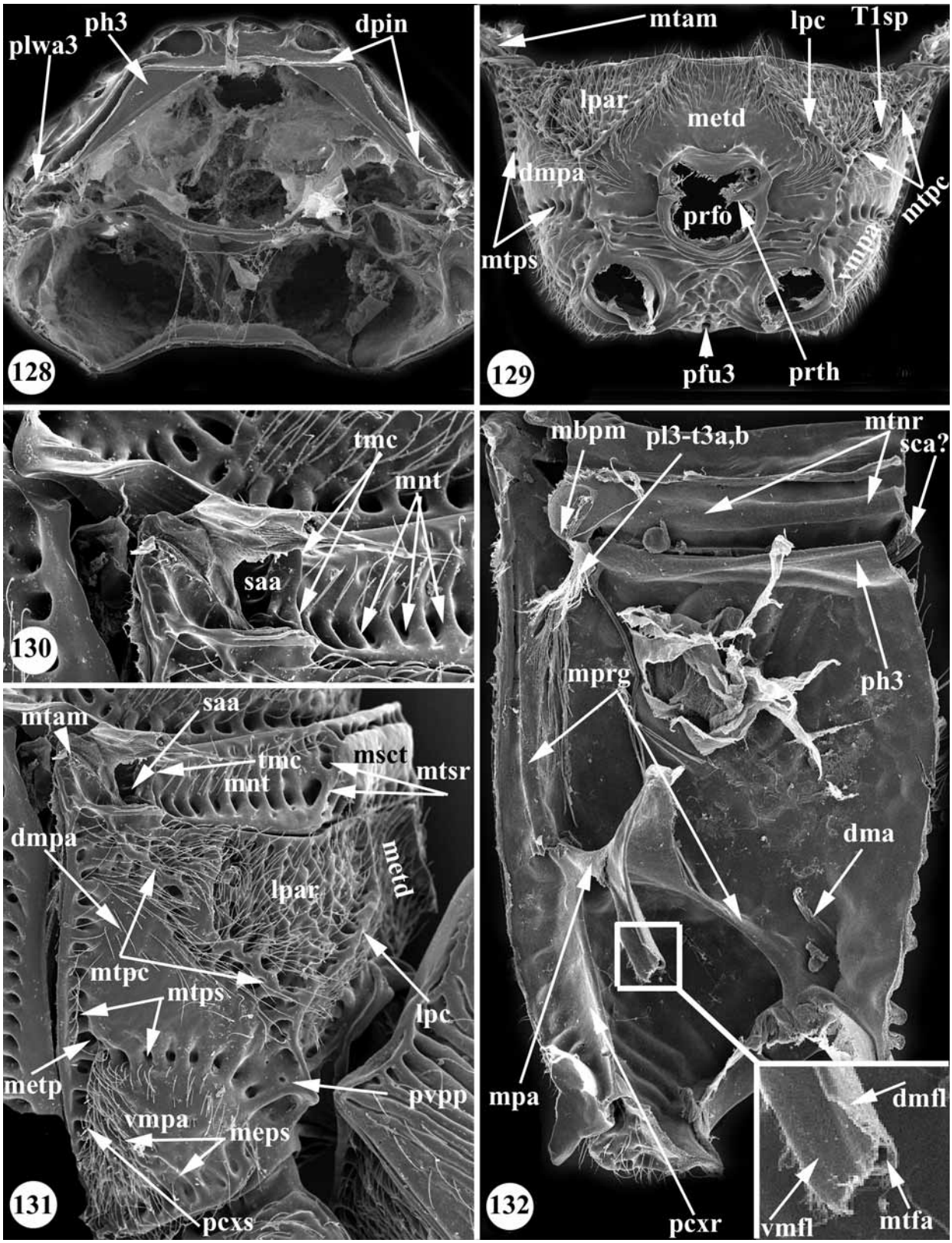

FIGURES 128–132. 128, *Telenomus sp.*, metapectal-propodeal complex, dorsal view; 129–132, *Archaeoteleia sp.*; 129, metapectal-propodeal complex, posterior view; 130, metanotum and metapleural arm, lateral view; 131, metapectal-propodeal complex, lateral view; 132, metapectal-propodeal complex and metanotum, median view.

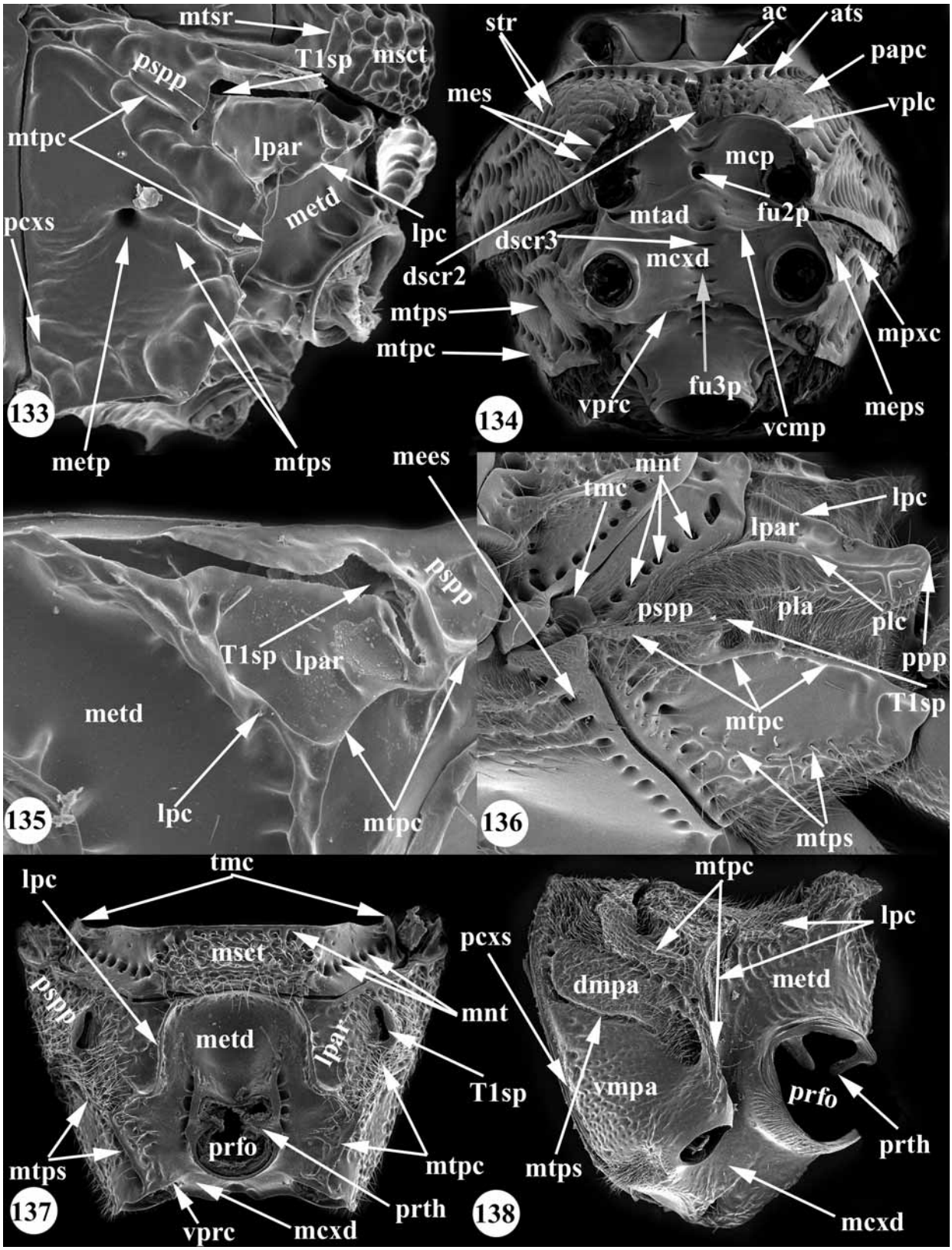

FIGURES 133–138. 133, *Telenomus sp.*, metapectal-propodeal complex, posterolateral view; 134, *Trimorus opacus*, mesosoma, ventral view; 135, *Telenomus sp.*, metapectal-propodeal complex, posterior view; 136, *Sparasion sp.*, metapectal-propodeal complex, metanotum, mesonotum and mesopleuron, lateral view; 137, *Calliscelio sp.*, metapectal-propodeal complex and metanotum, posterior view; 138, *Nixonia sp.*, metapectal-propodeal complex, posterolateral view.

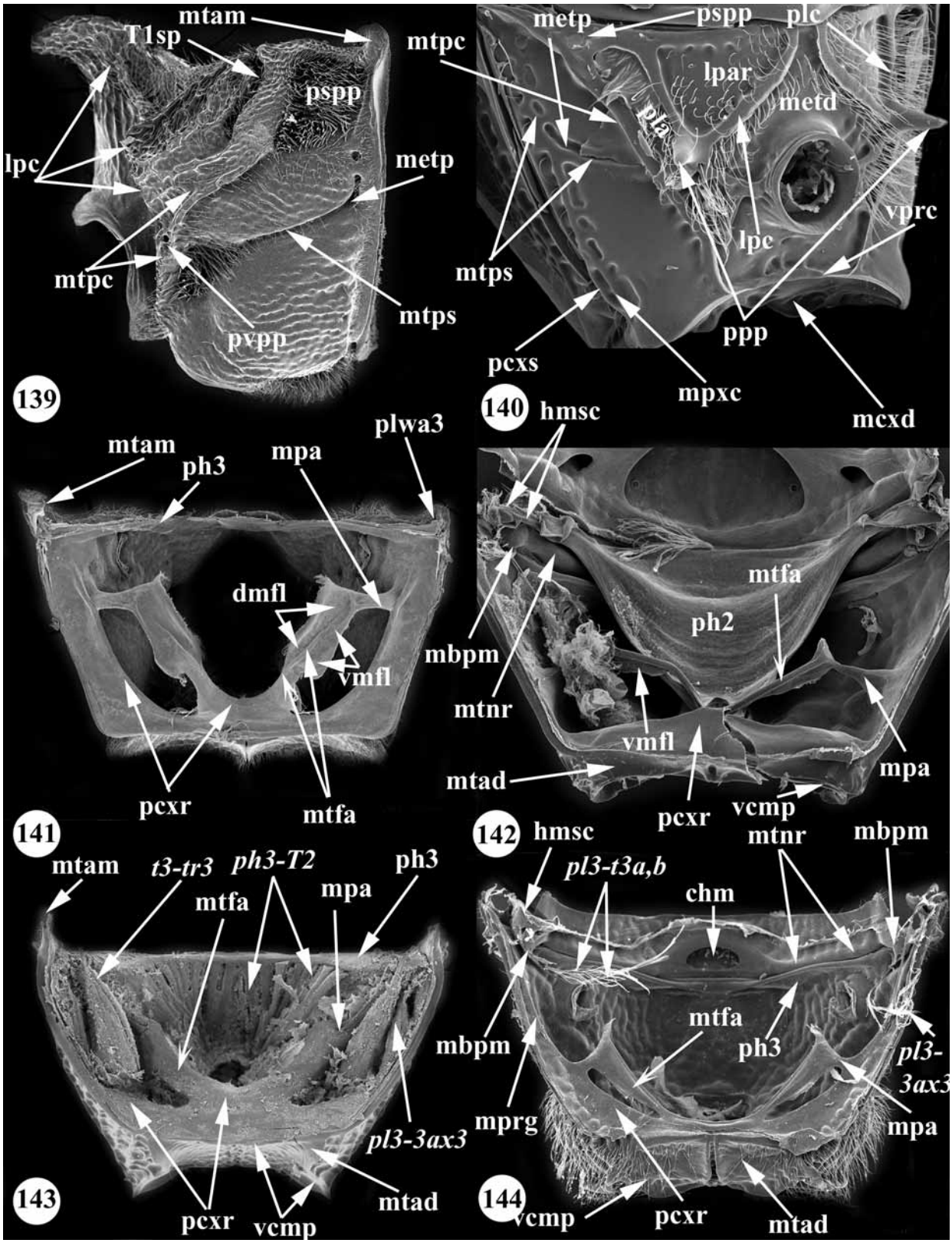

FIGURES 139–144. 139, *Nixonia sp.*, metapectal-propodeal complex, posterolateral view; 140, *Trimorus sp.*, metapectal-propodeal complex, posterolateral view; 141, *Sparasion sp.*, metapectal-propodeal complex, anterior view; 142, *Telenomus sp.*, metapectal-propodeal complex, second phragma and mesoscutellum, anterior view; 143, *Scelio sp.*, metapectal-propodeal complex, anterior view; 144, *Archaeoteleia sp.*, metapectal-propodeal complex, anterior view.

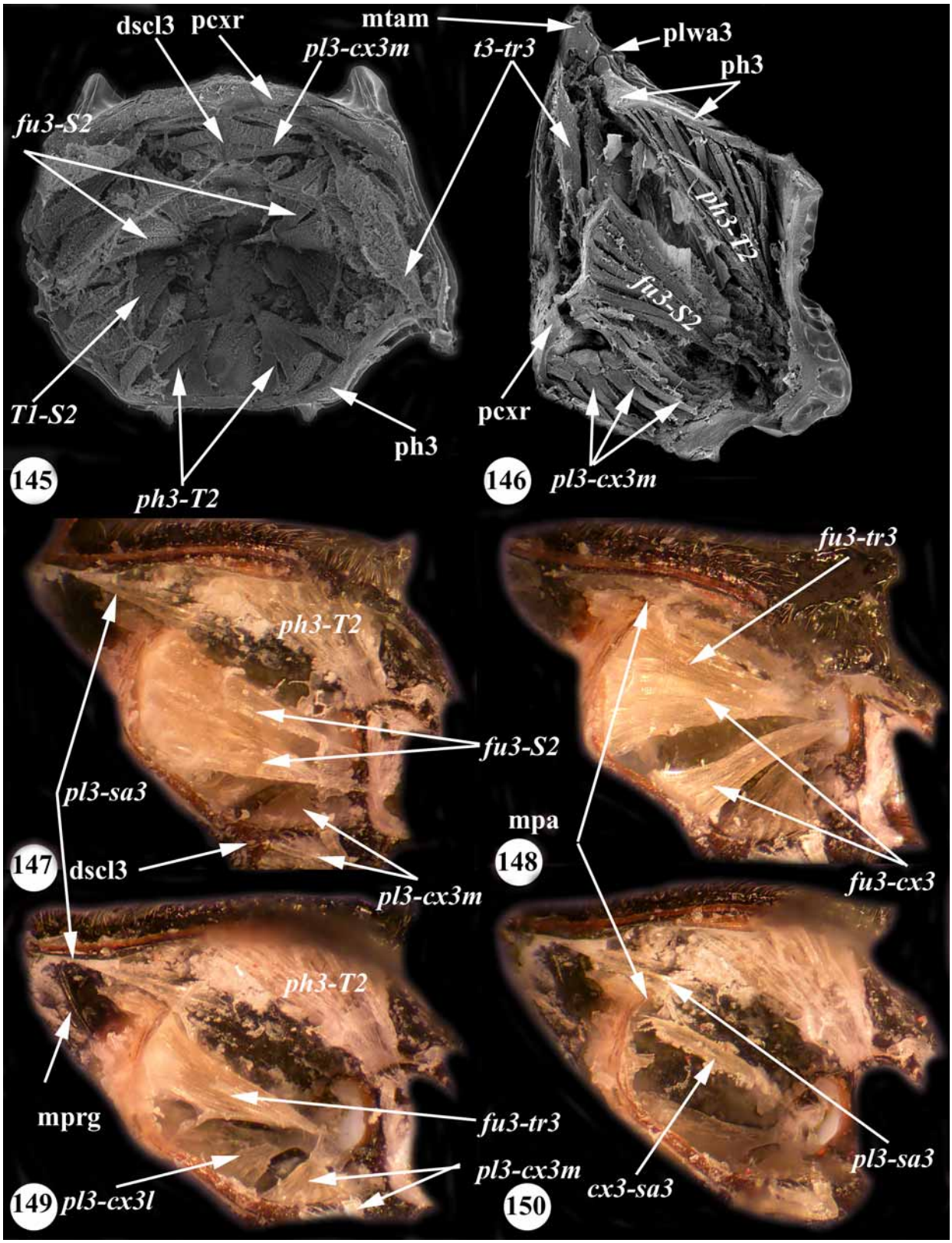

FIGURES 145–150. 145, *Idris sp.*, metapectal-propodeal complex, dorsal view; 146, *Scelio sp.*, metapectal-propodeal complex, median view; 147–150, *Sparasion sp.*, metapectal-propodeal complex, median view.

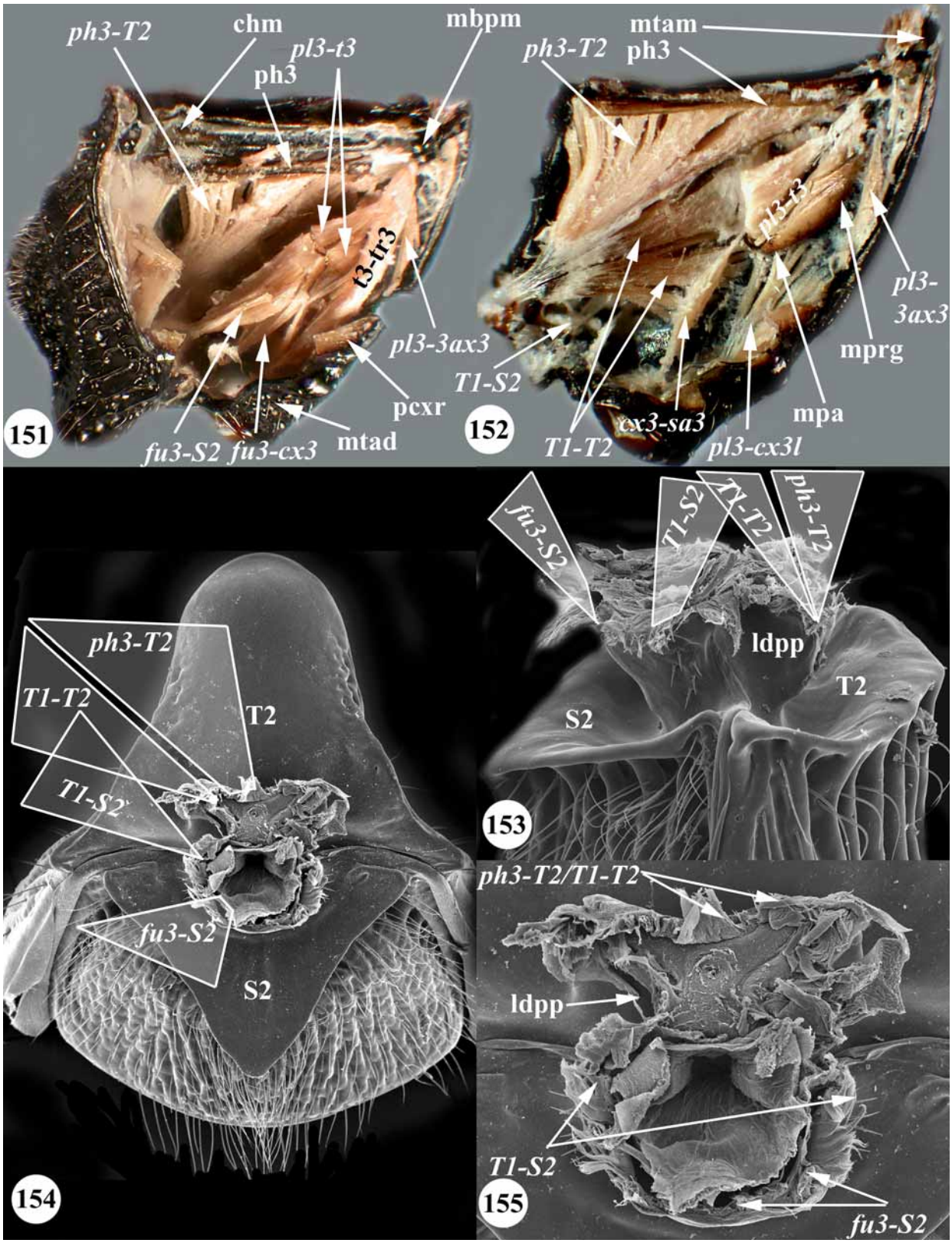

FIGURES 151–155. 151, 152, *Scelio sp.*, metapectal-propodeal complex, median view; 153–155, *Archaeoteleia sp.*; 153, first metasomal segment, lateral view; 154, metasoma, anterior view; 155, first metasomal segment, anterior view.

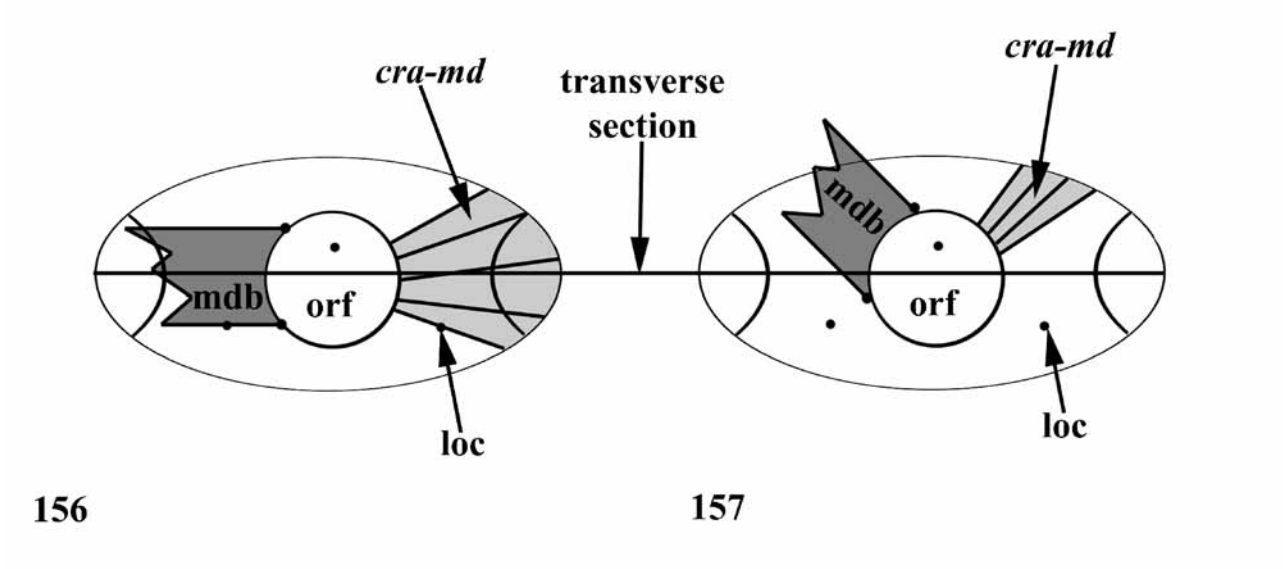

FIGURES 156, 157. 156,157, schematized head of scelionids, ventral view.